Localization and Function of RNases in *Bacillus subtilis*

Dissertation

for the award of the degree

"Doctor rerum naturalium"

of the Georg-August-Universität Göttingen

within the doctoral program

Molecular Biology

of the Georg-August University

School of Science (GAUSS)

submitted by

Nora Cascante Estepa

from Soria (Spain)

Göttingen 2016

Thesis Committee

Prof. Dr. Jörg Stülke
(Institute of Microbiology and Genetics, Department of General Microbiology)

Prof. Dr. Markus Bohnsack
(Institute of Molecular Biology, Department of Molecular Biology)

Prof. Dr. Ivo Feussner
(Albrecht-von-Haller Institute for Plant Sciences, Department of Plant Biochemistry)

Members of the Examination Board

Prof. Dr. Jörg Stülke
(Institute of Microbiology and Genetics, Department of General Microbiology)

Prof. Dr. Markus Bohnsack
(Institute of Molecular Biology, Department of Molecular Biology)

Prof. Dr. Ivo Feussner
(Albrecht-von-Haller Institute for Plant Sciences, Department of Plant Biochemistry)

Prof. Dr. Stefanie Pöggeler
(Institute of Microbiology and Genetics, Department of Genetics of Eukaryotic Microorganisms)

PD Dr. Wilfried Kramer
(Institute of Microbiology and Genetics, Department of Molecular Genetics)

Dr. Fabian Commichau
(Institute of Microbiology and Genetics, Department of General Microbiology)

Date of oral examination: 22nd February 2017

Herewith I declare, that I prepared the Doctoral Thesis "Localization and Function of RNases in *Bacillus subtilis"* on my own and with no other sources and aids than quoted.

Göttingen, 21st December 2016

Nora Cascante Estepa

Acknowledgements

In the first place I would like to express my sincere gratitude to my supervisor Prof. Dr. Jörg Stülke for this opportunity and for the guidance throughout these years. Besides my supervisor, I would like to immensely thank Prof. Dr. Markus Bohnsack and Prof. Dr. Ivo Feussner for being part of my Thesis Advisory Committee, and for their insightful comments during the committee meetings. I thank Prof. Dr. Stefanie Pöggeler, Prof. Dr. Heike Krebber, and Dr. Fabian Commichau for taking part in the Examination Board.

I would like to thank Achim Dickmanns, Johannes Arens, and Piotr Neumann for the work performed on PNPase, as well as Prof. Dr. Ficner for the opportunity of working together with his group in that project.

I would also like to express my gratitude to Prof. Dr. Diederichsen for the possibility of performing experiments in his department. Thank you to Daniel Frank for his technical support in managing the HPLC, and for his infinite patience.

During my secondment in Amsterdam I had an amazing time and I would like to thank Prof. Dr. Leendert Hamoen for the opportunity of spending two months in his lab. Also I would like to thank Laura C. Bohórquez for helping me in the lab and in the city, and for the nice time that I had there. ¡Gracias! Of course, I also want to thank the rest of the Hamoen's lab for the nice environment and for making me feel very welcome. Also, thank you to Henrik Strahl for the very interesting talks that we had and for the brief time we worked together on RNase Y, I learnt a lot during this time.

Thank you to the fellows and all the members of the AMBER Consortium. I really had a very nice time in all the meetings, courses, conferences, and, of course, the free time that we spent together. Also thank you to the EU FP7 Marie Curie Initial Training Network on Molecular Bacteriology for financial support.

I would like to thank the Molecular Biology program of the University of Göttingen for this amazing opportunity, and especially to Kerstin Grüniger and Dr. Steffen Burkhardt for their organization and their constant support.

I am very grateful to all the members of the AG. Stülke, AG. Commichau, and AG. Hoppert (past and present), for the great time that I had these years and for the nice working environment. Especially, I would like to thank Christina Herzberg, who was there from the very beginning, and taught me everything. Also for the conversations that we shared while filling tip boxes, that made it much less boring ;). Very especial thanks to Jan Kampf and Daniel Reuß, as well as Ingrid Quintana and Blanca Rincón for the nice conversations, meals, and kitchen times.

Table of contents

Summary

The ability to adapt to changing environmental conditions is essential for every organism to survive. In bacteria, this adaptation relies on the control of the mRNA synthesis, stability, and turnover, which allows the expression of different sets of proteins as a response to the external conditions. In many bacteria, the enzymes responsible for the degradation of the mRNA interact to form multi-enzyme complexes, the RNA degradosomes. In the Gram-positive model organism *Bacillus subtilis*, several binary interactions were detected amongst RNA-related proteins *in vivo*, and it has been hypothesized that an RNA-degrading complex exists in this organism. These interactions involved the endoribonuclease RNase Y, the RNA helicase CshA, the exoribonucleases RNase J1 and PNPase, and the glycolytic enzymes enolase and phosphofructokinase. Moreover, the paralogue of RNase J1, RNase J2 was shown to only interact with RNase J1. However, some of these interactions could not be reproduced and the complex could never be purified as a whole, questioning the possibility of its existence. In this work, I have studied the subcellular localization of the components of the RNA degradosome of *B. subtilis*. The differential localization of each protein rules out the existence of a stable RNA degradosome. Furthermore, I have studied the interaction and oligomerization between the paralogous RNases J1 and J2 *in vivo,* and analyzed the importance of the C-terminal domain for this interaction. The results confirm the interaction of the RNases J1 and J2 through the C-terminal domain, and show that they oligomerize as dimers and tetramers. However, it is possible that the tetramers can only be formed in the presence of RNA. Moreover, it seems that the RNase J2 cannot interact with RNA on its own.

Although the enzymes of the putative RNA degradosome have been extensively studied, many questions regarding activity and regulation remain open. Amongst them, the enzyme PNPase is one of the best studied, since PNPase from *Escherichia coli* has been studied for many decades. It has been shown that ATP, c-di-GMP and citrate, amongst others, can regulate its activity. However, the regulation of the PNPase from *B. subtilis* is not known. In this work, I have studied the effect of citrate, c-di-GMP and c-di-AMP, as well as enolase and phosphofructokinase, on the RNA degradation activity of PNPase. None of these metabolites and enzymes seems to have an effect on this activity.

Altogether, these findings contribute to a better understanding of the complex picture of RNA degradation, while opening ways for further investigations.

1. Introduction

It is essential for any organism to establish a dynamic equilibrium that allows the proper interplay and regulation of the different molecular mechanisms. This should permit the maintenance of the homeostasis as well as enable the organism to be able to swiftly respond to sudden environmental changes. To achieve this, the organisms need to have access to a different set of proteins for every specific condition, to ensure the possibility of accommodating their internal molecular mechanisms to the new environment. This is achieved by the control of the gene expression. This can be exerted at several levels; however, the protein levels are ultimately dependent on, not only the amount of mRNA, but also of other RNA species, such as rRNA, tRNA and non-coding regulatory RNAs. The RNA turnover relies on transcriptional and post-transcriptional regulation; however, its stability and functionality are dependent on the latter. This regulation, that occurs after the RNA has been synthesized, is what is referred to as RNA processing.

RNA processing exists and is essential in every domain of life (archaea, bacteria and eukarya). It is a general name that describes very different mechanisms that modulate the gene expression, such as capping, splicing, nuclear export, polyadenylation, editing, maturation or decay. These are regulated all together to ensure that a proper amount of functional RNA species is provided at all times.

1.1. RNA processing in bacteria: maturation and decay

The ability to adapt to external changes is especially important in bacteria, since they are often subject to extreme environmental variations (in temperature, salt concentration, nutrient availability, presence of antibiotics), for example in the change from saprophyte to pathogenic. In prokaryotes, however, the majority of the RNA processing events are minor or non-existing, so they rely almost exclusively on RNA maturation and degradation to exert the post-transcriptional control of the gene expression.

Maturation occurs in rRNA and tRNA species, which are synthesized as precursor molecules that need to undergo several modifications to become fully functional. These include base modification and nucleolytic cleavage. Prokaryotic ribosomes (70S) are complex ribonucleoproteins composed of the large (50S) and the small (30S) subunits. The proteins serve as a scaffold for the proper organization of the complex, whereas the RNAs possess catalytic activity. There are three rRNA molecules within the ribosome: 5S and 23S in the large subunit and 16S in the small subunit. They are encoded in a single operon that is present several times in the

genome, depending on the microorganism, for example, seven times for *Escherichia coli* (Deutscher, 2009) and ten for *B. subtilis* (Loughney *et al.*, 1982; Stewart *et al.*, 1982; Jarvis *et al.*, 1988). The ribosomal RNAs are transcribed together in one molecule, consequently, a downstream processing is necessary to obtain the mature forms that can be assembled into the ribosomal subunits. This maturation processing is very conserved amongst bacteria, although the mechanisms through which they are performed differ substantially (Arraiano *et al.*, 2010).
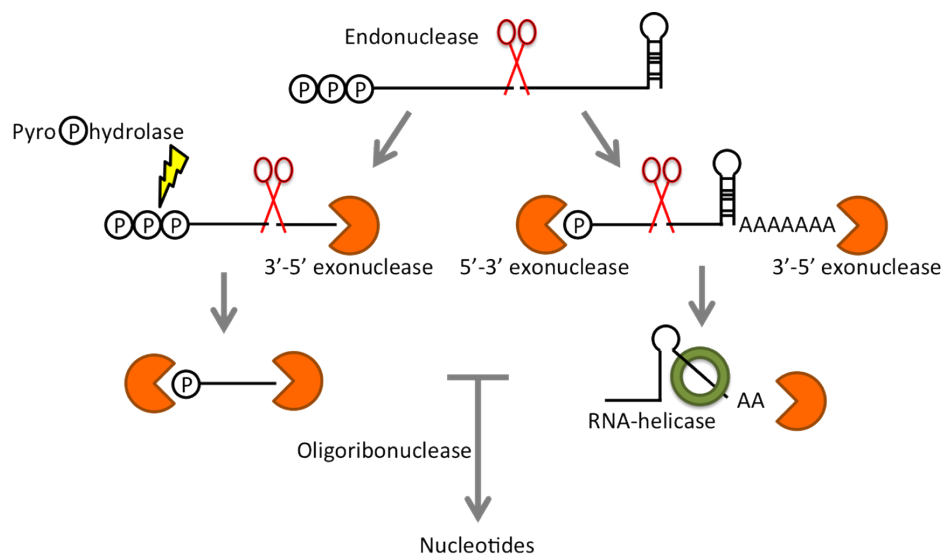
Figure 1. **Pathways for RNA degradation in bacteria.** Messenger RNAs are generally protected in both ends to prevent their fast degradation. They possess a triphosphorylated 5' end and secondary structures at the 3', as well as in the body of the transcript. The degradation of an mRNA can occur starting with an endonucleolytic cleavage or by exonucleolytically processing the extremes of the transcripts. However, for the latter, other enzymes have to take part in surpassing the protection of the ends. Pyrophosphohydrolases can remove the phosphates at the 5' and RNA helicases, with the help of poly(A)-polymerases can overcome the secondary structures. Once the protections have been removed or the transcript has been cut in the body by an endonuclease, the degradation of the transcript is very fast, and the pool of nucleotides is restored with the help of oligoribonucleases.

Once the ribosomes are correctly assembled, the tRNAs act as adaptors for decoding the information on the mRNAs in the process of translation. Transfer RNAs are also often encoded in operons, so they must undergo nucleolytic processing similar to ribosomal RNA. Once the single tRNAs have been released, further processing is required (like base modification or CCA signal at 3' end) for the mature form to be able to fold properly and to be recognized for specific aminoacylation (Hartmann *et al.*, 2009). Incorrect folding implies rapid decay, less fidelity of aminoacylation and less efficiency in the binding to ribosomes. Altogether, the proper regulation of the rRNA and tRNA post-transcriptional modification is mandatory for an appropriate protein synthesis. Nonetheless, quality control mechanisms exist to eliminate defective species that threaten the accuracy of the process. Nucleolytic processing is responsible for the degradation of

2

rRNAs and tRNAs when needed, sometimes after addition of a destabilising poly(A) tail (in the case of tRNAs) (Arraiano *et al.*, 2010).

The turnover of the messenger RNAs is also a highly regulated process and a crucial event for the control of the gene expression. It is necessary for the rapid adaptation of the organism to the environment (Wilusz and Wilusz, 2004), as well as for the maintenance of the pool of ribonucleotides that have to be available for incorporation in newly synthesized molecules. It is, thus, essential to have the mechanisms for mRNA degradation under strict control (Laalami *et al.*, 2014). However, the only way of efficiently regulating the degradation of mRNA is to control the steps for the initial cleavage, which commits the molecule to decay (Górna *et al.*, 2012). There are three theoretical ways of initiating the degradation of the mRNA molecules: an endonucleolytic cleavage or an exonucleolytic cleavage from the 5' or 3' end (Laalami *et al.*, 2014) (Figure 1). The decay of mRNA has been extensively studied especially in the Gram-negative model organism *E. coli*, where the processes and enzymes involved are well characterized (Carpousis, 2002; Marcaida *et al.*, 2006; Bandyra *et al.*, 2013). For many years it was assumed that these mechanisms and enzymes for mRNA degradation in other bacteria would be very similar to the ones previously described for *E. coli* (Deutscher, 2015). Surprisingly, new functional studies as well as the sequencing of the whole genome of the Gram-positive model organism *Bacillus subtilis* (Kunst *et al.*, 1997) proved that what was known for the Gram-negative could not be fully extended to *B. subtilis* (Deutscher, 2015). The study of the mechanisms for the decay of mRNA in *B. subtilis* revealed major differences in the enzymes taking part in this process (Górna *et al.*, 2012; Deutscher, 2015). The search for homologues of the known enzymes was not fruitful, and it seemed that, while the processes were conserved, the players were not (Laalami *et al.*, 2013; Bandyra *et al.*, 2013).

1.2. mRNA turnover in *Escherichia coli*

The pathways for the degradation of mRNA in bacteria have been studied for many years and continue to be extensively studied. Almost every year a review is published that gathers the recent discoveries on the topic (Condon, 2007; Arraiano *et al.*, 2010; Condon and Bechhofer, 2011; Bechhofer, 2011; Lehnik-Habrink *et al.*, 2012; Laalami *et al.*, 2014; Hui *et al.*, 2014; Deutscher, 2015; Mohanty and Kushner, 2016). The decay of mRNA has been mostly studied in the Gram-negative model organism *E. coli*. It is generally accepted that the degradation of the mRNA can occur following two different pathways: the direct entry pathway and the 5' end-dependent pathway. In the direct entry, the transcript, protected with a triphosphate at the 5' end is attacked by a single endonucleolytic cut by the endonuclease RNase E. Subsequently, the

two fragments that are released are differentially processed. The upstream fragment is degraded by 3'-5' exonucleases, like RNase II, PNPase or RNase R. The downstream fragment, unprotected of the 5' triphosphate, can now be recognized by the 5' sensor of RNase E. The 5' end is bound in a pocket of RNase E and the fragment is cleaved several times, releasing fragments that are degraded by 3'-5' endonucleases. The small fragments that are released are then further degraded to monomers by the oligoribonuclease, restoring like this the pool of ribonucleotides. The second pathway depends on the phosphorylation of the 5' end. The pyrophosphohydrolase RppH is responsible for cleaving the 5' triphosphate structure that protects the transcript. Once the 5' is unprotected, the RNase E is able to bind the transcript and perform several cleavages, releasing several fragments that are degraded by 3'-5' exonucleases as described above. In the case of secondary structures, the transcript can be polyadenylated by a poly(A) polymerase, allowing the 3'-5' exoribonucleases to re-engage until the fragments have been processed to ribonucleotides. Furthermore, the RNA helicases can help in the process of degrading fragments with secondary structures. A general overview of the process can be seen in Figure 1.

It can be appreciated that the decay of mRNA transcripts is not dependent on one single enzyme, but is a collaboration of several activities. Interestingly, it has been shown for *E. coli* and other prokaryotes that the RNases associate with other RNA-related activities to form active complexes, the RNA degradosome. The RNA degradosome of *E. coli* is described below.

1.3. The RNA degradosome in *Escherichia coli*

The RNA degradosome is a multi-enzyme complex formed by RNA-related proteins and whose function is the processing and degradation of RNA. The complex is formed around a central endonuclease, RNase E, which interacts with the 3'-5' exoribonuclease PNPase (Carpousis *et al.*, 1994; Braun *et al.*, 1996), the DEAD-box RNA helicase RhlB (Py *et al.*, 1996), and the glycolytic enzyme enolase (Miczak *et al.*, 1996; Py *et al.*, 1996). The complex exists associated to the membrane through the N-terminal domain of the RNase E (Liou *et al.*, 2001; Strahl *et al.*, 2015). Furthermore, the complex has been reconstituted *in vitro* (RNase E, PNPase, and RhlB), where it forms spontaneously and is active as the native complex (Coburn *et al.*, 1999). The complex with its four subunits could also be reconstituted by another group (Worrall *et al.*, 2008). Moreover, the interactions of the proteins within the RNA degradosome have also been studied *in vivo* and the distances between subunits could be measured by fluorescence microscopy (Domínguez-Malfavón *et al.*, 2013). Interestingly, the complex has also been shown associated to the RNase II (Lu and Taghbalout, 2014) and the chaperone DnaK (Miczak *et al.*, 1996), although the latter interaction seems to occur when the degradosome forms abnormally under stressful conditions

(Regonesi *et al.*, 2006). This, however, shows that the complex can interact with more proteins in a dynamic manner. A general study of these interaction partners was performed by proteomics and several partners could be identified for the wild type degradosome (Mauri and Dehò, 2008). The role of this minor interactions and their relevance was assessed by Kaberdin and Lin-Chao, 2009. A study of the function of the RNA degradosome *in vivo* found out that the four integral members of the complex are necessary for proper mRNA turnover in *E. coli* but that the complex acted upon some specific transcripts while others were not affected. It was proposed that there are structural or biochemical determinants that selectively target some transcripts over other (Bernstein *et al.*, 2004).

The individual proteins of the RNA degradosome are described below.

1.3.1. The RNase E of *E. coli*

The endoribonuclease RNase E belongs to the RNase E/G family, which is present throughout the bacterial domain (proteobacteria, actinobacteria, firmicutes, and in some cyanobacteria). RNase E is the central endoribonuclease. It does not only affect the global RNA stability and decay, but is responsible for the processing of RNA precursors of rRNA (Apirion, 1978; Roy and Apirion, 1983; Bouvet and Belasco, 1992; Ow and Kushner, 2002). It was discovered as the enzyme responsible for the cleavage between the 26S and the 5S, although the gene could only be later identified (Apirion, 1978). Interestingly, the gene *rne* turned out to be identical to the *ams* (<u>a</u>ltered <u>m</u>RNA <u>s</u>tability), the long-time known responsible for the global altered stability of the mRNAs (Mudd *et al.*, 1990; Taraseviciene *et al.*, 1991). Although RNase E shows no sequence specificity for its cleavages, it preferentially cuts in A/U-rich unpaired regions (Bouvet and Belasco, 1992; Carpousis, 2007). Furthermore, it is sensitive to the phosphorylation state of the 5' end, cutting preferentially when the 5' is monophosphorylated (Mackie, 1998).

The enzyme is divided into two major domains: the N-terminal or catalytic domain, and the C-terminal or scaffolding domain (Figure 2). The crystal structure of the N-terminal domain is available, and it has shed some light on the preferences of the enzyme for its cleavage (Callaghan *et al.*, 2005a; Koslover *et al.*, 2008). Furthermore, this catalytic domain is responsible for the tetramerization of the enzyme. For this oligomerization and for the functionality of the catalytic domain, the protein must be bound to zinc and magnesium ions (Callaghan *et al.*, 2005b). The C-terminal domain is predominantly disordered, and it harbours several micro-domains, that interact with the members of the RNA degradosome: enolase, RhlB, and PNPase (Callaghan *et al.*, 2004; Bouvier and Carpousis, 2011). It also contains two RNA-binding domains (Taraseviciene *et al.*, 1995; Leroy *et al.*, 2002) and an amphipathic α-helical membrane domain that associates the

multi-protein complex to the cell membrane (Khemici *et al.*, 2005; Khemici *et al.*, 2008; Strahl *et al.*, 2015). This helix is conserved in homologues of RNase E of β- and γ-proteobacteria, and its deletion causes slow growth in *E. coli* (Khemici *et al.*, 2008; Aït-Bara *et al.*, 2014).
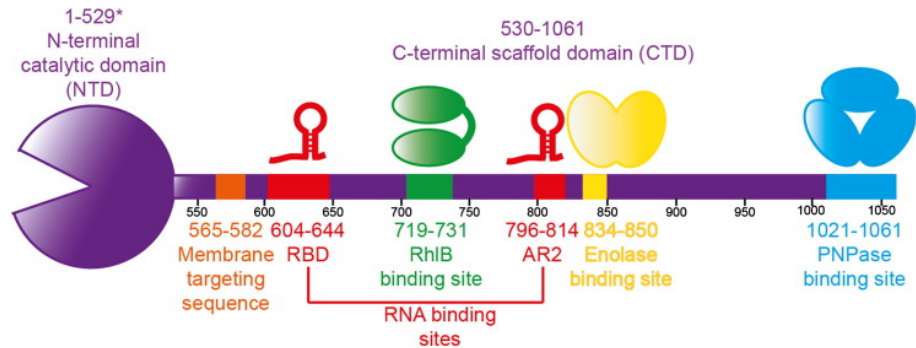
Figure 2. **Domain organization of the endoribonuclease RNase E.** From Bandyra *et al.*, 2013. RNase E possesses tow distinct domains: the catalytic N-terminal domain and the unstructured C-terminal domain. The catalytic domain contains the active site and allows the enzyme to tetramerize, as a dimer of dimers. The unstructured C-terminal domain contains several micro-domains, and serves as a scaffold for interacting proteins of the RNA degradosome. The canonical interaction partners Rhlb, PNPase, and enolase are depicted. Furthermore, the C-terminal domain contains two RNA binding sites (red) and an amphipathic α-helix that associates the enzyme to the membrane (orange).

1.3.2. RhlB, a DEAD-box RNA helicase of *E. coli*

RhlB is an ATP-dependent RNA helicase that belongs to the DEAD-box RNA helicase family (Kalman *et al.*, 1991), and it is one of 5 members of this family present in *E. coli* (Worrall *et al.*, 2007). RhlB is, however, the only helicase to have been found associated with the RNA degradosome. The presence of an RNA helicase within this RNA-degrading complex suggests that it is necessary for the proper degradation of structured RNA by the exo- and endonucleases, PNPase and RNase E (Py *et al.*, 1996). In the degradosome, RhlB interacts with the essential scaffolding protein RNase E. This interaction is necessary for the activity of RhlB, and increases the ATPase activity of RhlB by an order of magnitude (Chandran *et al.*, 2007; Worrall *et al.*, 2007). Furthermore, it has been seen that RraA, a regulator protein of *E. coli*, binds RhlB and RNase E, inhibiting the activity of the helicase and, indirectly, the activity of PNPase in the complex (Górna *et al.*, 2010; Pietras *et al.*, 2013). However, several reports suggest that a mini-degradosome can be formed by the polynucleotide phosphorylase PNPase and the helicase RhlB. It was shown that RhlB interacts with PNPase *in vivo* and *in vitro*, but not with enolase, another member of the degradosome. The RhlB-PNPase complex is also active, without the interaction to RNase E (Liou *et al.*, 2002). Furthermore, it was proved that a loss of interaction between RhlB and PNPase but not of RhlB with RNase E greatly affects the expression of genes involved in the cysteine metabolism, and increases the response to oxidative stress (Tseng *et al.*, 2015). These studies confirm that

RhlB and PNPase can be active on their own and not necessarily being part of the RNase E-based RNA degradosome.

For extensive reviews on DEAD-box RNA helicases in RNA degradosomes and involved in RNA metabolism consult (Carpousis *et al.*, 2008; Hardwick and Luisi, 2013).

1.3.3. The glycolytic enzyme enolase of *E. coli*

Enolase is a metallo-enzyme that catalyses the conversion of 2-phosphoglycerate into phosphoenolpyruvate, in the penultimate step of glycolysis. It is universally conserved and present in the three domains of life, as is glycolysis. Although the enolase of *E. coli* has been characterized for many decades (Spring and Wold, 1971), the knowledge of its relationship with RNA metabolism is more recent (Miczak *et al.*, 1996). Enolase is part of a multi-protein RNA-degrading machine, the RNA degradosome, and interacts directly with the core of the complex, RNase E (Chandran and Luisi, 2006). Although the presence of enolase within this complex has been known for a number of years (Miczak *et al.*, 1996), the function of the glycolytic enzyme in such remains obscure. It is known, however, that the interaction of enolase with the degradosome is essential for the degradation of the glucose transporter mRNA *ptsG* under conditions of phosphosugar stress (Morita *et al.*, 2004) and that the disruption of its interaction with RNase E affects the global mRNA turnover in *E. coli* (Bernstein *et al.*, 2004). Nonetheless, it is yet unclear what is the role of the enzyme in the degradation of mRNA. It has been proposed that enolase could have a structural or allosteric role within the degradosome, connecting the RNA degradation with the central carbon metabolism pathways (Kühnel and Luisi, 2001). It has been shown, however, that a reconstitution *in vitro* of the RNA degradosome without the presence of enolase possesses activity like a wild type degradosome (Coburn *et al.*, 1999).

1.3.4. Polyribonucleotide phosphorylase of *E. coli*

Polyribonucleotide phosphorylase (PNPase) was first identified as an RNA polymerase. The studies on PNPase from *Azotobacter vinelandii* granted in 1959 the Nobel Prize in Physiology or Medicine to Severo Ochoa, shared with Arthur Kornberg, *"for their discovery of the mechanisms in the biological synthesis of ribonucleic acid and deoxyribonucleic acid"*. Many studies were performed in the following decades to elucidate the mechanism of action and regulation of the protein *in vitro*. The results from these studies have been reviewed by Littauer and Grunberg-Manago in 1999. The enzyme requires magnesium and catalyses the phosphorolytic cleavage of RNA molecules utilizing inorganic phosphate (Pi). This reaction is reversible, and thus the enzyme can use NDPs to synthesize RNA, releasing a Pi moiety (see Figure 3). In 1963, it was first

discovered to play a role in the degradation of an mRNA from *E. coli* (Andoh *et al.*, 1963; Sekiguchi and Cohen, 1963). This required Pi, which was calculated to be in the cell at a concentration of 30 mм (Andoh *et al.*, 1963). PNPase is a 3'-5' exoribonuclease, which means that it degrades RNA from the 3' end. In *E. coli*, a second 3'-5' exoribonuclease exists, RNase II, which also catalyzes the degradation of RNA molecules, although in a hydrolytic manner. Interestingly, it was shown that 90% of the RNA degradation in *E. coli* was performed hydrolytically, making PNPase not likely a major player in the RNA turnover in this organism (Deutscher and Reuven, 1991). Furthermore, studies of both RNases *in vivo* showed that the activity of neither of these enzymes could participate in the rate-limiting step of RNA degradation (Belasco and Higgins, 1988). It was later proposed that the enzyme responsible for the rate-determining step of RNA decay was the newly discovered endoribonuclease, RNase E (Babitzke and Kushner, 1991).
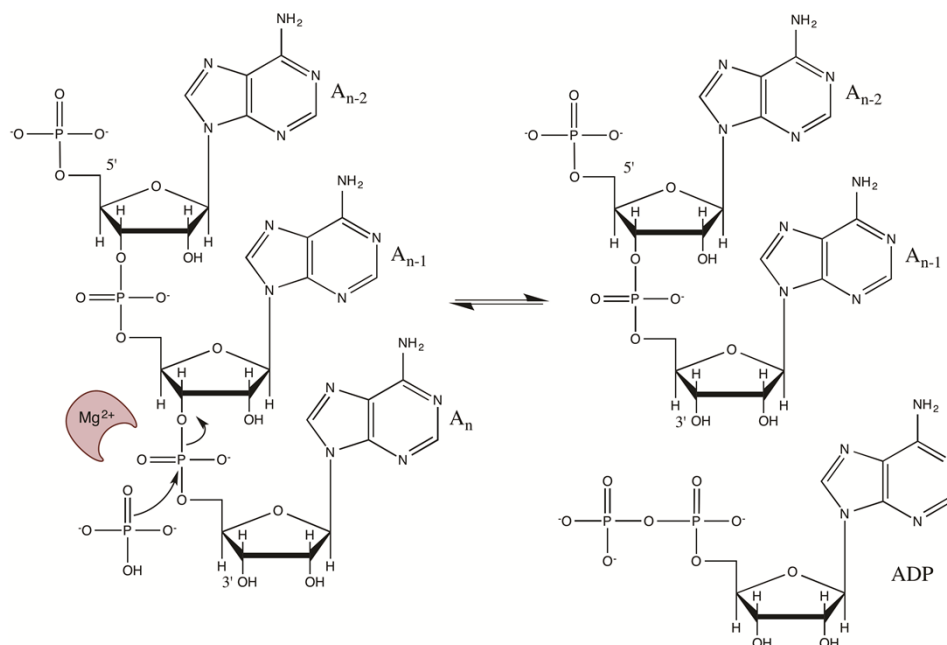
Figure 3.   **Reaction catalysed by PnpA. PNPase catalyses the reversible reaction of phosphorolytic cleavage of RNA.** The enzyme needs a divalent cation as cofactor (Mg^{2+} or Mn^{2+}, for example) and inorganic phosphate to produce a nucleophilic attack on the RNA strand. As a result, one molecule of NDP is produced and the RNA molecule is shortened by one monomer. In the appropriate conditions the enzyme can elongate an RNA molecule by incorporating NDPs and releasing inorganic phosphate.

Further studies were performed to elucidate the role of this enzyme *in vivo.* It was shown that polyadenylation was required for the processive degradation by PNPase (Xu and Cohen, 1995). Moreover, even though the responsible enzymes (PAPI and PAPII) for polyadenylation in *E. coli* had been identified (Sarkar, 1997), it was discovered that PNPase possessed poly(A)polymerase activity (Mohanty and Kushner, 2000), that could account for the residual polyadenylation in the absence of the PAPs. Interestingly, the PNPase from spinach chloroplasts could also function as

exonuclease and poly(A) polymerase (Yehudai-Resheff *et al.*, 2001). It was later demonstrated, however, that the polymerization activity of PNPase in *E. coli* is not relevant *in vivo* (Jarrige *et al.*, 2002). Furthermore, it was discovered that PNPase was necessary for the survival of the organism at cold temperatures, and that the exonucleolytic function and not the polymerization activity was critical in these conditions (Matus-Ortega *et al.*, 2007; Awano *et al.*, 2008). Although PNPase has a clear and important role in the RNA metabolism, it is obvious that, since others can replace the activity of the enzyme within the cell, PNPase is yet another player in the complex picture of RNA degradation. Interestingly, the enzyme has been shown to be regulated by several metabolites and signalling molecules such as ATP (Del Favero *et al.*, 2008), citrate (Nurmohamed *et al.*, 2011), and c-di-GMP (Tuckerman *et al.*, 2011). The regulation of an RNA-degrading enzyme by such molecules raises interesting questions regarding the relationship between RNA processing and other cellular pathways.

PNPase is also involved in DNA metabolism, as it takes part in DNA repair after damage. It participates in nucleotide excision repair after UV damage (Rath *et al.*, 2012) and it is involved in the protection against oxidative stress (Wu *et al.*, 2009). Furthermore, it has been proved to be involved in the quality control of precursors for rRNA (Cheng and Deutscher, 2003).

The crystal structure of PNPase has been obtained (Shi *et al.*, 2008; Nurmohamed *et al.*, 2009). The enzyme presents a trimeric, ring-like structure, as was reported for enzymes from other organisms in previous studies (Portier, 1975a; Portier, 1975b; Symmons *et al.*, 2000; Jarrige *et al.*, 2002; Symmons *et al.*, 2002). The central channel enclosed by the trimeric structure could be a means for the access of the RNA molecules to the active site of the enzyme. A close-up of the structure pointed to a role of the helical domain in catalytic activity, and unravelled the residues participating in the coordination of divalent metal ions, which are conserved amongst PNPases (Nurmohamed *et al.*, 2009). PNPase has a subdomain organization composed of two RNase PH-like sub-domains, surrounding an α-helical domain (Shi *et al.*, 2008). Crystallographic studies in *Streptomyces antibioticus* suggest that only the most C-terminal PH domain is catalytically active (Symmons *et al.*, 2000). At the C-terminal end the protein contains two RNA-binding domains KH and S1. They have been proposed to be the RNA binding surface that confers processivity to the enzyme (Jarrige *et al.*, 2002; Stickney *et al.*, 2005), but they do not participate in the catalysis (Stickney *et al.*, 2005; Briani *et al.*, 2007). A study of 55 sequences of bacterial PNPases has shown that the protein is highly conserved, except the α-helical domain (Bermúdez-Cruz *et al.*, 2005).

PNPase from *E. coli* has been shown to interact with several proteins *in vivo*. It was first identified to be present in the ribosomal fraction when this was isolated (Wade and Lovett, 1961). Moreover, it is part of a multi-protein RNA-degrading complex, the RNA degradosome. In the RNA degradosome, PNPase is bound to a characterized micro-domain in the C-terminal domain of

RNase E (Vanzo *et al.*, 1998), the central endoribonuclease of the RNA degradosome (see 1.3.1). The crystal structure of the *E. coli* PNPase has been solved bound to the aforementioned micro-domain of RNase E (Nurmohamed *et al.*, 2009). This complex comprises the central endoribonuclease RNase E, the DEAD-box RNA helicase RhlB, the glycolytic enzyme enolase, and the exoribonuclease PNPase (see 1.3). Furthermore, it has been reported that PNPase and the RNA helicase RhlB can interact *in vivo* independent of RNase E (Liou *et al.*, 2002).

An extensive review on the regulation, expression, structure and activity of different PNPases of prokaryotes was recently published (Briani *et al.*, 2016).

1.4. mRNA turnover in *Bacillus subtilis*

Although the pathways for the degradation of mRNA in *B. subtilis* have been extensively studied, many question marks remain. The mechanisms are very similar to those of the Gram-negative *E. coli*, however, the players are not well conserved (see 1.2). As for *E. coli*, the transcripts can be degraded in two pathways, the direct entry and the 5' end-dependent pathway. In the direct entry a first endonucleolytic cleavage is performed that commits the transcript to degradation, being the rate-limiting step. It is performed by RNase Y, although it can, in a lesser extent be performed by the RNases J1/J2 or another endonuclease (Laalami *et al.*, 2014). Consequently, two fragments are released. The upstream fragment is degraded by the 3'-5' exonuclease polynucleotide phosphorylase (PnpA); the downstream fragment is degraded by the 5'-3' exonuclease RNase J1/J2. The latter was the first enzyme to be found that could degrade RNA in the 5'-3' direction in prokaryotes (Mathy *et al.*, 2007). Alternatively, the protection of the triphosphate at the 5' end can be removed by a pyrophosphohydrolase (RppH 1 or 2). Subsequently, the transcript is sensitive to be attacked by the exonuclease activity of RNase J1/J2. However, RNase J1/J2 has also been shown to cut endonucleolytically close to the 5' end. Furthermore, RNase Y preferentially cuts RNAs with a monophosphorylated 5' end. This translates on a competition between RNase Y and both activities of RNase J1/J2 for the degradation of the unprotected transcript (Laalami *et al.*, 2014). The smaller fragments generated by the consecutive action of several RNases are further degraded to ribonucleotides by oligoribonucleotides. Interestingly, no poly(A) polymerase has been identified in *B subtilis.* However, there is evidence that the intermediates of degradation are polyadenylated. It is not clear, nonetheless, whether the polyadenylation is this organism contributed to the degradation of structured mRNAs. The existence of RNA helicases may be critical for the degradation of highly structures transcripts. A simplified overview of the degradation of mRNAs in bacteria is depicted in Figure 1.

As for *E. coli*, many of the RNases and RNA-related proteins have been shown to interact amongst each other, in a putative RNA degradosome (see 1.3)*. These interactions and their relevance are described below.

1.5. The RNA degradosome of *Bacillus subtilis*

To increment the effectivity of a pathway, proteins can arrange in multi-enzyme complexes. Many of the activities that in *B. subtilis* take part in the degradation of RNA have been shown to interact amongst each other. They have been proposed to form an RNA-degrading complex, similar to the well-studied RNA degradosome of *E. coli* (see 1.3).
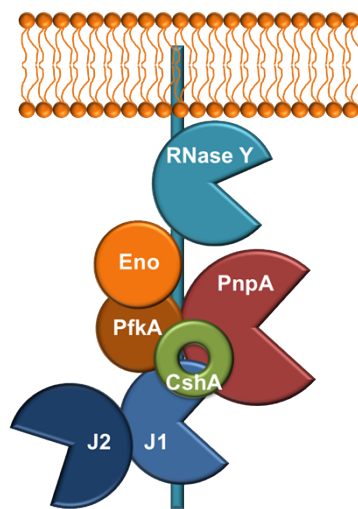
Figure 4.   **RNA degradosome of *Bacillus subtilis*.** Interaction of proteins to form the RNA-degrading machine, the degradosome, following experiments from Commichau *et al.*, 2009 and Lehnik-Habrink *et al.*, 2010. RNase Y is the protein that attaches the complex to the membrane through its N-terminal membrane domain. The rest of the proteins interact amongst each other and with RNase Y at its scaffolding C-terminal unstructured domain.

The interactions were initially found by bacterial two-hybrid (B2H), as binary protein-protein interactions (Commichau *et al.*, 2009). The model for the degradosome represented in Figure 4, is a complex of the exonuclease PNPase, the RNases J1 and J2, and the glycolytic enzymes enolase and PfkA, interacting with the unstructured C-terminal domain of RNase Y. RNase Y serves as a scaffolding protein, that attaches the putative RNA degradosome to the cell membrane thanks to its membrane-spanning α-helix at its N-terminal end (see 1.5.1). CshA was later identified as the DEAD-box RNA-helicase attached to the complex, as an analogy to RhlB in the *E. coli* RNA degradosome. Interestingly, among these RNA-related enzymes two glycolytic enzymes could be found, enolase and phosphofructokinase (PfkA or PFK). This is the case as well for enolase in the *E. coli* RNA degradosome. The interactions could later be reproduced by crosslinking *in vivo* pull-

down experiments (Lehnik-Habrink *et al.*, 2011a). Some of the binary interactions could also be analysed *in vitro* (enolase-RNase Y and PNPase-RNase Y), although some could no be detected (PfkA-PNPase, PfkA-RNase J1, and RNase J1-RNase Y) (Newman *et al.*, 2012). Furthermore, the interaction of PNPase and RNase Y could be reproduced *in vivo* by a different group (Salvo *et al.*, 2016). However, the existence of this complex in *B. subtilis* is still under debate, since it could never be isolated as a whole. Furthermore, *in vivo* pull-down experiments of RNase J1 indicate that RNase J2 is most likely the major interacting protein, forming a complex of their own (Mathy *et al.*, 2010), with no sign of additional interactions.

1.5.1. RNase Y

RNase Y is encoded in *B. subtilis* by the gene *ymdA*, later re-named to *rny* (Commichau *et al.*, 2009). The protein is an endoribonuclease that not only is involved in the processing of many individual transcripts (Commichau *et al.*, 2009; Shahbabian *et al.*, 2009; Lehnik-Habrink *et al.*, 2011b; Noone *et al.*, 2014), but also is of great importance for the general mRNA decay in this organism (Durand *et al.*, 2012; Laalami *et al.*, 2013). RNase Y is, however, sensitive to the phosphorylation state of the transcript, and it is not able to cut endonucleolytically when the 5' is triphosphorylated (Shahbabian *et al.*, 2009). RNase Y is highly conserved in bacteria, especially in firmicutes. In the bacterial groups that do not contain a homologue of RNase Y it is likely to find a member of the E/G or the J RNases, although some exceptions exist that contain none of these known RNases (Commichau *et al.*, 2009).

RNase Y has been shown to play an important role in global mRNA decay in *B. subtilis.* There is evidence that this enzyme is responsible for the initial step, the rate-limiting step, of the decay, and that a depletion affects the expression of 25% of the genome (Durand *et al.*, 2012). In other studies, however, the effect of the depletion of RNase Y seems to be not as strong. Moreover, among the transcripts found to be affected in both studies, only 10% overlap (Laalami *et al.*, 2013). It seems that the level of depletion and the conditions in which the experiments are performed highly affect the outcome. Furthermore, similar studies with the depletion of RNase J1, that also possesses endonuclease activity, show that this enzyme also greatly affects the global mRNA decay. Therefore, the possibility of RNase J1 being responsible for the initial step of mRNA decay cannot be completely excluded (Durand *et al.*, 2012). Interestingly, it has been shown that RNase Y plays a role in biofilm formation (Lehnik-Habrink *et al.*, 2011b; Lehnik-Habrink *et al.*, 2011a). The *rny* gene is encoded in a bi-cistronic operon with *ymdB*, a gene encoding a phosphodiesterase that is involved in bi-stability and biofilm formation in *B. subtilis* (Diethmaier *et al.*, 2011).

Since the discovery of the enzyme it has been thought that the enzyme was essential, meaning it cannot be deleted from the genome (Hunt *et al.*, 2006; Commichau *et al.*, 2009; Shahbabian *et al.*, 2009; Lehnik-Habrink *et al.*, 2011b). Indeed, the depletion of the enzyme caused a strong phenotype with slower growth, elongated and anucleate cells and mini-cells. In 2013, the gene could, however, be completely knocked-out of the genome, showing an even more severe phenotype. The mutant strain is defective in competence and sporulation, hypersensitive to antibiotics and shows strong defects in cell morphology (Figaro *et al.*, 2013).
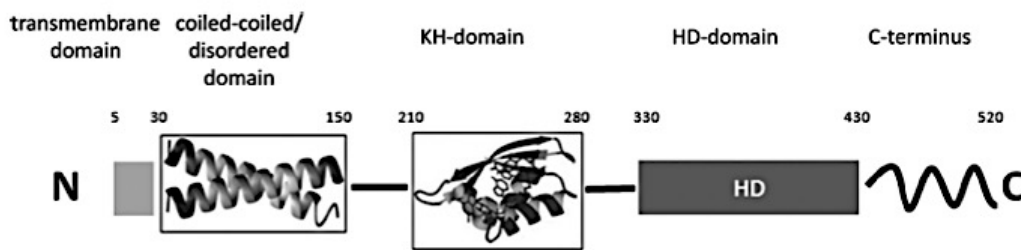
Figure 5.   **Domain organization of the RNase Y endoribonuclease.** From Lehnik-Habrink *et al.*, 2011a. RNase Y is composed of five domains. From N-terminal to C-terminal: membrane-spanning α-helix, coil-coiled of unknown function, KH domain for RNA binding, HD domain with the active site and unstructured C-terminal domain of unknown function.

Structurally, the enzyme is composed of several domains (see Figure 5). It possesses a HD domain (His Asp) that is responsible for the enzymatic catalysis. This domain is highly conserved in the superfamily of metal-dependent phosphohydrolases (Aravind and Koonin, 1998). Indeed, it has been shown that the enzyme requires magnesium to perform the catalytic activity, although it can be replaced by manganese and zinc ions (Shahbabian *et al.*, 2009). Furthermore, it contains a KH domain (ribonucleoprotein K homology) that is the RNA-binding domain and is typically found in RNases (Aravind and Koonin, 2001). Additionally, it contains two domains of unknown function, the coil-coiled domain and the unstructured but conserved C-terminal domain (Lehnik-Habrink *et al.*, 2011a). A membrane-spanning α-helix is found at the N-terminal end of the protein (Shahbabian *et al.*, 2009; Lehnik-Habrink *et al.*, 2011a). This membrane anchor is fundamental to the enzyme. Releasing RNase Y from the membrane results in reduced viability and hindered protein-protein interactions (Lehnik-Habrink *et al.*, 2011a). Interestingly, it was recently found that in the Gram-positive *Staphylococcus aureus* the membrane localization of RNase Y is essential for growth. Furthermore, the membrane-anchor seems to be necessary to bring related proteins to the proximity of the membrane (Khemici *et al.*, 2015). Furthermore, the localization pattern at the membrane is influenced by the dissipation of the membrane potential (Strahl *et al.*, 2014).

In *B. subtilis*, RNase has been found to interact with several proteins from the RNA metabolism as well as from the carbon metabolism, namely glycolysis (Commichau *et al.*, 2009). Indeed, it has been proposed as a scaffold for RNA-related proteins in a degradosome-like complex. The interactions involved in the formation of this RNA-degrading machine have been previously described (see 1.5).

1.5.2. Enolase and phosphofructokinase in *B. subtilis*

Enolase and phosphofructokinase (PFK) are enzymes from the glycolysis, a pathway that is conserved amongst bacteria, eukaryotes and archaea. Furthermore, enolase is one of the few enzymes that is universally conserved (Commichau *et al.*, 2009). The essentiality of these enzymes has been an extensive field of study. Enolase has been reported as essential (Kobayashi *et al.*, 2003) although the *eno* gene, could also be deleted in several studies (Leyva-Vazquez and Setlow, 1994; Commichau *et al.*, 2013). The mutant is, however, not able to grow in LB complex medium. PFK was also considered essential for many years (Kobayashi *et al.*, 2003) although deletion mutants have been isolated, with slower growth in sporulation medium or minimal media with glucose as a single carbon source (Muñoz-Márquez and Ponce-Rivas, 2010; Commichau *et al.*, 2013). Even though some results seem contradictory, it is important to consider that, as metabolic enzymes, the growth media and the conditions in which the mutants were obtained greatly influence the possibility of deleting their respective genes.

Enolase and PFK have, interestingly, been associated with the RNA-degrading machinery in *B. subtilis.* This is of great importance, since enolase is an integral member of the *E. coli* RNA degradosome (see 1.3.3). Enolase has been shown to interact *in vivo* by bacterial two-hybrid assays (B2H) and crosslinking with RNase Y and the RNA helicase CshA (Commichau *et al.*, 2009; Lehnik-Habrink *et al.*, 2010; Lehnik-Habrink *et al.*, 2011a). PFK has been shown in the same experiments with CshA, RNase Y, PNPase and RNase J1 (Commichau *et al.*, 2009; Lehnik-Habrink *et al.*, 2010; Lehnik-Habrink *et al.*, 2011a). However, the interaction between PFK and PNPase, and PFK and RNase J1 could not be confirmed *in vitro*, unlike the interaction enolase-RNase Y, that was confirmed by surface-plasmon resonance (SPR) (Newman *et al.*, 2012).

1.5.3. CshA, a DEAD-box helicase of *B. subtilis*

CshA in encoded by the *ydbR* gene, later renamed to *cshA* (cold shock helicase-like protein A) (Hunger *et al.*, 2006). It has been characterized as an ATP-dependent RNA binding protein, with RNA-dependent ATPase activity (Ando and Nakamura, 2006) that is able to destabilize RNA duplexes (Hunger *et al.*, 2006). Furthermore, it is one out of four members of the DEAD-box RNA

helicase family, present in *B. subtilis* (Redder and Linder, 2012). The expression of *cshA* is increased 2.6-fold as a response to cold shock, and it has been related to the cold-shock proteins (CSPs) (Beckering *et al.*, 2002; Hunger *et al.*, 2006). Furthermore, the deletion of this gene leads to growth defect and altered morphology at temperatures under 22°C (Ando and Nakamura, 2006; Lehnik-Habrink *et al.*, 2013). Another group, however, could not see a cold sensitivity in the mutant (Hunger *et al.*, 2006). CshA has been shown to be the most abundant helicase in *B. subtilis* and to be able to interact with ribosomal proteins. Interestingly, the protein is located to the same area as the ribosomes (Hunger *et al.*, 2006), and its deletion leads to a defect in ribosome biosynthesis, as shown by a reduced number of them within the cell (Lehnik-Habrink *et al.*, 2013). Moreover, CshA has been proposed as the functional homologue of RhlB in *E. coli* as it is able to interact with several RNases, in a putative RNA degradosome (Lehnik-Habrink *et al.*, 2010). The C-terminal domain of CshA is necessary for interaction with these proteins and for its own dimerization. It can interact *in vivo* under crosslinking conditions with RNase Y, PNPase, the glycolytic enzymes enolase and PfkA and RNase J1. Furthermore, it was shown by differential centrifugation that CshA is mostly attached to the membrane fraction (Lehnik-Habrink *et al.*, 2010).

1.5.4. The polynucleotide phosphorylase of *B. subtilis*

Polynucleotide phosphorylase, or PNPase in *B. subtilis,* is a 3' to 5' exoribonuclease that catalyses the phosphorolytic attack on RNA, releasing a molecule of NDP. Moreover, the reaction is reversible and the enzyme is able to polymerize RNA, liberating a molecule of inorganic phosphate. It is encoded by the *pnpA* gene, formerly *comR* (it is involved in the expression of late competence genes (Luttinger *et al.*, 1996). The enzyme is 50% identical and 67% similar to the homologue of *E.coli*. Interestingly, the global mRNA decay in *B. subtilis* is mostly depending on a phosphorolytic activity, in contrast to *E. coli* that relies on a hydrolytic RNA degradation (Deutscher and Reuven, 1991). It is, therefore, likely that the PNPase in *B. subtilis* is one of the major activities in RNA metabolism. It has been speculated, however, that this effect could be artifactual, since the exonucleolytic activity of the, by the time unknown, RNase J1/J2 (see 1.5.5) could have been overlooked by using a 5' triphosphorylated transcript (Laalami *et al.*, 2014). This would explain why the deletion of PNPase is not only viable but does not show a strong general effect on the gene expression (Luttinger *et al.*, 1996). Nonetheless, a deletion strain of PNPase presents reduced competence, elongated filamentous cells and cold-sensitivity at 16°C and 23°C (Luttinger *et al.*, 1996), but shows a relatively normal growth in other conditions (Wang and Bechhofer, 1996). The phenotype of long chained cells could be explained by a decrease in the

expression of sigma D and the effect on the downstream genes (Liu *et al.*, 2014). The enzyme was first confirmed as a polynucleotide phosphorylase upon *in vitro* activity assays, where it was able to cleave single-stranded RNA dependent on Pi (Mitra *et al.*, 1996). Furthermore, the enzyme shows a similar processing function of the PNPase of *E. coli* (Wang and Bechhofer, 1996). *In vivo* the enzyme is required for the decay of specific transcripts, and can be stalled by secondary structures of the RNA (Bechhofer and Wang, 1998; Farr *et al.*, 1999). Moreover, the enzyme has been shown to be involved in DNA metabolism, since it can degrade single-stranded DNA under conditions where manganese is available and the concentration of Pi is low. Interestingly, under high concentrations of Pi, the enzyme preferentially degrades RNA, suggesting a dual function depending on the status of the cell (Cardenas *et al.*, 2009). Since the enzyme catalyses a reversible reaction, its polymerization as well as its degradation activity have been shown to be involved in DNA repair mechanisms, regulated by RecN and RecA, respectively (Cardenas *et al.*, 2011). Furthermore, its polymerization activity has led to the investigation of whether PNPase is the missing poly(A) polymerase of *B. subtilis*, since in *E. coli* PNPase accounts for the residual polyadenylation after deletion of the main PAP (see 1.3.4). However, two activities able to polyadenylate in the absence of PNPase have been found, although they could not be identified (Sarkar *et al.*, 1997). Furthermore, a comparison of polyadenylation in *B. subtilis* in the presence and absence of PNPase proved that the polyadenylation profile was similar in both situations, ruling out the possibility that PNPase is the major poly(A) polymerase of this organism (Campos-Guillén *et al.*, 2005). In the meantime, the enzyme responsible for addition of poly(A) tails in *B. subtilis* remains unknown (Mohanty and Kushner, 2010).

1.5.5. The paralogous RNases J1 and J2

RNase J1 and J2 are two paralogous enzymes with a 49 % sequence identity and 70 % sequence similarity. They are encoded by the genes *rnjA* (*ykqC*) and *rnjB* (*ymfA*), respectively. They were first identified as members of the β-CASP protein family (metallo-β-lactamase-associated CPSF Artemis SNM1/PSO2), as they contain the characteristic β-lactamase and β-CASP domains that name the family. These proteins contain three conserved motifs (A, B, and C) that are necessary for the enzyme's activity and that were predicted to be present in both paralogues, RNase J1 and J2. This family is present in all three domains of life (eukaryota, bacteria, and archaea) and its members are involved in DNA and RNA metabolism. However, all archaeal and bacterial members of this family have only been described to be active on RNA (Callebaut *et al.*, 2002).

RNases J1 and J2 were first identified in *B. subtilis* as functional homologues of the well-studied endoribonuclease RNase E from *E. coli*, since they were able to cleave the *thrS* leader sequence from *B. subtilis* at the same place where RNase E can also process it. This discovery was a breakthrough because RNases J1 and J2 were the first proteins from the β-CASP family from prokaryotes demonstrated to take part on the RNA metabolism (Even *et al.*, 2005). Furthermore, these enzymes seemed to have sensitivity to the phosphorylation state of the 5' end of the transcript, showing a preference for monophosphorylated over triphosphorylated substrates. Interestingly, RNase J2 has an unexpected substitution in the conserved motif C, that seems to not affect its endoribonucleolytic activity (Even *et al.*, 2005). Further studies implicated RNase J1 in the maturation of the 5' end of the 16S rRNA form *B. subtilis* (Britton *et al.*, 2007; Mathy *et al.*, 2007) but it was discovered that this processing occurred 5'-3' exonucleolytically (Mathy *et al.*, 2007). This was a major discovery since this activity had never been seen in prokaryotes and it was thought to only exist in eukaryotes. This activity seemed to be sensitive to the phosphorylation state of the 5' end, and was also present in RNase J2, although much weaker: RNase J2 had a 100 times lower catalytic constant that RNase J1/J2 (Mathy *et al.*, 2010). Since the first discovery of these enzymes, they have been shown to affect the expression of many transcripts. RNase J1 was proven to be responsible for the degradation of the destabilized *glmS* mRNA after metabolite-induced ribozyme-dependent self-cleavage (Collins *et al.*, 2007). It was also shown to endonucleolytically process the *ermC* mRNA (Yao *et al.*, 2008) although the 5'-3' exoribonucleolytic activity of RNase J1 could also take part in this degradation (Yao *et al.*, 2009). Furthermore, RNase J1 was found to be responsible for the turnover of the *trp* leader RNA, which was processed both endo- and exonucleolytically (Deikus and Bechhofer, 2007; Deikus *et al.*, 2008; Deikus and Bechhofer, 2011) and of the *hbs* transcript (Daou-Chabo *et al.*, 2009). Moreover, RNase J1 is responsible for the decay of the RNAs from the toxin/antitoxin systems *bsrE/SR5* and *bsrG/SR4* in *B. subtilis* (Müller *et al.*, 2016; Jahn and Brantl, 2016)*.* Although these enzymes affected many individual transcripts, the complete picture of their activity in the cell was missing. A proteome and transcriptome analysis performed on the single and double mutants showed that a great amount of transcripts were affected by the lack of the enzymes, but much more in the double mutant than in the single mutants (Mäder *et al.*, 2008). A deeper analysis of individual transcripts confirmed the -omics analysis. Moreover, an analysis by tiling microarrays was performed that demonstrated that 25 to 30 % of the transcripts in the cell were affected by a more than 30-fold depletion of RNase J1 (Durand *et al.*, 2012).

RNase J1 was described as essential in a study where the essentiality of several genes was evaluated (Hunt *et al.*, 2006). The depletion of this enzyme caused an elongated phenotype and affected distribution of nucleoids, even with the presence of anucleate cells. This phenotype is

similar to a mutant with blocked DNA replication. However, in a more recent study a deletion mutant of RNase J1 was obtained. As was observed for the depletion of RNase J1, the cells were filamentous and curly, although the phenotype could not be rescued by addition of magnesium. This filamentous phenotype could be explained by an 11-fold stabilization of the *mreBH* transcript (Durand *et al.*, 2012). An increase in the expression of MreB has been shown to produce similar spirals in *B. subtilis* (Kawai *et al.*, 2009; Figaro *et al.*, 2013). It also showed other interesting phenotypes like hypersensitivity to antibiotics, cold-sensitivity (even at room temperature), and impaired competence (Figaro *et al.*, 2013). Interestingly, a double RNase J1/J2 mutant was also viable. The deletion of RNase J2 has been shown to increase fitness under low-pressure conditions. An evolutionary experiment under these conditions has also shown a 9-nucleotide in-frame deletion that also confers increased fitness compared with the parental strain (Waters *et al.*, 2015). Although RNase J1 was shown to not be essential, the importance of the enzyme for the cell is undeniable. However, it is still unclear which function of the enzyme is responsible for the severe phenotype of RNase J1 deletion mutant. Both RNase J1 and RNase J2 have endonuclease activity, but the exonuclease activity of RNase J2 is very weak. Since the deletion of RNase J2 shows no clear phenotype it has been proposed that the most important activity is the 5'-3' exonucleolytic (Condon, 2010; Durand *et al.*, 2012). Indeed, a double RNase J1 and PNPase (3'-5' exoribonuclease) mutant was not possible to be obtained (Figaro *et al.*, 2013). This could be explained by a recent discovery that the bacterium relies on the 5'-3' exonuclease activity for the turnover of 3' processing fragments, if such activity is present in the cell (DiChiara *et al.*, 2016). Interestingly, many other β-CASP family members have both activities (Dominski *et al.*, 2013; Clouet-d'Orval *et al.*, 2015) but little is known about how these activities are related. The first crystal structure of an RNase J was obtained from *Thermus thermophilus*, which is 61 % similar to either RNase J1 or J2 (Li de la Sierra-Gallay *et al.*, 2008). The enzyme possessed, as expected, the β-lactamase and β-CASP domains, as well as a C-terminal domain.

The catalytic site was defined by the presence of two zinc ions, coordinated in an octahedral environment. These were located in the cleft between the β-lactamase and the β-CASP domains. However, this depicted one only active site for a dual activity. Nonetheless, the confirmation that the active site was responsible for both activities was confirmed by the mutation of the amino acids responsible for the coordination of the zinc ions, which severely impaired the exo- and the endonucleolytic activities. Soon after, the paradox of one active site-two functions could be explained, when the crystal structure of *B. subtilis* RNase J1 was obtained (Newman *et al.*, 2011), as well as the crystal structure of *T. thermophilus* RNase J bound to RNA (Dorléans *et al.*, 2011). The structure of RNase J1 (Figure 6) is very similar to the previous one for *T. thermophilus*. Interestingly, some key amino acids for the coordination of the zinc ions in the active site are

missing in the RNase J2 of *B. subtilis* (Newman *et al.*, 2011). Furthermore, another two amino acids that seem to be important for the correct positioning of RNA are also substituted in RNase J2. These phenomena could explain the loss of exonuclease activity of RNase J2, but they cannot explain why the endonuclease activity is maintained. However, the structural studies from Dórleans and colleagues and Newman and colleagues could provide an explanation for both activities being performed in the same active site. Further crystal structures exist for RNase J from *Streptomyces coelicolor* and *Deinococcus radiodurans* (Pei *et al.*, 2015; Zhao *et al.*, 2015)*.
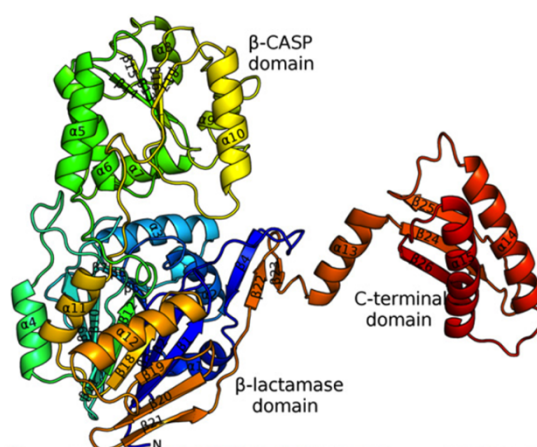
Figure 6. **Crystal structure of a monomer of RNase J1.** From Newman *et al.*, 2011. The three domains β-lactamase, β-CASP, and C-terminal are depicted. The active site localizes in the cleft between the two first, where the zinc ions are coordinated. The C-terminal domain is connected to the other two *via* the α13 helix. The structure is depicted as ribbons, with a rainbow color-coded from blue in the N-terminal to red in the C-terminal.

RNase J1 and RNase J2 have been shown to form a complex *in vivo*, that also modifies the individual specificities of the enzymes (Mathy *et al.*, 2010). However, there is still controversy as in what is the oligomeric state of the proteins *in vivo.* It has been shown *in vitro* that the proteins are able to form dimers and tetramers, with a 1:1 stoichiometry, although the major form *in vivo* is still under discussion (Mathy *et al.*, 2010; Newman *et al.*, 2011). It is also not known whether the enzymes interact as heterodimers, which, in turn, interact amongst each other, or as homodimers that interact to form a heterotetramer (see Figure 7). However, after the study of association and dissociation constants it was hypothesized that the homodimers interact to form heterotetramers (Newman *et al.*, 2011). Interestingly, when the proteins are purified independently, the synergistic effect of the complex is no longer visible (Mathy *et al.*, 2010), suggesting that the enzymes can form homodimers and heterodimers with similar stabilities, and that subunit exchange is unlikely.

It is known by structural and functional analysis that the C-terminal domain of RNase J1 (see Figure 6) is necessary for its dimerization and for its activity *in vitro.* Furthermore, the C-terminal

domain of other members of the β-CASP family is important for the modulation of their activity (Li de la Sierra-Gallay *et al.*, 2008). However, the relevance of the C-terminal domain for the *in vivo* interaction and activity of RNase J1 and J2 of *B. subtilis* is not known.
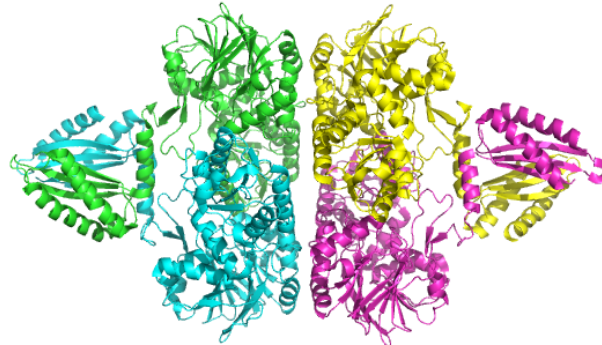
Figure 7. **Ribbon representation of the RNase J1 homotetramer.** Structure from Newman *et al.*, 2011 (Entry 3ZQ4 in the Protein Data Bank). Each monomer has been coloured differently. The pink and yellow, and the green and blue form both dimers. It is visible the intimate contact of the C-terminal domains in the dimer interface, and the less extensive surface of the tetramer interface.

Furthermore, the subcellular localization of RNase J1 was studied some years ago (Hunt *et al.*, 2006). The enzyme is present in the cytoplasm in a ribosome-like distribution, and this localization was affected by the interruption of transcription by rifampicin (Hunt *et al.*, 2006), as is the case for ribosomes (Mascarenhas *et al.*, 2001). The distribution and effect of rifampicin were recently confirmed in another publication (Cascante-Estepa *et al.*, 2016), also for RNase J2. Interestingly, a complex of RNase J associated with translating ribosomes was observed in Gram-negative bacterium *Helicobacter pylori* (Redko *et al.*, 2013).

Although these enzymes have been extensively studied in *B. subtilis* and other organisms, many features remain unknown and many other controversial.

1.6. Objectives

The study of the RNA processing in bacteria has been extensive. In *B. subtilis*, however, much is still not known of this important regulatory mechanism of gene expression. In my thesis I have tried to fill some of those gaps in the story of RNA metabolism in this Gram-positive organism. It has been known for many years that in *E. coli* there is a complex of RNases and RNA-related proteins, the RNA degradosome that interacts to make the process more efficient. Although many interactions among RNA-related proteins have been detected in *B. subtilis,* there was no real evidence for the presence of such a complex *in vivo.* I have analysed the localization of the proteins supposed to be part of this putative degradosome by GFP fusions, to detect possible

interactions *in vivo* and common localization patterns. Furthermore, I have studied the localization of the RNases J1 and J2 in the cell by GFP fusions, and the effect of the deletion of one of the paralogues on the localization of the other. Moreover, I have analysed the interaction of these paralogues *in vivo* and the importance of the C-terminal domain for such interaction. Last but not least, I have studied the activity of the conserved 3'-5' exonuclease polynucleotide phosphorylase *in vitro* and the possible effectors of this activity, including members of the putative RNA degradosome of *B. subtilis.*

2. Materials and methods

2.1. Materials

Materials used in this work such as chemicals, enzymes, oligonucleotides and commercial kits and equipment are listed in the appendix.

2.2. Strains and plasmids

A list of the strains and plasmids generated and used in this work can be found in the appendix.

2.3. Methods

2.3.1. General methods

Some general methods used in this work that are mentioned in the literature are listed in **Table 1.**

Table 1.   **General methods**

Method	Reference
Absorption measurement	Sambrook *et al.*, 1989
Gel electrophoresis of DNA	Sambrook *et al.*, 1989
Plasmid preparation from *E. coli*	Sambrook *et al.*, 1989
Ligation of DNA fragments	Sambrook *et al.*, 1989
Determination of protein amounts	Bradford, 1976
Gel electrophoresis of proteins (denaturing)	Laemmli, 1970
Sequencing according to the chain termination method	Sanger *et al.*, 1977

2.3.2. Cultivation of bacteria

E. coli and *B. subtilis* were grown in LB medium at 37°C or 28°C and 200 rpm in tubes and Erlenmeyer flasks. Fresh colonies from plates, glycerol stocks or overnight liquid cultures were used for inoculation. Growth was measured at a wavelength of 600 nm using a Ultrospec 2100 Pro Spectrophotometer (Amersham Biosciences).

Bacterial growth media and supplements

Solutions, buffers and media were prepared with deionized water and autoclaved (20 minutes at 121°C and 2 bar) (Autoclave LA 2x3x4, Zirbus Technology GmbH). Substances sensitive to high temperatures were sterilized by filtration through a 20 μm Filtropur S plus syringe filter (Sarstedt). *E. coli* was cultured in Luria Bertani's (LB) medium or agar plates, both supplemented with the necessary antibiotics. *B. subtilis* was grown in LB medium or SP-agar and LB-agar plates supplemented with appropriate antibiotics. Agar was added to basic media in a concentration of 15 g/l.

Table 2.   Growth media

LB medium	Tryptone	10 g
(1 l)	Yeast extract	5 g
	NaCl	10 g
	dH$_2$O	add to 1 l
SP medium	Nutrient broth	8 g
(1 l)	MgSO$_4$ · 7H$_2$O	0.25 g
	KCl	1 g
	dH$_2$O	add to 1 l
	autoclave; after cooling down addition of	
	MnCl$_2$ (10 mм)	1 ml
	Ferric ammonium citrate (CAF; 2.2 mg/ml)	2 ml
	CaCl$_2$ (0.5 м)	1 ml
CE minimal medium	KH$_2$PO$_4$	0.4 g
(100 ml)	K$_2$HPO$_4$ · 3H$_2$O	1.6 g
	(NH$_4$)$_2$SO$_4$	0.33 g
	MnSO$_4$ · 4H$_2$O	0.232 mg
	MgSO$_4$ · 7H$_2$O	12.3 mg
	Tryptophan (5 mg/ml)	1 ml
	Ferric ammonium citrate (CAF; 2.2 mg/ml)	1 ml

Potasium Glutamate (40 % w/v)	2 ml

Antibiotics

Antibiotics were prepared as 1000-fold concentrated stock solutions. Ampicillin, spectinomycin and kanamycin were dissolved in deionized water and chloramphenicol in 70% ethanol. All solutions were sterile filtrated and stored at -20°C. The antibiotics were added to the media before inoculation. The agar media were cooled down before addition of the antibiotics.

Table 3.   Antibiotic selection

Selection in *E. coli*	
Ampicillin	1 µg/ml
Selection in *B. subtilis*	
Spectinomycin	150 µg/ml
Chloramphenicol	5 µg/ml
Kanamycin	10 µg/ml

Storage of bacteria

E. coli was kept on LB medium agar plates up to 4 weeks at 4°C. For long-term storage, bacterial stocks were prepared in 10% DMSO (Roth), and stored at -80°C. SP-plates at room temperature were used for the long-term storage of *B. subtilis*, as well as 50 % glycerol stocks prepared from overnight cultures and stored at -80°C.

2.3.3. Transformation of *E. coli*

Preparation of competent DH5α cells

A single colony was inoculated to 20 ml LB medium and incubated with agitation for 24 hours at 28°C. A 250 ml culture of SOB medium was inoculated to an OD_{600} of 0.1 with the preculture and cells were grown with agitation to an OD_{600} of 0.5 at 16°C (20 hours). The culture was incubated for 10 minutes on ice, and cells were harvested by centrifugation for 10 minutes at 5000 rpm and 4°C (Sorvall RC 6+, Thermo Scientific). The pellet was resuspended in 80 ml ice-cold TB and incubated for another 10 minutes on ice, after which the cells were centrifuged for 5 minutes at 5000 rpm and 4°C. After resuspension of the pellet in 20 ml ice-cold TB, DMSO was

added to a final concentration of 7% (v/v). Aliquots of 0.2 ml were frozen in liquid nitrogen and stored at -80°C.

Table 4.   Buffers and media for competent _E. coli_

TB	PIPES	3.46 g
(1 l)	$CaCl_2 \cdot 2H_2O$	2.2 g
	KCl	18.64 g
	dH_2O	add to 1 l
	adjust pH to 6.7	
	autoclave; after cooling down addition of	
	$MnCl_2$ (1M, sterile)	55 ml
SOB	Tryptone	20 g
(1 l)	Yeast extract	5 g
	NaCl	0.58 g
	KCl	0.186 g
	dH_2O	add to 1 l
	autoclave; after cooling down addition of	
	$MgCl_2$ (1 M, sterile)	10 ml
	$MgSO_4$ (1 M, sterile)	10 ml

Transformation of _E. coli_ competent cells

The aliquots of 200 µl of competent cells were thawed on ice. Alternatively, the freshly prepared competent cells were divided in aliquots to a volume of 200 µl and kept on ice. The cells were mixed with 10-100 µg of DNA, and kept on ice for 30 minutes. The samples were subjected to heat-shock for 90 seconds at 42°C (ThermoStat Plus, Eppendorf), after which they were put back on ice for an additional 5 minutes. After addition of 800 µl of LB medium, the samples were incubated with agitation for an hour at 37°C. The transformation samples were propagated in LB-agar plates supplemented with the appropriate antibiotic, and left to grow overnight at 37°C.

2.3.4. Transformation of *B. subtilis* cells

Preparation of competent cells

Competent cells were prepared freshly the same day of the transformation. A colony from an SP-agar plate was inoculated in 4 ml LB and was incubated overnight at 28°C with agitation. With the overnight culture, 10 ml of MNGE supplemented wit 0.1% CAA were inoculated to an OD_{600} of 0.1 and grown at 37°C with agitation until an OD_{600} of 1.3. The culture was diluted with 10 ml of MNGE without CAA and incubated for another hour at 37°C with agitation. For transformation, 400 μl aliquots were used.

Transformation of competent cells

The aliquots of competent bacteria were mixed with the DNA and incubated for further 30 minutes at 37°C. Then, 100 μl of expression mix were added to the samples and incubated for another hour at 37°C with agitation, after which they were propagated in SP-agar or LB-agar plates supplemented with the appropriate antibiotic.

Table 5.   Media for transformation of *B. subtilis*

10X MN medium	$K_2HPO_4 \cdot 3H_2O$	136 g
(1 l)	KH_2PO_4	60 g
	Sodium citrate · $2H_2O$	10 g
	dH_2O	add to 1 l
MNGE medium	MN medium (10X)	1 ml
(10 ml)	Glucose (20%)	1 ml
	Potassium glutamate (40%)	50 μl
	Ferric ammonium citrate (CAF; 2.2 mg/ml)	50 μl
	Tryptophan (5 mg/ml)	100 μl
	$MgSO_4$ (1 M)	30 μl
	dH_2O	add to 10 ml
	+/- Casamino acids (CAA; 10%)	100 μl

Expression mix	Yeast extract (5%)	500 µl
(1 ml)	Casamino acids (CAA; 10%)	250 µl
	Tryptophan (5 mg/ml)	50 µl
	dH$_2$O	250 µl

2.3.5. Preparation and detection of DNA

Preparation of plasmid DNA from *E. coli*

For the isolation of plasmid DNA from *E. coli* 2 ml of an overnight culture of the desired strains were harvested at 14.500 rpm for 1 minute (Heraeus Fresco 21, Thermo Scientific). After discarding the supernatant the NucleoSpin® Plasmid Kit (Macherey-Nagel) was used to extract the DNA, following the manufacturer's instructions. The plasmid DNA was eluted from the column with deionized water that had been pre-warmed to 70°C.

Polymerase chain reaction (PCR)

DNA was amplified by PCR with specific oligonucleotide, using Phusion DNA polymerase (Thermo Scientific) in a thermocycler (SensoQuest). Oligonucleotides were designed using the software Geneious 7.0.2 (Biomatters). All oligonucleotides were purchased from Sigma-Aldrich and are listed in the appendix. The PCR reactions were performed in a total volume of 50 µl, and 30 cycles of amplification. The PCR reaction and program used are described below (elongation time is specific for every PCR product).

Table 6.   **Polymerase Chain Reaction (PCR)**

Compound	Volume (µl)
Template DNA	1
5X Phusion HF buffer*	10
dNTP mix (12.5 mM each)	2
Forward oligo (5 µM)	2
Reverse oligo (5 µM)	2
Phusion polymerase*	0.5
dH$_2$O	32.5

Step	Temperature (°C)	Time
Initial denaturation	98.5	2'
Denaturation	98.5	20''
Annealing	54	30''
Elongation	72	variable
Final elongation	72	10'
Hold	4	hold

*Thermo Scientific

Isolation of genomic DNA from *B. subtilis*

The genomic DNA was purified from the desired strains using the peqGOLD Bacterial DNA kit (PEQLAB Biotechnologie GmbH). For that purpose, a single colony was inoculated to 4 ml of LB medium containing, if necessary, the appropriate antibiotics, and grown overnight at 28°C at 200 rpm. The cells (2 ml) were collected by centrifugation for 2 minutes at 14.500 rpm. The extraction of the DNA was performed following the manufacturer's instructions. For the elution deionized water pre-warmed to 70°C was used.

Agarose gel electrophoresis

DNA fragments were separated and analyzed in gels prepared from 1% (w/v) peqGOLD Universal-Agarose (PEQLAB Biotechnologie GmbH) disolved in TAE buffer. For staining of the DNA fragments HD Green Plus DNA stain (INTAS Science Imaging Instruments GmbH) was mixed with the dissolved agarose solution (1 µl / 10 ml). The DNA samples were mixed with self-made 5-fold DNA loading dye. After the samples were loaded, 130 V were applied to the gel until the bromophenol blue had migrated two thirds of the gel. As a molecular weight marker λ-DNA digested with the restriction enzymes BamHI and EcoRI was used. The DNA was detected and documented *via* its fluorescence under UV light (λ= 254 nm) by GelDoc™ (BioRad).

Table 7.   **Materials for agarose gel electrophoresis**

50X TAE buffer	Tris	121.14 g
(500 ml)	Acetic acid (100%)	57.1 ml
	EDTA (0.5 м, pH 8)	100 ml
λ-DNA marker	λ-DNA* (0.3 mg/ml)	240 µl

(840 µl)	FD EcoRI (1U/µl)*	14 µl
	FD HindIII (1U/µl)*	14 µl
	10X FD Buffer Green*	84 µl
	dH$_2$O	488 µl
	2 hours at 37°C; store at -20°C	
5X DNA loading dye	Glycerol	5 ml
(10 ml)	50X TAE buffer	200 µl
	Bromophenol blue	10 mg
	Xylene cyanol	10 mg
	dH$_2$O	4.5 ml

* Thermo Scientific

Digestion and dephosphorylation of DNA

For the digestion of DNA fragments, Fast Digest (Thermo Scientific) endonucleases and buffers were used. Vectors were first digested for 15 minutes at 37°C. The samples were cooled on ice while 2.5 µl were anlyzed by agarose gel electrophoresis. Then the second enzyme was added to the mixture and the sample was further digested for another 15 minutes at 37°C. Digested vectors were dephosphorylated by adding 5 units of FastAP Alkaline phosphatase (Thermo Scientific) to the sample and incubating for 5 minutes at 37°C. PCR products were digested simultaneously with both restriction enzymes for 30 minutes at 37°C. Fragmets were purified and ligated for subsequent transformation.

Purification of DNA fragments

The QIAquick® PCR purification kit (QIAGEN, Hilden) was used for purification of linear DNA fragments such as PCR products or digested vectors as described by the manufacturer. The column was incubated in pre-warmed deionized water (70 °C) for 5 minutes at room temperature and DNA was eluted by centrifugation for 1 minute at 14.500 rpm.

Ligation of DNA

DNA fragments were ligated using T4-DNA ligase (Thermo Scientific) in the buffer supplied by the manufacturer. The ligation reaction contained 20 - 200 ng of vector DNA and an excess of the DNA fragment (insert to vector molar ratio of 10:1 to 20:1). After addition of 5 U of T4-DNA ligase

to a final volume of 20 µl, the fragments were allowed to ligate for 2 hours at room temperature or overnight at 16°C. Subsequently the ligated samples were transformed into *E. coli* competent cells.

Analysis of clones by cracking

Colonies from transformation plates were inoculated in 4 ml LB medium supplemented with the appropriate antibiotic, and incubated at 37°C overnight or until growth was visible. For the analysis, 50 µl of the preculture were harvested for 1 minute at 14.500 rpm, and resuspended in resuspension buffer. For the disruption of the cells, 25 µl of freshly prepared crack buffer were added and the samples were incubated for 5 minutes at 70°C. After cooling on ice, 5 µl of crack staining were added and the samples were left on ice ofr 10 minutes. Insoluble particles were eliminated by centrifugation at 14.500 rpm for 5 minutes at 4°C, and the soluble fraction was loaded on an agarose gel for electrophoresis.

Table 8.   Cracking buffers

Resuspension buffer	Na_2-EDTA · $3H_2O$	37 mg
(10 ml)	*adjust pH to 8.0*	
	dH_2O	add to 10 ml
Crack buffer	*D*-(+)-Sucrose	200 mg
(1 ml)	SDS (20%)	25 µl
	NaOH (2 M)	100 µl
	dH_2O	add to 1 ml
Crack staining	KCl (4 M)	150 µl
(200 µl)	5X DNA loading dye	50 µl

Long-flanking homology PCR (LFH-PCR)

The attempt for the introduction of a modified gene in its original locus in *B. subtilis* was performed with the flanking homology PCR (LFH-PCR) technique (Wach, 1996). For this purpose three fragments were amplified by PCR. A DNA fragment of about 1000 bp with homology to the upstream region of the gene to be modified, a DNA fragment of similar length and region homologous to downtream region of the gene to be modified, and a third fragment to amplify the resistance gene. The usptream and downstream fragments have to harbor a 20 bp flank that anneals with the resistance fragment. These flanks were introduced *via* oligonucleotide. The

concentration of the three purified fragments was measure using a NanoDrop ND-1000 Spectrophotometer (PEQLAB)and they were then joined through a PCR reaction described below. *B. subtilis* was transformed with the LFH-PCR products and clones were examined by PCR to screen for the correctly integrated fragment.

Table 9. **LFH-PCR reaction and program**

Compound	Volume (μl)
5X Phusion HF buffer	20
dNTP mix (12.5 mм each)	4
upstream fragment (100 ng)	-
cassette fragment (150 ng)	-
dowstream fragment (100 ng)	-
Phusion polymerase	2
dH$_2$O	to 100

Step	Temperature (°C)	Time	Cycles
1.	98.5	1′	
2.	98.5	15″	10
3.	52	30″	10
4.	72	2′ 15″	10
5.	4	hold	
addition of oligonucleotides 8 μl of 5 μм stocks			
6.	98.5	15″	21
7.	52	30″	21
8.	72	4′ + 5″/cycle	21
9.	72	10′	
10.	4	hold	

Sequencing of DNA

Sequencing of PCR or plasmid samples premixed with the sequencing primer was performed by SeqLab Sequence Laboratories Göttingen GmbH .

2.3.6. Preparation and analysis of proteins

Cell disruption by French press

The bomb (French Pressure Cell, Thermo Scientific) was pre-cooled on ice for 20 minutes before usage. The cell pellets were resuspended in buffer W (described in Table 17) and applied to the bomb. Before closing the air was squeezed out of the pump. A pressure of 18,000 psi was applied (G. Heinemann press) and the cell extract was recovered slowly and conserved on ice. The samples were disruped 1-3 times depending on the concentration and organism.

Cell disruption by Tissue Lyser

The cells were disrupted by addition of 0.5 g of 0.1 mm diameter glas beads (Roth) to a 2 ml Eppendorf tube. Afterwards, 1 ml of cell culture resuspended in buffer W was added and the cells were disrupted three times at 30 s^{-1} for 3 minutes. The samples were placed on ice for cooling after each disruption cycle.

Discontinuous SDS polyacrylamide gel electrophoresis (SDS-PAGE)

Proteins were analysed by SDS-PAGE following the principle described by Laemmli in 1970. Protein samples were denatured by boiling in SDS loading dye at 95°C for 30 minutes. The polyacrylamide concentration of the gels was 12% (v/v). Samples were loaded onto the prepared gel and electrophoresis was performed at 120 V – 200 V at 4°C until the bromophenol blue had reached the lower end of the gel. The self constructed protein marker *Page King* (Pietack, 2010) or the PageRulerTM Plus Prestained Protein Ladder (ThermoFischer Scientific) were used as size standards. Gels were stained with Coomassie Brilliant Blue G-250, Silver staining of were used for specific protein detection *via* Western blot.

Table 10.   SDS-PAGE materials

5X SDS loading dye	Tris (1.5 м; pH 6.8)	1.33 ml
(10 ml)	Glycerol	5 ml
	SDS (20%)	2.5 ml
	2-mercaptoethanol	1.6 ml
	Bromophenol blue	20 mg
5% Stacking gel	Acrylamide:bisacrylamide (37.5:1) (30%)	0.83 ml
(5 ml)	Tris (1.5 м; pH 6.8)	0.63 ml

	SDS (20%)	25 µl
	dH$_2$O	3.46 ml
	APS (10%)	50 µl
	TEMED	5 µl
12% Running gel (5 ml)	Acrylamide:bisacrylamide (37.5:1) (30%)	2 ml
	Tris (1.5 M; pH 8.8)	1.25 ml
	SDS (20%)	25 µl
	dH$_2$O	1.67 ml
	APS (10%)	50 µl
	TEMED	2 µl
10X Running buffer (500 ml)	Glycine	72 g
	Tris	30 g
	SDS	0.5 g

Native-PAGE gels

Protein samples are kept always on ice and mixed with 5-fold native loading dye. The samples were applied to Native-PAGE gels with or without stacking gel. The separating gels we prepared at 8%. Samples. The electrophoresis was performed overnight at 20 V at 4°C. As a marker PageRulerTM Plus Prestained Protein Ladder (ThermoFischer Scientific) was used.

Table 11.   Native-PAGE materials

5X SDS loading dye (10 ml)	Tris (1.5 M; pH 6.8 or pH 8.8)	1.33 ml
	Glycerol	5 ml
	Bromophenol blue	20 mg
5% Stacking gel (5 ml)	Acrylamide:bisacrylamide (37.5:1) (30%)	0.83 ml
	Tris (1.5 M; pH 6.8)	0.63 ml
	dH$_2$O	3.46 ml
	APS (10%)	50 µl
	TEMED	5 µl
8% Running gel	Acrylamide:bisacrylamide (37.5:1) (30%)	1.33 ml

(5 ml)	Tris (1.5 M; pH 8.8)	1.25 ml
	dH$_2$O	2.34 ml
	APS (10%)	50 µl
	TEMED	2 µl
10X Running buffer	Tris	30.3 g
(1 l)	Glycine	144.1 g
	dH$_2$O	add to 1 l

Native-PAGE gels for basic proteins

For the visualization of native basic proteins on a gel was performed as previously described (Niepmann and Zheng, 2006). Briefly, a polyacrylamide gradient gel 6-20% was prepared from 40% acrylamide:bisacrylamide 29:1 stock solution. The proteins were incubated for 10 minutes at room temperature with loading dye containing Coomassie Blue G. The gel was run overnight at 15 V, using a histidine pH 8.0 cathode and Tris-HCl pH 8.8 anode buffer system. The gel was destained and fixated overnight in silver stain destaining solution and developed by silver stain method (see Table 14).

Coomassie staining for polyacrylamide gel

Protein gels can be stained with Coomassie Brilliant Blue G-250 (Roth) to visualize the proteins. For this, the gels were incubated in staining solution for 30 minutes at room temperature with agitation. To destain the background and make the proteins visible, the gel was incubated in destaining solution until the contrast was sufficient.

Table 12.   Solutions for Coomassie gel staining

Staining solution	Coomassie Brilliant Blue G-250	2.5 g
(1 l)	Acetic acid	100 ml
	Methanol	500 ml
	dH$_2$O	add to 1 l
Destaining solution	Ethanol	200 ml
(1 l)	Acetic acid	50 ml
	dH$_2$O	add to 1 l

Western blot

After polyacrylamide gel electrophoresis the proteins were immobilized in a PVDF membrane (Biorad) that had previously been activated in methanol. The proteins from the gel were transferred to the membrane in a semidry blotting apparatus for 2 hours with a current of 80 mA per gel. The membrane was blocked for 30 minutes in blocking solution and incubated overnight with the primary antibodies in TBS-T at 4°C: 1:1000 anti-FLAG or anti-Strep (PromoKine) and 1:30,000 anti-GapA (Meinken *et al.*, 2003). The membranes were washed three times for 15 min with TBS-T. The secondary antibody (Anti-Rabbit IgG (Promega), 1:100,000 in TBS-T) was added for 1 hour and then the membrane was washed again three times for 20 min with TBS-T.
Before the addition of the CDP-Star reagent (Roche) for development of the membrane, it was incubated for 5 minutes in buffer III. The CDP-Star was then added in buffer III (5 µl/500µl).

Table 13.   Buffers for Western blot

10X TG buffer	Tris	30.3 g
(1 l)	Glycine	144.1 g
	dH$_2$O	add to 1 l
1X Transfer buffer	10X TG buffer	100 ml
(1 L)	Methanol	200 ml
	dH$_2$O	add to 1 l
10X TBS	Tris	60.57 g
(1 l)	NaCl	87.6 g
	adjust pH to 7.5	
	dH$_2$O	add to 1 l
1X TBS-T	10X TBS	100 ml
(1 l)	Tween-20	500 µl
	dH$_2$O	add to 1 l
Blocking solution	TBS-T	50 ml
(20 ml)	Skimmed milk powder	2.5 g
Buffer III	Tris	12.11 g
(1 l)	NaCl	5.84 g
	adjust pH to 9.5	
	dH$_2$O	add to 1 l

Silver stain for polyacrylamide gel

The proteins separated by SDS-PAGE can be visualized by the method of the Silver stain. It is more sensitive than other staining methods like Coomassie when detecting low amounts of proteins (up to 1 ng (Weiss *et al.*, 2009)). The staining proceeds in several steps were the gel is incubated in different solutions, all described below.

Table 14.   Silver stain protocol

Fixing solution 1	Methanol (100%)	25 ml
(100 ml)	Acetic acid (100%)	6 ml
	Formaldehyde (37%)	50 µl
	ddH$_2$O	add to 50 ml
Na$_2$S$_2$O$_3$ solution 2	Na$_2$S$_2$O$_3 \cdot$ 5H$_2$O	10 mg
(100 ml)	ddH$_2$O	add to 50 ml
Impregnating solution 3	AgNO$_3$	0.1 g
(100 ml)	Formaldehyde (37%)	18.5 µl
	ddH$_2$O	add to 50 ml
Developing solution 4	Na$_2$CO$_3$	3 g
(100 ml)	Na$_2$S$_2$O$_3$ solution **2**	1 ml
	Formaldehyde (37%)	25 µl
	ddH$_2$O	add to 50 ml
STOP solution 5	Na$_2$-EDTA	0.93 g
(100 ml)	ddH$_2$O	add to 50 ml

Step	Reagent	Duration
Fixing	Fixing solution **1**	1-24 h
Washing	EtOH 50%	3 x 20'
Reduction	Na$_2$S$_2$O$_3$ solution **2**	1' 30''
Washing	dH$_2$0	3 x 20''
Staining	Impregnating solution **3**	15'-25'
Washing	dH$_2$0	2 x 20''
Development	Developing solution **4**	until stained
Washing	dH$_2$0	2 x 20''

Overexpression of proteins in *E. coli*

The 1 liter LB cultures of the desired strains were inoculated from overnight cultures and incubated at 37°C. When the cultures had reached adn OD_{600} of 0.5, the expression of heterologous proteins was induced by addition of isopropyl-β-D-thio-galactopyranoside (IPTG) to a final concentration of 1 mM (PEQLAB). The cultures were incubated for three hours at 37°C and harvested before storing the pellets at -20°C.

Purification of His$_6$-tagged proteins

For protein purification, the frozen pellets were resuspended in cold cell disruption buffer, and the cells were disrupted by 3 passages through the French pressure cell (Thermo Scientific) at 18,000 psi. Cell debris and other insoluble material was removed by ultracentrifugation for 1 hour at 35,000 rpm at 4°C in a Sorvall WX Ultra Series Centrifuge (Thermo Scientific). For purification of recombinant His$_6$-tagged proteins the supernatant fraction was loaded onto a bed of 500 µl of Ni^{2+}-NTA resin (IBA) in a Poly-Prep Chromatography Column (Biorad) that had been pre-equilibrated in disruption buffer. After applying the cell extract, the column was washed 5 times with 5 ml of disruption buffer containing 10 mM imidazole. The elution was performed in steps of 5 ml, with increasing concentrations of imidazole (30 mM, 50 mM, 75 mM and 100 mM). The relevant fractions were combined and concentrated by centrifugation through Vivaspin turbo 15 (Sartorius) for 15 minutes at 4.000xg and 8°C in Heraeus Megafuge 16R (Thermo Scientific). Protein concentration was determined following the Bradford assay as described further in this section. The pooled fraction was further purified and analysed *via* Size-exclusion chromatography (SEC).

Table 15. Disruption buffer

10X HEPES buffer	HEPES	119.15 g
(1 l)	NaCl	116.8 g
	adjust pH to 7.5	
	dH$_2$O	add to 1 L
	add imidazole to different concentrations	

Size exclusion chromatography

The experiments were performed at room temperature in a HiLoad 16/600 Superdex 200 pg using an ÄKTAprime plus (GE Healthcare Life Sciences). Purified protein was applied to the column equilibrated with 20 mM Tris-HCl, 50 mM NaCl, pH 8.0 buffer. The program was set to 1 ml/min and several elution fractions were recovered, where protein concentration was measued by a spectrophotometer coupled to the column. A calibration run was performed with molecular weight standards and related to their elution volumes for both column sizes. The elution volume presents a linear relationship to the $\log_{10}$(Mw).

Table 16. Standard curve for HiLoad 16/600 Superdex 200 pg

Mw (KDa)	log Mw	Retention volume (ml)
670	2.83	50.45
158	2.20	64.92
44	1.64	81.19
17	1.23	93.02
1.35	0.13	111.92
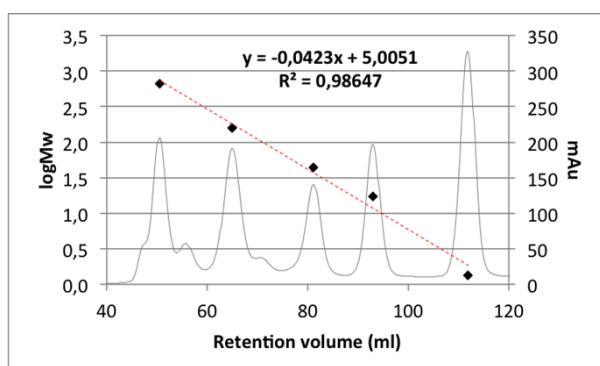
Figure 8.   Standard curve in a HiLoad 16/600 Superdex 200 pg chromatography column. Proteins of different sizes were injected into the size-exclusion chromatography column. The grey line, corresponding to the secondary vertical axis, represents the spectrum of elution. The logarithm of the molecular weight of each protein was plotted against its retention volume. The standard curve was then used to interpolate molecular weight from experimental retention times.

SPINE (Strep-protein interaction experiment)

The SPINE experiment was performed as described (Herzberg *et al.*, 2007). Briefly, the cultures of the relevant strains of *B. subtilis* were grown to the desired OD_{600}. For the experiments that required crosslinking, half of the cultures were incubated for 20 minutes with 0.6% formaldehyde (FA) solution. The prepared cultures were harvested by centrifugation at 5,000 rpm in a Sorvall RC

6+ Centrifuge (Thermo Scientific). The pellets were washed in buffer W and disrupted by 3 passages through the French pressure cell. The cells debris was eliminated by ultracentrifugation at 35,000 for 30 minutes and 4°C. The crude cell extracts were applied to a Poly-Prep Chromatography column (Biorad) that contained 50% Streptactin Sepharose (IBA) pre-equilibrated in buffer W. The matrix specifically binds the Streo sequence of eight amino acids (WSHPQFEK). The amount of resin was 500 µl / 250 ml of culture. After the proteins were allowed to bind the resin, it was washed 5 times with 5 ml of buffer W. The elution was performed with one bed volume of buffer E, which contains D-desthiobiotin (IBA). The fractions were analysed *via* SDS-PAGE, Native-PAGE and Western blot.

Table 17.   Buffers for Strep-protein purification

Buffer W	Tris	12.11 g
(1 l)	NaCl	8.76 g
	adjust pH to 7.5	
	dH$_2$O	add to 1 L
Buffer E	Buffer W	250 ml
(250 ml)	*D*-desthiobiotin	134 mg

Calculation of protein amounts by the Bradford method

To measure the concentration of protein in solution we made use of the principle for protein-dye binding described by Bradford in 1976. For this we prepared a one-fold solution of the Bradford reagent by diluting the 5 fold Roti-Quant (Roth) with distilled water.

$$y = 0.0301x - 0.0055$$
$$R^2 = 0.98854$$
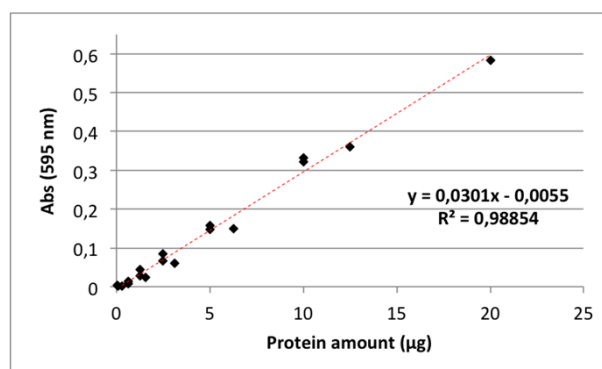
Figure 9.   Standard curve for Bradford protein amount calculation. Different concentrations of BSA diluted in water were measured using the Bradford reagent. The protein amount in micrograms was plotted against the absorbance obtained at 595 nm. The measurements were adjusted to a linear function whose slope was used to interpolate amount of protein from the absorbance measured.

The protein samples were mixed with the Bradford reagent to a total volume of 1 ml and the absorbance was measured in an Ultrospec 2100 Pro spectrophotometer (Amersham Biosciences) at a wavelength of 595 nm. A blank sample was prepared by mixing the buffer with the Bradford reagent in the same proportion as the protein samples. The protein amount per sample was interpolated from the standard curve depicted in Figure 9 that was prepared using bovine serum albumin (BSA) protein (AppliChem).

PNPase *in vitro* degradation assay

The purified protein PNPase from *B. subtilis* was used for analysis of its *in vitro* activity similar to previously described (Nurmohamed *et al.*, 2011). For this, the protein (250 nM) was mixed with 40 mM inorganic phosphate (Pi) a divalent cation ($MgCl_2$ or $MnCl_2$) and a short fragment of poly(A) RNA of 15 bases (15-mer RNA) (50 μM) (Sigma Aldrich).
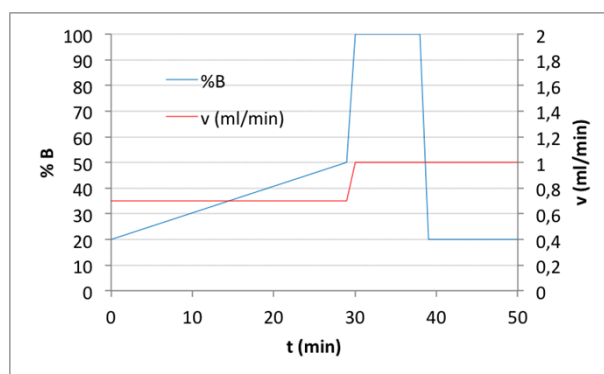
Figure 10. **Elution program ion-exchange HPLC.** Percentage of buffer B (20 mM Tris-HCl, 1 M NaCl, pH 8.0) is represented by a blue line and corresponds to the primary vertical axis. The red line represents the flow though the HPLC system and corresponds to the seconday vertical axis.

The reaction was performed in 5 μl of final volume witin a buffer solution of 20 mM Tris-HCl, pH 8.0 and incubated at 25°C for a determined amount of time. Purified PfkA, enolase, Mg-citrate as well as c-di-AMP and c-di-GMP (Biolog) were added to the reactions to assay possible effects on the reaction. The reaction was stopped and analysed *via* ion-exchange HPLC through a BioLC DNA Pac PA200 4x250 mm Analytical column and 4x50 mm Guard (Dionex) associated with a JASCO chromatography system. The reaction samples ware monitored through a spectrophotometer that was coupled to the column (260 nm). The spectra were analysed by Borwin 1.50 software (Jasco). The equipment for ion-exchange HPLC that I had access to was in the Institute for Organic and Biomolecular Chemistry, in the group of Prof. Dr. Ulf Diederichsen, with the technical support of Mr. Daniel. The buffer system used for the HPLC was 20 mM Tris-

HCl, pH 8.0 (A) and 20 mм Tris-HCl, 1 м NaCl, pH 8.0 (B). The program used for the HPLC is depicted in Figure 10.

2.3.7. Light and fluorescence microscopy

For the microscopic analysis the samples of *B. subtilis* were grown in LB medium at 37°C or 28°C to the desired DO_{600}. A total of 0.3 µl were placed on a slide covered with a thin layer of 1% agarose dissolved in water. When the sample had dried a coverslip was placed over the sample. The pictures were taken using the AxioImager M2 equipped with a digital camera AxioCam MRm and the AxioVision Rel 4.8 software for image uptake (Zeiss). The objectives used ECPlan-NEOFLUAR 100X/1.3 (Zeiss). For the fluorescence images the applied filtersets used were 49 G365, FT395, BP445/50 (Zeiss) for DAPI detection, the Filterset 38 BP470/40, FT495, BP525/50 (Zeiss) for GFP detection and the Filterset 43 BP545/25, FT570, BP605/70 (Zeiss) for Nile Red detection. The Axioskop 40 (Zeiss) was equipped with an AxioCam MRm and the objectives Plan Neofluar 100x/1.30 and Plan Neofluar 40x/0.75 (Zeiss). The filterset used for visualization of GFP was Filterset 2 (AHF Analysentechnik). For DAPI and Nile Red, the filtersets described above were used. For uptake of images the AxioVision Rel. 4.7 (Zeiss) was used. The software Image J 1.49p (National Institutes of Health, USA) was used for processing of the images. The cells were incubated for 5 minutes at 37°C and 200 rpm with the Nile Red (Sigma-Aldrich) or DAPI (AppliChem) dyes at a final concentration of 1 µl/ml to visualize the cell membrane or the genetic material, respectively. To perform the experiments where the transcription was interrupted, the cells were incubated for 10 minutes at 37°C and 200 rpm with rifampicin (dissolved in methanol; Sigma) at a final concentration of 200 mg/ml. As a negative control the same amount of methanol was added to the cells in the same conditions. To induce the expression of GFP protein fusion whose expression was under control of a xylose-inducible promoter, 0.1% of xylose was added to the cell cultures. The exposure times were 1 s for GFP (except for Eno-GFP, 500 ms), 500 ms for Nile Red and 100 md for DAPI. (Adapted from Cascante-Estepa *et al.*, 2016).

3. Results

3.1. Localization of components of the RNA-degrading complex of *B. subtilis*

This chapter is extracted from the previously published material in Cascante-Estepa N., Gunka K. and Stülke J. (2016) Localization of components of the RNA-degrading machine in *Bacillus subtilis*. *Front. Microbiol.* **7**:1492.

For years it has been known that, not only in eukaryotes but also in bacteria, compartmentalization and subcellular organization are essential for the normal functioning of a cell (Shapiro and Losick, 2000; Lewis *et al.*, 2000; Errington, 2003). The possibility of fusing fluorescent proteins to visualize the *in vivo* localization of proteins has greatly improved our understanding of the cell dynamics in the past years. Indeed, the researchers that discovered and described the green fluorescent protein (GFP) were awarded in 2008 the Nobel Prize in Chemistry (Chalfie *et al.*, 1994). However, the ability of the green fluorescent protein (GFP) to dimerize can cause artifacts in the localization of the fusion protein within the cells, which can be avoided by the use of monomeric fluorescent proteins (Miyawaki, 2011; Margolin, 2012). Moreover, the addition of a tag to a protein could affect its functionality and localization *in vivo*, by avoiding interactions, conformational changes or proper folding (Gunka *et al.*, 2013). Furthermore, the overexpression of labeled proteins may result in aggregation and mis-localization (Miyawaki, 2011; Margolin, 2012). For these reasons, to study the localization of the proteins implicated in RNA degradation in *B. subtilis*, we used a monomeric GFP variant (Oliva *et al.*, 2010) and integrated the constructs into the original *loci* of the chromosome, ensuring that the labeled proteins are expressed from their native promoters. Additionally, we verified that these fusion proteins had retained their native activity *in vivo*.

Several ribonucleases, RNA helicases and glycolytic enzymes were proposed to form an RNA-degrading complex in *B. subtilis* (see 1.5). However, the subcellular localization of some of these proteins has not yet been determined *in vivo* by fluorescence labeling

3.1.1. Functionality of the proteins fused to GFP *in vivo*

To confirm that the fusion proteins had retained their original activity, we compared the strains harboring said fusions to the wild type and to their respective deletion mutants. We considered that, if the fusion to GFP rendered the proteins inactive, the strains would show a phenotype similar to the corresponding deletion mutants.

The deletion of the *pnpA* gene encoding polynucleotide phosphorylase causes the cells to grow in long cell chains and results in cold sensitivity (Wang and Bechhofer, 1996). The *B. subtilis* GP1698 strain, which harbors the PNPase-GFP fusion, was able to grow with a normal cell length (Figure 11A). RNase J1, encoded by the *rnjA* gene, has been regarded as essential until recently. Even though the construction of a deletion mutant is possible, this strain shows severely affected cell morphology, with cells growing in curly long chains (Figaro *et al.*, 2013). Our strain GP1722 expresses the RNase J1-GFP fusion and showed normal cell morphology and not a filamentous and curly-cell phenotype (Figure 11B).

Although RNase J2, the paralogue of RNase J1, can be deleted without any visible phenotype, it has been proven to interact *in vitro* with RNase J1 with a 1:1 stoichiometry (Mathy *et al.*, 2010). Moreover, we have observed a strong interaction of both proteins by *in vivo* co-purification (Figure 12). As we cannot assay the functionality of RNase J2, we would assume that a similar localization of RNases J1 and J2 indicates that the GFP tag did not affect J2 activity and localization (see Figure 16).
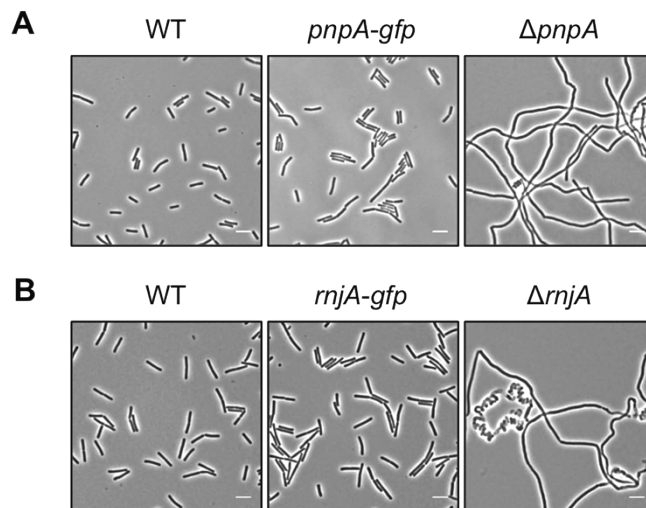
Figure 11.   The strains that contain the GFP fusions to PNPase and RNase J1 have a wild type phenotype under the microscope. Light microscopy of strains **(A)** 168 (WT), GP1698 (*pnpA-gfp*), and GP1748 (Δ*pnpA*) and **(B)** 168 (WT), GP1722 (*rnjA-gfp*), and GP2502 (Δ*rnjA*). The strains were grown in LB medium at 37°C to stationary phase. Both strains harboring the GFP fusions form short cells comparable to the wild type strain and are not elongated as their respective deletion mutants. Scale bar, 5 μm. WT, wild type.

RNase Y is encoded by *rny*, the first gene of the bi-cistronic *rny-ymdB* operon (Diethmaier *et al.*, 2011). To avoid interference with the expression of the phosphodiesterase YmdB, we constructed a strain expressing the RNase Y-GFP fusion under the control of a xylose-inducible promoter. As membrane localization of RNase Y has been demonstrated in several independent

studies (Hunt *et al.*, 2006; Lehnik-Habrink *et al.*, 2011a; Bürmann *et al.*, 2012), no further functional analyses were performed.
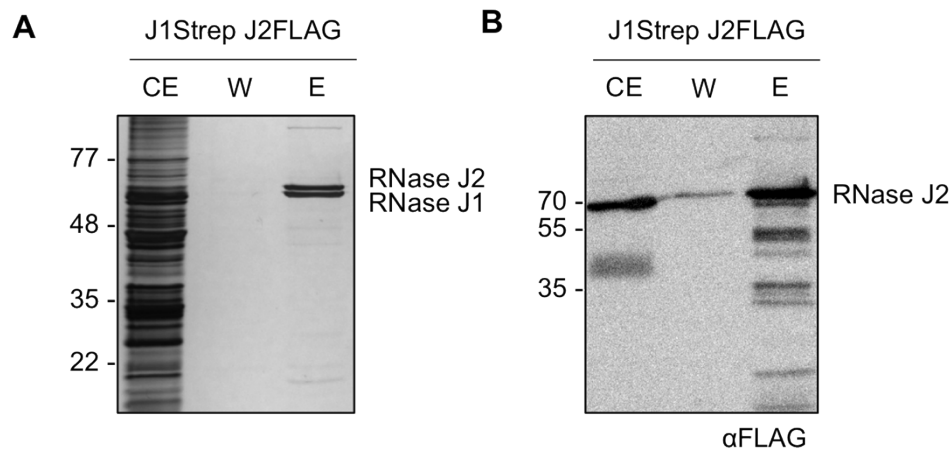
Figure 12. **RNase J1 and J2 interact *in vivo* forming a complex.** Cells from strain GP1048 (*rnjA*-Strep *rnjB*-3xFLAG) were cultured in LB medium at 37°C to an OD_{600} of 1. The cells were then disrupted and RNase J1-Strep was purified by StrepTactin column as described above. **(A)** The fractions were analyzed by denaturing PAGE and visualized by silver staining. The faint eluted bands at the top and the bottom of the gel correspond to PycA and AccB, respectively, the two biotin-containing proteins of *B. subtilis* (Meyer *et al.*, 2011). **(B)** The identity of RNase J2 was proven by Western blot analysis. CE, cell extract; W, wash fraction; E, elution fraction.

The *cshA* deletion mutant, however, grows poorly at temperatures lower than 28°C (Lehnik-Habrink *et al.*, 2013) but the strain GP1721, which harbours the CshA-GFP fusion, was able to grow at 28°C like the wild type (Figure 13A). The glycolytic enzymes enolase and phosphofructokinase (PfkA) were for years thought to be essential for the growth of *B. subtilis* (see 1.5.2)*.* This essentiality, however, has been recently re-analyzed (Muñoz-Márquez and Ponce-Rivas, 2010; Commichau *et al.*, 2013). There, enolase was shown to be essential for the growth of *B. subtilis* in LB medium, while the *pfkA* gene, albeit not essential, was proven to be required for normal growth on minimal medium with glucose as carbon source. For strain GP1720 expressing the phosphofructokinase fused to GFP, we observed growth on minimal medium with glucose as the carbon source, indicating activity of the fusion protein (Figure 13B). The strain encoding the fusion of enolase to GFP (GP1700) was viable and grew as the wild type strain, indicating functionality of enolase when fused to GFP (Figure 13C).
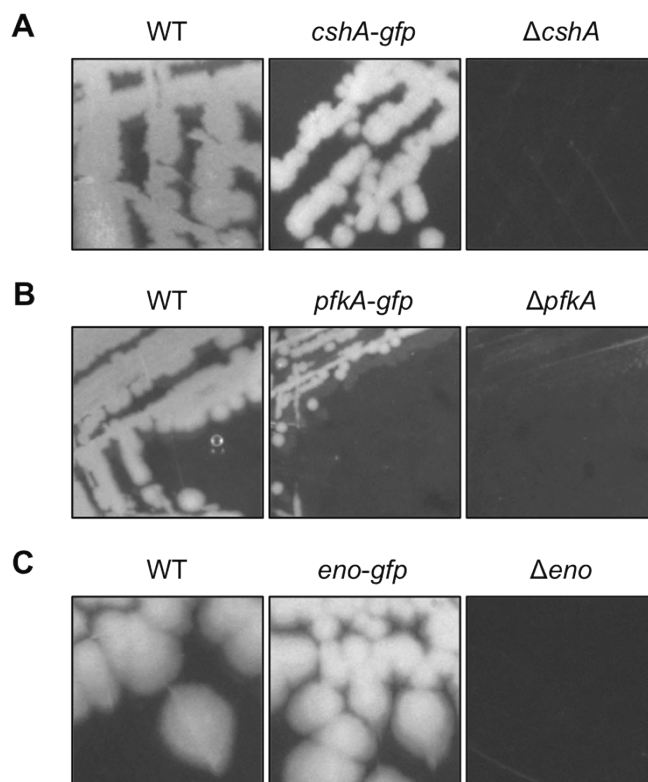
Figure 13. **The strains harbouring GFP fusions to CshA, PfkA and enolase show no growth defect. (A)** Strains 168 (WT), GP1721 (*cshA-gfp*), and GP1035 (Δ*cshA*) were streaked on LB agar and incubated at 28°C overnight. The strain harboring the *cshA-gfp* fusion in the genome is able to grow under these conditions while the deletion mutant has a growth defect. **(B)** Strains 168 (WT), GP1720 (*pfkA-gfp*), and GP1747 (Δ*pfkA*) were streaked on CE minimal medium plates with 0.5% glucose and incubated for 48 hours at 37°C. The strain with the *pfkA-gfp* fusion is able to grow under these conditions, in contrast to the deletion mutant. **(C)** Strains 168 (WT), GP1700 (*eno-gfp*), and GP594 (Δ*eno*) were streaked on LB plates and incubated at 37°C overnight. The strain harboring the *eno-gfp* fusion can grow under these conditions, while the deletion mutant is unable to grow. WT, wild type.

3.1.2. Localization of the proteins fused to GFP within the *B. subtilis* cell

RNase Y has been proposed to provide the scaffold for RNA-degrading enzymes in *B. subtilis*, while anchoring this putative complex to the cell membrane. In fact, several studies have reported membrane localization of this protein (Hunt *et al.*, 2006; Zweers *et al.*, 2009; Lehnik-Habrink *et al.*, 2011a; Bürmann *et al.*, 2012; Strahl *et al.*, 2014). The fluorescence microscopy on the strain GP1684, which expresses the RNase Y-GFP fusion protein, shows that the localization of the enzyme perfectly co-localized with the membrane (Figure 14). Interestingly, we observed a higher intensity of RNase Y localization at the division septa. We investigated afterwards the localization of the exoribonucleases PNPase, RNase J1 and RNase J2. For PNPase, we observed that it was localized with a uniform distribution throughout the cell cytoplasm (Figure 15A). The GFP fusions of the RNases J1 and J2 were found to localize in the cytoplasm with a lower

concentration of fluorescence at central region of the cell, that was identified by DAPI stain as the location for the nucleoid (Figure 16).
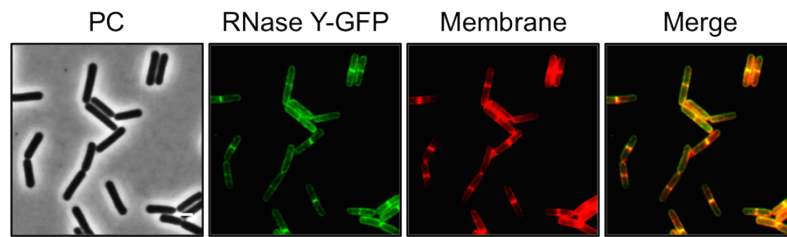
Figure 14.   RNase Y localizes to the cell membrane. Fluorescence microscopy of the strain GP1684 (Pxyl-*rny-gfp*) grown in LB medium at 28°C to stationary phase. The expression of the fusion protein was induced by addition of 0.1% xylose to the culture medium. The membrane was stained with Nile Red. RNase Y-GFP co-localizes with the Nile Red staining, confirming the membrane localization of the protein. Scale bar, 2 μm. PC, phase contrast.

In order to confirm the exclusion of RNases J1 and J2 from the nucleoid region, we treated cultures expressing the fusion proteins with rifampicin to stop transcription. The stop in transcription results in relaxation of the nucleoid and, as a result, it delocalizes from the central region of the cell and spreads to the whole cytoplasm (Hunt *et al.*, 2006). This effect is accompanied by a complete delocalization of RNases J1 and J2, which now are evenly distributed throughout the cytoplasm (Figure 17). Similar localization and delocalization pattern upon rifampicin treatment have been shown previously for ribosomes in *B. subtilis* (Mascarenhas *et al.*, 2001).
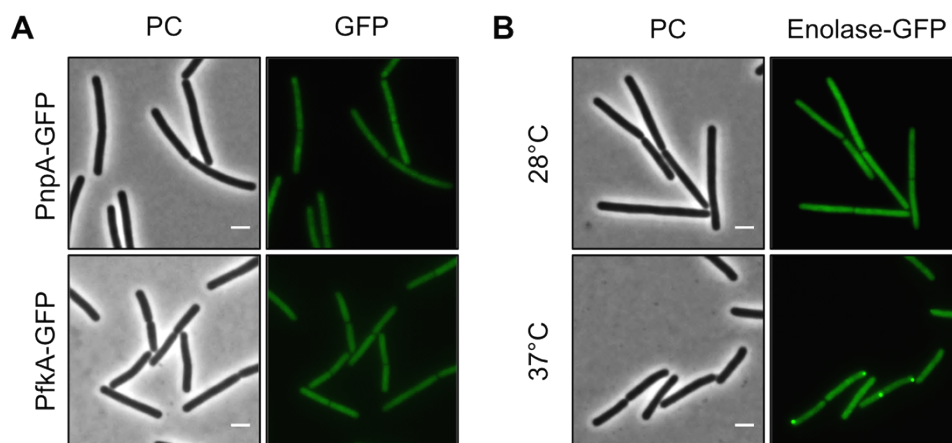
Figure 15.   The enzymes PNPase, PfkA, and enolase show a cytosolic localization. Fluorescence microscopy of strains harboring GFP fusions. **(A)** The strains GP1698 (*pnpA*-gfp) and GP1720 (*pfkA-gfp*) were grown in LB medium at 28°C to mid-exponential phase. The fusion proteins are homogenously distributed within the cytoplasm. **(B)** Strain GP1700 (*eno-gfp*) was grown to mid-exponential phase in LB medium at 28°C or 37°C. The protein appears widespread in the cytoplasm at both temperatures but at 37°C some cells show bright spots localized at the poles. Scale bar, 2 μm. PC, phase contrast.

We were able to confirm the localization of the CshA around the nucleoid (Figure 16) and its delocalization upon rifampicin-inhibited transcription (not shown). Taken together, these observations suggest that both RNase J1 and J2 are localized to those areas in the cytoplasm where the RNA target molecules are present. Interestingly, very similar results have been obtained for the localization of the DEAD box helicase CshA (Hunger et al., 2006).

For the glycolytic enzymes enolase and phosphofructokinase, we detected an even distribution in the cytoplasm (Figure 15). Interestingly, enolase formed bright spots at the polar regions of some cells at 37°C but not at 28°C.
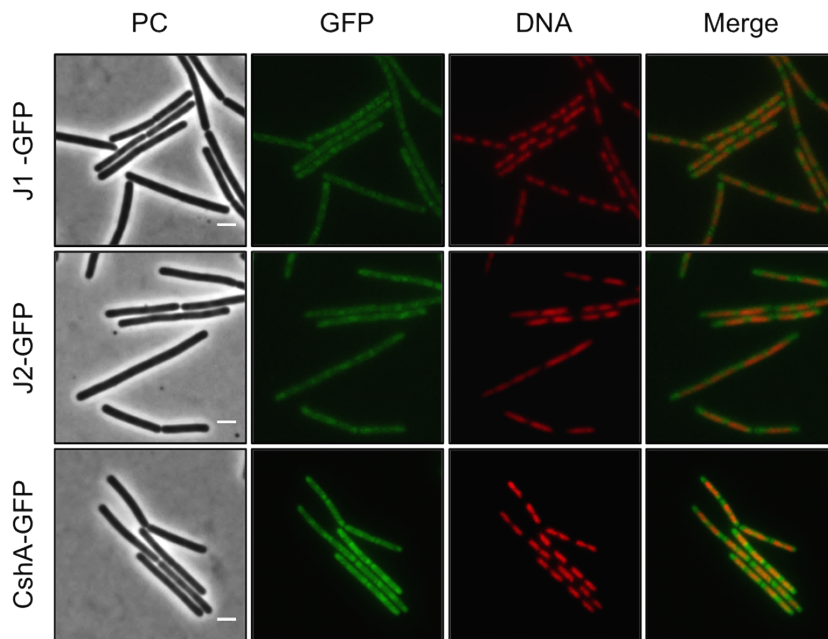
Figure 16. **The RNases J1 and J2, as well as the RNA helicase CshA are localized to the cytosol, surrounding the nucleoid.** Fluorescence microscopy of strains GP1722 (*rnjA-gfp*), GP1699 (*rnjB-gfp*), and GP1721 (*cshA-gfp*). The cells were grown in LB medium at 28°C to mid-exponential phase. The nucleoid was stained by DAPI as described above in the materials and methods section. The proteins are distributed in the cytoplasm concentrating at the poles. The concentration of the proteins is lower at the centre of each cell, where the nucleoid is positioned, as can be observed by DAPI stain. Scale bar, 2 μm. PC, phase contrast.
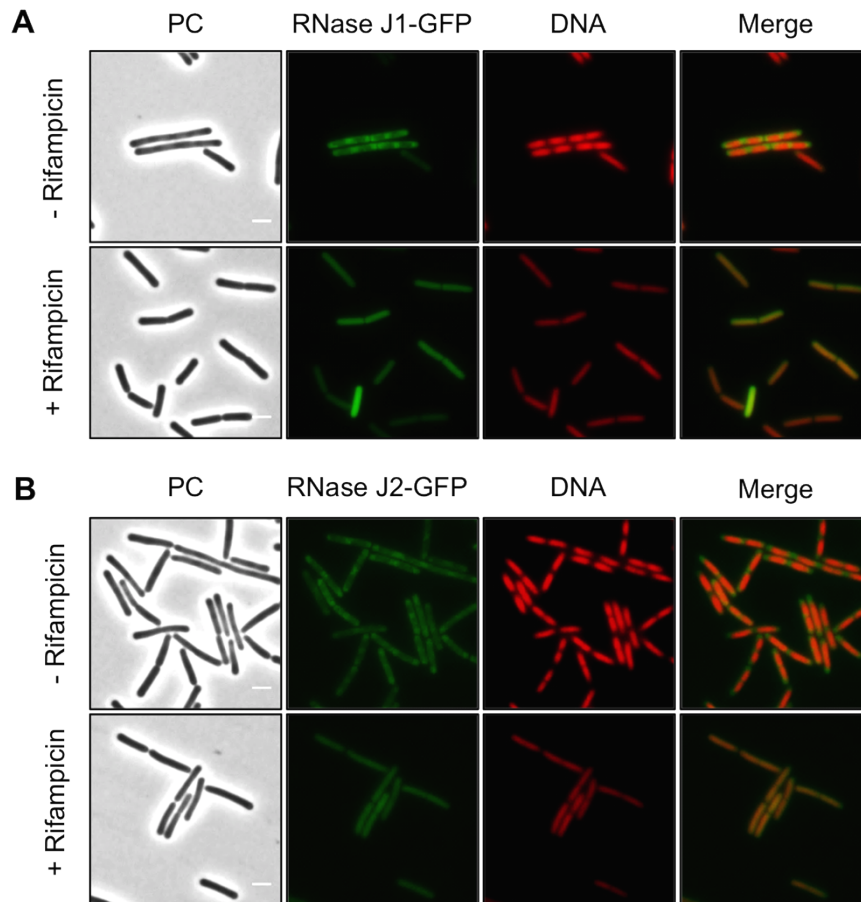
Figure 17. **RNase J1 as well as its paralogue RNase J2 delocalize upon treatment with rifampicin**. Fluorescence microscopy of strains **(A)** GP1694 (Pxyl-*rnjA-gfp*) and **(B)** GP1695 (Pxyl-*rnjB-gfp*). Bacteria were grown in LB medium at 37°C to mid-exponential phase, when rifampicin or methanol was added to the cultures as described above. The expression of RNase J1-GFP and RNase J2-GFP was induced by addition of 0.1% xylose to the culture medium. The nucleoid was stained by DAPI as described in the Material and methods section. The sub-polar localization of both RNases J1 and J2 is lost as the RNA synthesis is inhibited and the proteins appear evenly distributed in the cytoplasm. Upon addition of rifampicin the nucleoid, stained by DAPI, spreads occupying the majority of the cell volume. Scale bar, 2 μm. PC, phase contrast.

3.1.3. Conclusions

We have performed a detailed analysis of the localization of the proteins involved in RNA degradation in *B. subtilis*. However, our results are in contradiction with the existence of an RNA degradosome in this bacterium: while RNase Y is located at the cytoplasmic membrane, the exoribonucleases RNase J1 and J2 as well as the RNA helicase CshA are localized in the peripheral regions of the cell, i. e., the region where the bulk of the RNA is localized. Moreover, the polynucleotide phosphorylase and the glycolytic enzymes are found homogeneously distributed in the cytoplasm.

3.2. *In vivo* interaction of the paralogous RNases J1 and J2

RNase J1 and RNase J2 have been shown to form a complex *in vivo*, that also modifies the individual specificities of the enzymes (Mathy *et al.*, 2010). However, there is still controversy regarding the oligomeric state of the proteins *in vivo.* It is known by structural and functional analysis that the C-terminal domain of RNase J1 (see Figure 6) is necessary for its dimerization and for its activity *in vitro.* However, the relevance of the C-terminal domain for the *in vivo* interaction and activity of RNase J1 and J2 of *B. subtilis* is not known.

3.2.1. RNases J1 and J2 interact *in vivo* through the C-terminal domain

To analyze the relevance of the C-terminal domain in the interaction of the paralogous RNases J1 and J2, several strains were constructed in which the proteins were fused to a tag that made them possible to be identified. The constructs were then integrated in the chromosome, so that the fusion proteins could be expressed from their native promoters. The addition of a tag was necessary to be able to purify the proteins through an affinity column. Furthermore, the tags serve the second purpose of identification, since the proteins have very similar molecular weights (see Table 18). Thus, the strains GP1048 (*rnjA*-Strep *rnjB*-3xFLAG), GP1731 (*rnjB*-Strep *rnjA*-3xFLAG) were used. Furthermore, two strains were created in which the C-terminal domain of RNase J2 (amino acids 450-555) was truncated (see Figure 6), assuming that the structures of RNase J1 and J2 are superimposable (sequences share 49% identity and 70% similarity). These strains were GP1740 (*rnjA*-Strep *rnjBΔCter*-3xFLAG) and GP1741 (*rnjBΔCter*-Strep *rnjA*-3xFLAG). To perform the experiment, the strains were grown in LB medium and the cultures were harvested. The pellets were resuspended in buffer and the cells were broken open by French press, and Strep-tagged proteins were purified as decribed above.

Table 18.   Molecular weight of proteins calculated by ExPASy from their amino acid sequence.

	WT	Strep	3xFLAG
RNase J1	61.52	63.43	65.10
RNase J2	61.17	63.09	64.76
RNase J2ΔCter	49.09	51.00	52.67

To analyse the interaction partners of the bait proteins we performed SDS-PAGE. Furthermore, the proteins could be identified by Western blot. Same concentration of each cell extract has been loaded in the gel, to confirm the expression of all the tagged proteins (Figure 18B and C). Interestingly, the expression of the truncated RNase J2 seems to be higher than that of the full

protein (Figure 18B lanes 5 and 7, and 17C lanes 1 and 3). This could indicate a destabilizing effect of the C-terminal domain, or a regulatory mechanism involving this part of the gene. The amounts of RNase J1 seem to also be slightly increased in presence of the truncated RNase J2 (Figure 18B lanes 1 and 3).
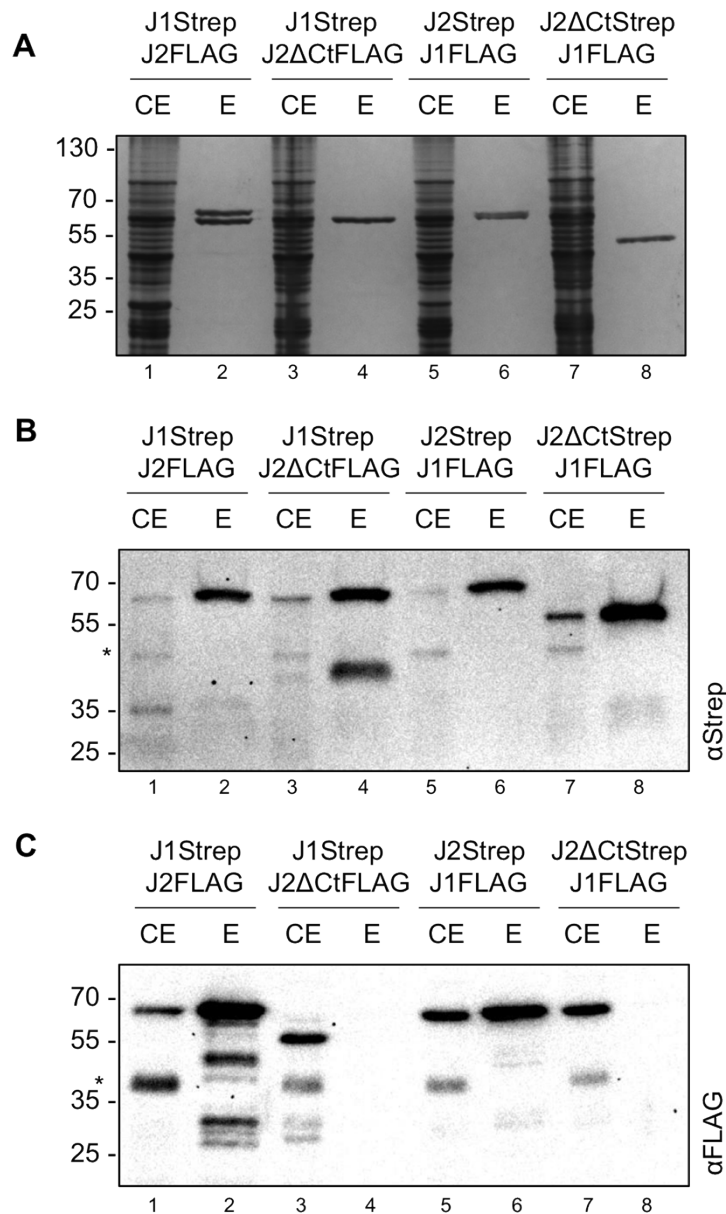
Figure 18. *RNase J1 and J2 interact thorugh the C-terminal domain of RNase J2 in vivo.* Cells from strains GP1048 (*rnjA*-Strep *rnjB*-3xFLAG), GP1731 (*rnjB*-Strep *rnjA*-3xFLAG), GP1740 (*rnjA*-Strep *rnjBΔCter*-3xFLAG) and GP1741 (*rnjBΔCter*-Strep *rnjA*-3xFLAG) were cultured in LB at 37°C to an OD$_{600}$ of 1. The cells were disrupted and proteins were purified though a StrepTactin chromatography column as described above. The fractions were analyzed by denaturing PAGE and visualized by silver staining **(A)**, and Western blot with antibodies anti-Strep **(B)**, and anti-Flag **(C)**. CE, cell extract; Ct, C-terminal domain; E, elution fraction; *, unspecific bands.

It was previously shown that a deletion of RNase J2 increases the expression of RNase J1 1.4-fold (Jamalli *et al.*, 2014). This could indicate that the truncated version of RNase J2 is not active. Furthermore, we can observe that RNase J2 co-purifies with RNase J1 and *vice versa* (Figure 18 lanes 2 and 6)*. We can also confirm that the C-terminal domain is necessary for the interaction between RNase J1 and J2, since the truncated RNase J2 cannot interact with the full-length RNase J1 (Figure 18 lanes 4 and 8). It is interesting to note that, in the presence of truncated RNase J2, there seems to be an accumulation of a smaller fragment of RNase J1 (Figure 18B lane 4). We can speculate that RNase J1 is less stable in the absence of interaction with RNase J2. Furthermore, we observe degradation products of RNase J2 (Figure 18C lane 2). These shorter protein fragments are not present when RNase J2 is Strep-tagged (Figure 18B lane 6), so we can hypothesize that the addition of the 3xFlag tag destabilizes the protein, making it more sensitive to degradation. Interestingly, the calculated isoelectric point (pI) of RNase J2 is very basic (pI calculated by ExPASy from the primary structure, 8.47). However, the calculated pI decreases drastically upon addition of the 3xFLAG tag to 6.43 (see Table 19).

Table 19.   Isoelectric point calculated by ExPASy from the amino acid sequence.

	WT	Strep	3xFLAG
RNase J1	5.93	5.97	5.57
RNase J2	8.47	8.41	6.43
RNase J2ΔCter	7.74	7.71	6.14

3.2.2. Oligomerization of the RNases J1 and J2 *in vivo*

As has been described before (see 1.5.5), RNases J1 and J2 interact *in vivo* and *in vitro*, and can form dimers and heterodimers. However, it is not known how these complexes exist *in vivo* naturally, and how the disruption of the interaction affects the complex formation. The native state of the complex in the cell was studied following the same procedure as described above (see 3.2.1), although disrupted by tissue lyser. The elution fractions were, however, loaded on a native-PAGE gel and the proteins were identified by Western blot. In Figure 19 we can observe that RNase J1/J2 exists as a dimer or tetramer, and both oligomers are present in similar amounts (lanes 1 and 3). It was shown that when its C-terminal domain is truncated, RNase J2 can no longer interact with its paralogue RNase J1 (Figure 18 lanes 4 and 8). Nonetheless, this does not impede the formation of homodimers and homotetramers by RNase J1 (Figure 19 lane 2). However, the truncated RNase J2 cannot self-interact, as it is demonstrated by the absence of oligomers (Figure 19A lane 4).

It is still unknown, however, if full-length RNase J2 was able to self-interact in the absence of RNase J1. Furthermore, it had not been assessed whether RNase J1 could also oligomerize when RNase J2 is completely deleted. Several strains were created in order to investigate these interactions further, combining Strep-tag fusion proteins and protein deletions. The strain GP1034 (*rnjA*-Strep) was transformed with genomic DNA from the srains GP1291 (*ΔrnjB*) and GP1732 (*rnjBΔCter*), to generate the strains GP1723 (*rnjA*-Strep *ΔrnjB*) and GP1736 (*rnjA*-Strep *rnjBΔCter*), respectively. Furthermore, the strain GP2318 (*rnjB*Strep *ΔrnjA*) was created by transforming chromosomal DNA from the GP2502 strain (*ΔrnjA*) into GP1687 (*rnjB*-Strep). The strain GP1737 harbors the fusion of a Strep-tag to the truncated RNase J2 protein.
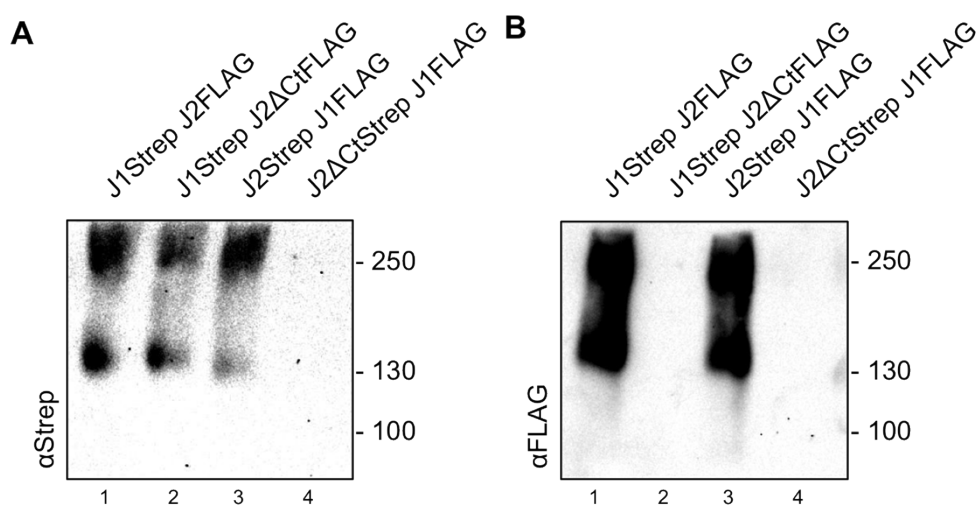
Figure 19. **RNase J1 and J2 oligomerize as dimer and tetramer *in vivo*. RNase J1 can also form dimers and tetramers itself.** Cells from strains GP1048 (*rnjA*-Strep *rnjB*-3xFLAG), GP1731 (*rnjB*-Strep *rnjA*-3xFLAG), GP1740 (*rnjA*-Strep *rnjBΔCter*-3xFLAG) and GP1741 (*rnjBΔCter*-Strep *rnjA*-3xFLAG) were cultured in LB at 37°C to an OD_{600} of 1. The cells were disrupted by tissue lyser and proteins were purified though a StrepTactin chromatography column as described. The fractions were analyzed by native PAGE and visualized by Western blot with antibodies anti-Strep **(A)** and anti-FLAG **(B)**. Ct, C-terminal domain.

The cells were grown in LB at 37°C and disrupted by French press as described. After purification through a Streptactin column, the elution fractions were analysed in a native-PAGE and Western blot, as for Figure 19A. However, the oligomerization of the proteins could not be detected, since the native-PAGE protocol used does not allow the migration of basic proteins. The homodimeric and homotrimeric forms of RNase J1 could be detected (not shown), but no oligomer involving RNase J2 was seen. The proteins RNase J1 and RNase J2 have very different calculated isoelectric points (pI) (see Table 19). For this reason, the elution fractions were analysed on a native-PAGE for basic proteins, where they are artificially charged by the dye Coomassie Brilliant Blue G, allowing the basic proteins to migrate towards the anode. The cell extracts were incubated for one hour with DNase I and RNase A, previous to centrifugation, and

subsequently applied to a Streptactin chromatography column. The elution fractions were loaded onto a gel, and the proteins could properly migrate and separate (Figure 20).
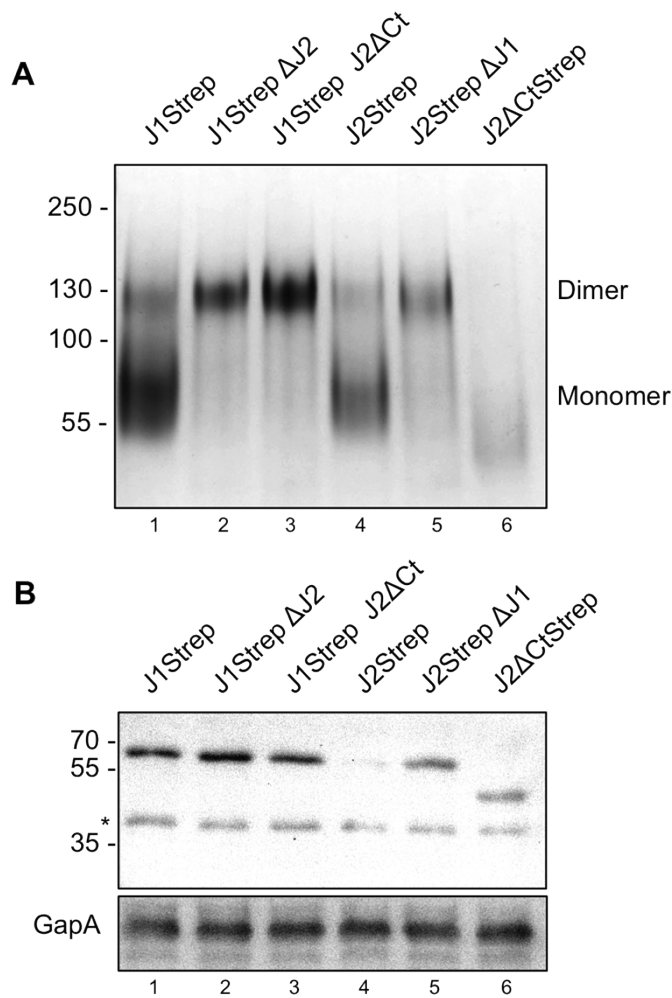
Figure 20. **RNase J1 and J2 interact *in vivo* forming hetero- and homodimers.** Cells from strains GP1034 (*rnjA*-Strep), GP1687 (*rnjB*-Strep), GP1723 (*rnjA*-Strep *ΔrnjB*), GP1736 (*rnjA*-Strep *rnjBΔCter*), GP1737 (*rnjBΔCter*-Strep), and GP2318 (*rnjB*Strep *ΔrnjA*) were cultured in LB at 37°C to an OD_{600} of 1. The cells were disrupted by French press and the cell extract was incubated for 1 hour on ice with 6.75 µg/ml RNase A and 5 µg/ml DNase I. **(A)** Proteins were purified though a StrepTactin chromatography column as described above. The fractions were analyzed by Native PAGE for basic proteins and visualized by silver staining. **(B)** A total of 15 µg of protein from the cell extracts were loaded on a denaturing PAGE and analyzed by Western blot with anti-Strep antibody. Antibody anti-GapA was used as a loading control. CE, cell extract; Ct, C-terminal domain; E, elution fraction; *, unspecific band.

In the absence of RNase J2 or in the presence of the truncated RNase J2 protein, RNase J1 is able to homodimerize (Figure 20A lanes 2 and 3). Interestingly, the dimer of RNase J1 and J2 was also present. However, a greater amount of monomer is visible (Figure 20A lane 1). This contradicts what was seen before (Figure 19 lanes 1 and 3). This effect is also visible when the pull-down is performed with RNase J2 as bait (Figure 20A lane 4). However, RNase J2, in the absence of RNase J1, is able to self-interact and form dimers (Figure 20A lane 5). The truncated

RNase J2 protein, as was shown before (Figure 19B lane 4), is not able to oligomerize. Interestingly, the presence of tetramers could not be observed. In this experiment, compared to the one described above (see 3.2.2), the cell extracts were incubated with RNase A and DNase I. It is tempting to speculate that the tetramers are formed when the proteins can bind to RNA. Furthermore, the addition of Coomassie Brilliant Blue G could have, indeed, affected the native oligomerization state. Moreover, the presence of monomers in the strains where RNase J1 and J2 can interact in a native state, but not when only one of the proteins is present, raises many questions.

Furthermore, the cell extracts were also analyzed by SDS-PAGE and Western blot. A total of 15 µg of protein were loaded in each lane. An antibody raised against GapA was used as a loading control. Interestingly, we observe again an increase in the protein amounts of RNase J2, when the C-terminal part is truncated (Figure 20B lanes 4 and 6). Moreover, the deletion of RNase J1 seems to affect the levels of RNase J2 in the same manner. However, silver stain analysis of the elution fractions after SDS-PAGE showed that several proteins that bind non-specifically to the column were also highly increased in this strain (not shown). This could be a consequence of the global effect of the deletion of RNase J1 on the mRNA levels (see 1.5.5). The increase in the levels of RNase J1 in the absence of RNase J2 is also visible (Figure 20 lanes 1 and 2); in the presence of the truncated RNase J2, however, it is not possible to appreciate.

3.2.3. Localization of the RNases J1 and J2 in different deletion mutants

To further investigate the behaviour of the RNases J1 and J2 *in vivo* in the absence or presence of the paralogues, fluorescence microscopy was performed, as described in materials and methods. Furthermore, the effect of the deletion or truncation of RNase J2 on the cell morphology was studied. The deletion of the *rnjA* gene, coding for RNase J1, shows very strong morphological defects, such as elongated and curly cells. The deletion of RNase J2, however, does not produce such a strong phenotype. Indeed, the majority of the cells within the population show a wild type phenotype. Some elongated cells are present, although they do not present the bulges and curls that exist in the deletion of *rnjA*. Furthermore, the elongated cells are not as long as those of the RNase J1 mutant (Figure 21). The same observations are true for the truncation of RNase J2. These results show that, although the deletion of RNase J2 causes a milder phenotype than that of RNase J1, the protein could also be involved in the processing of certain transcripts necessary for proper cell division. Furthermore, the truncation of the RNase J2 produces a same effect, raising the question of whether the activity of RNase J2 or its oligomerization is necessary for a normal phenotype.

To address the question of the localization of these paralogous RNases several strains were constructed. RNase J1 was fused to GFP and combined with the deletion and truncation of RNase J2 (strains GP1722 (*rnjA-gfp*), GP1734 (*rnjA-gfp rnjBΔCter*), and GP2317 (*rnjA-gfp ΔrnjB*)). Furthermore, RNase J2 was fused to GFP in the presence and absence of RNase J1, generating strains GP1749 (*rnjB-gfp*), and GP1750 (*rnjB-gfp ΔrnjA*), respectively. To answer the question of whether the truncation of RNase J2 altered its normal localization, the truncated protein was fused to GFP in the strain GP1733 (*rnjBΔCter-gfp*). All the GFP fusions were expressed from the native locus of the proteins, and a second copy of the tagged protein was not present. As was shown before, RNase J1 and J2 localize to the cytoplasm of the cell, surrounding the nucleoid (Figure 22A and B). As its is shown, the absence of RNase J2 or the truncation of its C-terminal domain does not seem to affect the localization of RNase J1 (Figure 22A). However, the morphology of the cell is affected, presenting elongated and thickened cells that even present bulges. This is interesting, since it only happens in when the fusion of RNase J1 to GFP is combined with either the deletion or truncation of RNase J2.
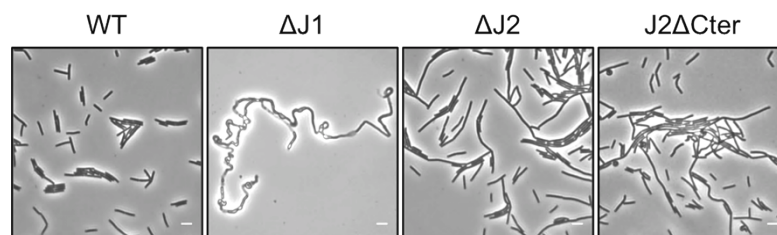
Figure 21. **The deletion strain of RNase J1 shows a filamentous and curly phenotype. The deletion of RNase J2 or truncation of the C-terminal domain causes some cells to be elongated.** Phase contrast images of strains 168 (WT), GP1291 (*ΔrnjB*), GP1732 (*rnjBΔCter*), and GP2502 (*ΔrnjA*) grown in LB medium at 37 °C to stationary phase. Scale bar 5 µm.

The impact of the deletion of *rnjA* on the localization of RNase J2 is, however, very strong. In the absence of RNase J1, RNase J2 localizes in defined spots, which are even visible in the light microscopy image (Figure 22B). This localization suggests that the protein is aggregating. However, it has been proven that RNase J2 does not aggregate but oligomerizes in the absence of RNase J1 (Figure 20A). Furthermore, the curly and elongated phenotype is more severe than that of the deletion of RNase J1 (Figure 21). Moreover, the truncated version of RNase J2 can be found evenly disperse in the cytoplasm, confirming that it cannot interact with RNase J1.
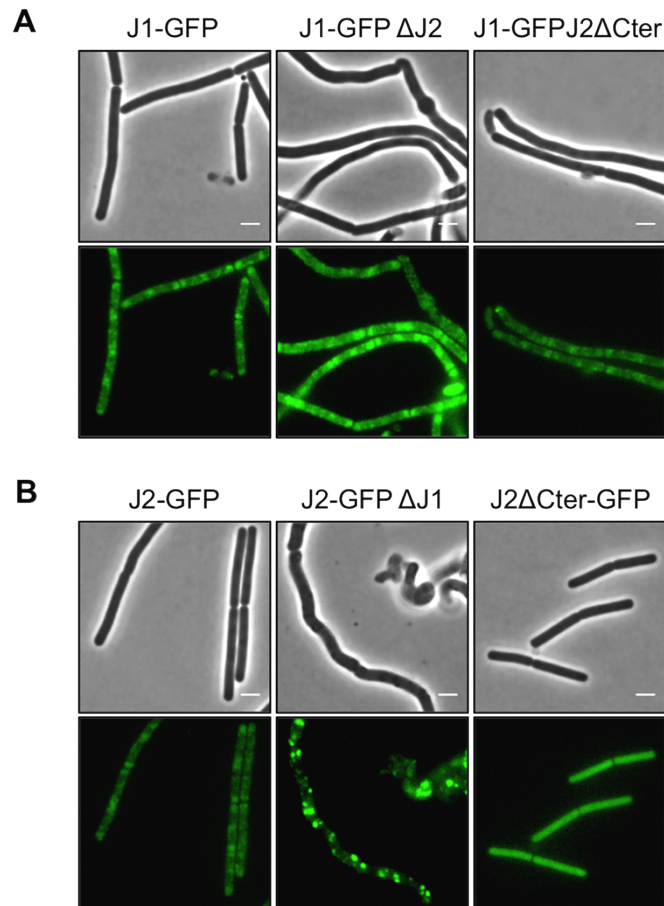
Figure 22. **RNase J1 maintains its localization when RNase J2 does not interact with it. RNase J2 can no longer interact with RNA when RNase J1 is not present.** Phase contrast and fluorescent microscopy of strains **(A)** GP1722 (*rnjA-gfp*), GP1734 (*rnjA-gfp rnjBΔCter*), and GP2317 (*rnjA-gfp ΔrnjB*) and **(B)** GP1733 (*rnjBΔCter-gfp*), GP1749 (*rnjB-gfp*), and GP1750 (*rnjB-gfp ΔrnjA*) grown in LB medium at 37 °C to mid-logarithmic phase.

3.2.4. Conclusions

RNases J1 and J2 can interact *in vivo* through their C-terminal domains. Furthermore, they oligomerize, forming dimers and tetramers in similar amounts. RNase J1 and J2 are both, however, able to interact amongst each other. Furthermore, the deletion of the RNase J1 affects the localization of RNase J2 in the cell, while RNase J1 remains localized as wild type in the absence of RNase J2. Although the absence of RNase J2 does not cause a very strogn phenotype alone, the additional fusion of RNase J1 to GFP increases the length and thickness of the cells. The truncation of the C-terminal domain of RNase J2 hinders its interaction with RNase J1 and with itself, as well as its localization in the cell.

3.3. *In vitro* activity of the enzyme PNPase of *Bacillus subtilis*

Several regulatory mechanisms have been described for PNPase of different organisms, however, not much is known about the regulation of the *B. subtilis* PNPase. PNPase has been related to carbon metabolism, since it is part of a putative complex with the glycolytic enzymes enolase and PfkA and several other RNA-related proteins (see 1.5). Thus, the enzymes enolase and PfkA have been purified to assay their effect on the *in vitro* degradation activity of PNPase. Furthermore, several metabolites affect the acitivity of PNPase, although it is not known whether they have any effect on the activity of PNPase. The affect of c-di-AMP, c-di-GMP and citrate was assayed. Furthermore, the crystal structure of PNPase from *B. subtilis* was obtained in collaboration with Johannes Arens, Achim Dickmanns and Piotr Neumann (Prof. Dr. Ficner, Dept. Molecular and Structural Biology, Göttingen Universität).

3.3.1. Crystal structure of PNPase from *B. subtilis*

The PNPases of several organisms have been crystallized (Symmons *et al.*, 2000; Shi *et al.*, 2008; Nurmohamed *et al.*, 2009; Hardwick *et al.*, 2012), however, the structure of the PNPase from *B. subtilis* was not available. During my Master's thesis I was able to purify the enzyme (Cascante-Estepa, 2014). Subsequently, the enzyme was crystallized and th ediffraction pattern could be used to obtain the crystal structure at a resolution of 2.3 Å, in the Department of Molecular Structural Biology (Arens, 2015).

The PNPase of *B. subtilis* possesses a domain organization similar to other PNPases. It is composed of five domains: two PH domains, of which only the second is active, a poorly-conseved helical domain, and two RNA-binding domains, KH and S1 (Figure 23).
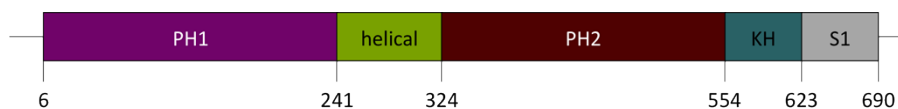
Figure 23. **Domain organization of the enzyme PNPase of *Bacillus subtilis*.** The enzyme possesses five defined domains. PH2 contains the active site, while PH1 has lost the enzymatic activity. KH and S1 domains are the RNA-binding domains. (Symmons *et al.*, 2000; Jarrige *et al.*, 2002; Stickney *et al.*, 2005; Briani *et al.*, 2007; Shi *et al.*, 2008).

PNPase is a trimer that oligomerizes as a ring-like structure, with a central channel that serves as the entrance for the RNA. Although the crystal structure of PNPase with an RNA molecule could not be obtained, the base stacking of the amino acid phenylalanine 77 with an RNA base in the center of the channel could be seen (Figure 24A). The PH domains form the ring in the structure, while the helical domain and the KH and S1 domains are localized outwards from the central

channel. The KH and S1 domains seem to be very flexible (Figure 24B). Only one of the PH domains is, however, active. The enzyme possesses one active site at the PH2 domain, which could be identified by the presence of an ADP molecule (Figure 24C). The color code of the structure corresponds to that of the domains in Figure 23.
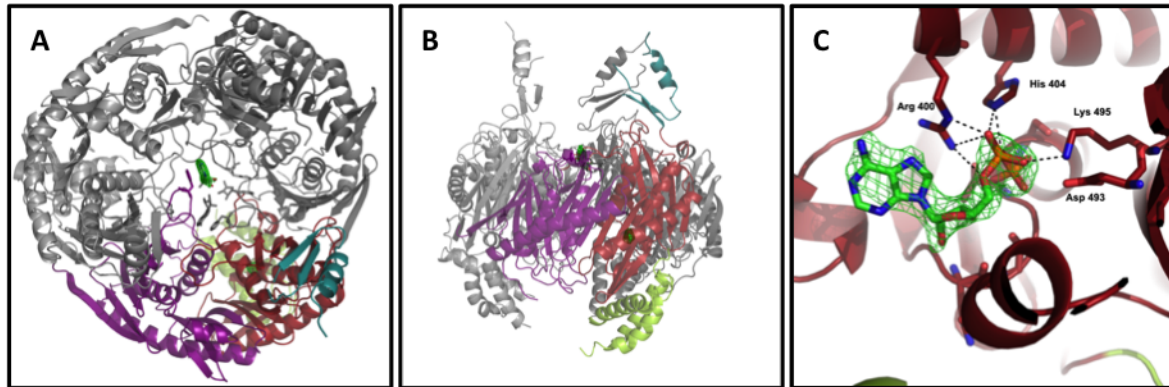
Figure 24.   Crystal structure of PNPase interacting with and RNA base, inorganic phosphate and ADP (2.3 Å). Johannes Arens, Achim Dickmanns, and Piotr Neumann crystallized and modelled the enzyme. The obtained crystal structure of His$_6$-PNPase has a resolution of 2.3 Å. The enzyme oligomerizes as a trimer with a ring-like structure. The central channel is the entry site for RNA, where it gains access to the active site. In the first image we can see a base of an RNA molecule base stacking with Phe77 of PNPase. The enzyme possesses one active site per monomer situated at the PH2 domain. In the second image we can see the active site identified by the presence of a Pi in the crystal structure. In the third image we can observe the interactions of adenosine diphosphate (ADP) with the amino acids of the active site. (Arens, 2015)

3.3.2. Purification of PNPase, enolase and PfkA

For the purification the enzymes PfkA, enolase, and PNPase the plasmids pGP393, pGP563, and pGP838 were used, respectively. The proteins are fused to an N-terminal His$_6$-tag. Briefly, the plasmids were transformed into a producer strain of *E. coli* and the expression of the proteins was induced in LB medium at 37°C by addition of IPTG. Upon disruption of the cells, the tagged proteins were purified through a Ni^{2+}-NTA sepharose column, and eluted by increasing amounts of imidazole as described (see Table 15). After analysis of the fractions by SDS-PAGE, the relevant fractions were pooled and applied to a size-exclusion chromatography (SEC). The fractions containing the protein were concentrated and stored in aliquots at -80°C.

The purification of PNPase had been previously performed (Cascante-Estepa, 2014) and the concentration of imidazole was known, so the protein was eluted from the column by directly applying buffer with 100 mM imidazole (Figure 25A). The elution fractions were very clean and were analyzed by SEC. This revealed a bigger peak with elution time 60.29 minutes, which corresponds to a molecular weight of 284.99 KDa. The molecular weight of a monomer of His$_6$-PNPase is 78.86 KDa; consequently, the peak would correspond to 2.6 ≈ 3 monomers. As

expected, PNPase is a trimer in solution. The presence of the protein in the peak at 60.29 was confirmed by analyzing the fractions 14, 15, and 16 by SDS-PAGE (Figure 25A). Subsequently, the protein was concentrated to 1.63 mg/ml or 20.66 µM.
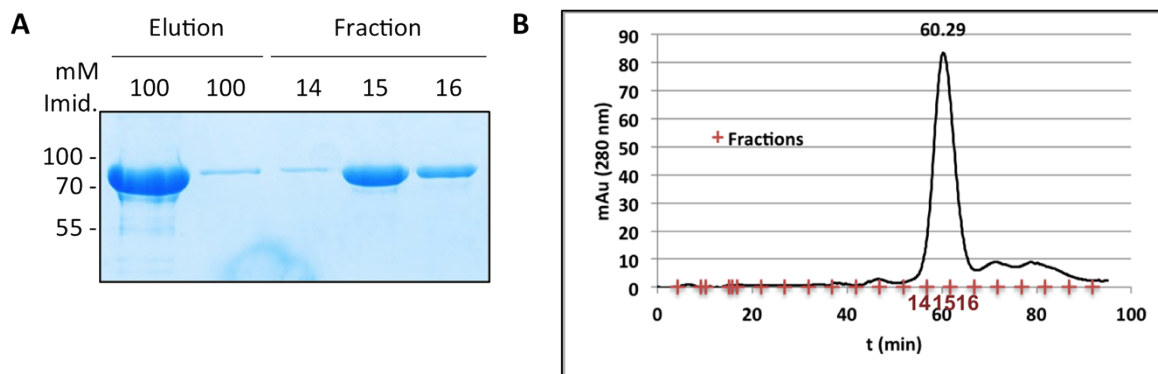
Figure 25. **Purification of His$_6$-PNPase from DH5α::pGP838 and size-exclusion chromatography.** Expression of His-tagged PNPase was induced by addition of 1 mM IPTG to a culture of *E. coli* harbouring the pGP838 plasmid. **(A)** The cells were disrupted and purification was performed as described above. **(B)** Relevant elution fractions were pooled and applied to a size-exclusion chromatography column as described in Materials and methods. The fractions were analysed by SDS-PAGE and Coomassie staining and the ones containing enzyme were concentrated and preserved in aliquots at -80 °C. Imid., imidazole.

For the purification of His$_6$-enolase several elution steps were performed with increasing amounts of imidazole. Although the wash fractions were already very clean, many additional bands were eluted with 30 mM imidazole (Figure 26A). Consequently, only the other three fractions were pooled and analyzed by SEC. This showed three major peaks with elution times of 35.60, 44.67, and 58.13 minutes (Figure 26B). Fractions 8, 10, 12, and 13, corresponding to the peaks, were analyzed by SDS-PAGE (Figure 26C). Fractions 8 and 12 contained no protein. The fractions 12 and 13 corresponded to the peak with 58.13 minutes elution time, which corresponds to a size of 351.72 KDa. The molecular weight of a monomer of His$_6$-eno is 47.98 KDa; consequently, the peak would correspond to 7.33 ≈ 7 monomers. However, the crystal structure of enolase revealed that the protein oligomerized as an octamer (Newman *et al.*, 2012). Nonetheless, the size-exclusion chromatography only offers an approximate size, which is more accurate for globular proteins. For this reason, it can be assumed that 7.33 corresponds to an octamer. Subsequently, the protein was concentrated to 0.23 mg/ml or 4.79 µM.

For the purification of His$_6$-PfkA several elution steps were performed with increasing amounts of imidazole. An intermediate washing step with 2.5 M NaCl had been performed. The elution fractions (Figure 27A) were pooled and analyzed by SEC. This showed two peaks with elution times 44.30, and 71.77 minutes (Figure 27B). Fractions 10, 15, and 16 corresponding to the peaks were analyzed by SDS-PAGE (Figure 27C). Fractions 10 contained little amounts of protein, while

fractions 15 and 16, corresponding to the peak with 71.77 minutes elution time, contained the majority of the protein.

Figure 26. **Purification of His$_6$-enolase from DH5α::pGP563 and size-exclusion chromatography.** Expression of His-tagged enolase was induced by addition of 1 mM IPTG to a culture of *E. coli* harbouring the pGP563 plasmid. **(A)** The cells were disrupted and purification was performed as described above, and the fractions were analysed by SDS-PAGE and Coomassie staining. **(B)** Relevant elution fractions were pooled and applied to a size-exclusion chromatography column as described in Materials and methods. **(C)** The fractions were analysed by SDS-PAGE and Coomassie staining and the ones containing enzyme were concentrated and preserved in aliquots at -80 °C. Inj., injection; Imid., imidazole; W5, wash 5.

The molecular weight of a monomer of His$_6$-PfkA is 35.65 KDa; consequently, the peak would correspond to 2.6 ≈ 3 monomers. However, the crystal structure of PfkA revealed that the protein oligomerized as a tetramer (Newman *et al.*, 2012). As was mentioned for the purification of enolase, the size-exclusion chromatography only offers an approximate size, which is more accurate for globular proteins. Nonetheless, it could be that the washing with high salt affected the oligomerization. However, this more likely would result in aggregation or complete disruption of the oligomer. The small peak at 45.30 elution time could be aggregated protein, but was still the smaller peak. The protein from fractions 15 and 16 was then concentrated to 0.75 mg/ml or 21.04 μM.
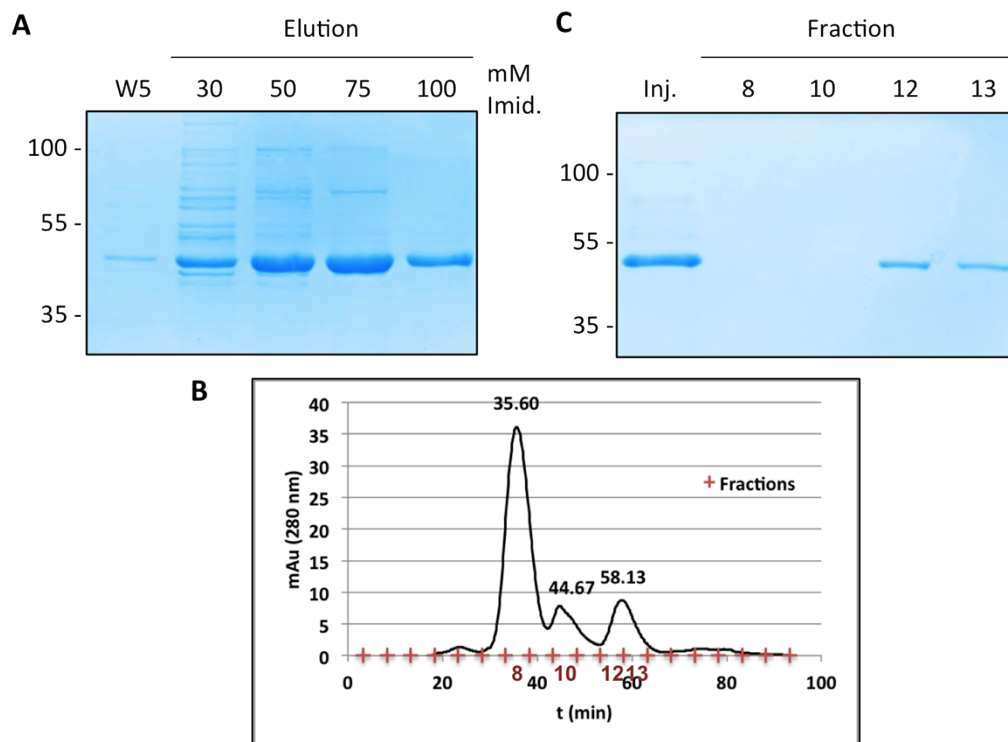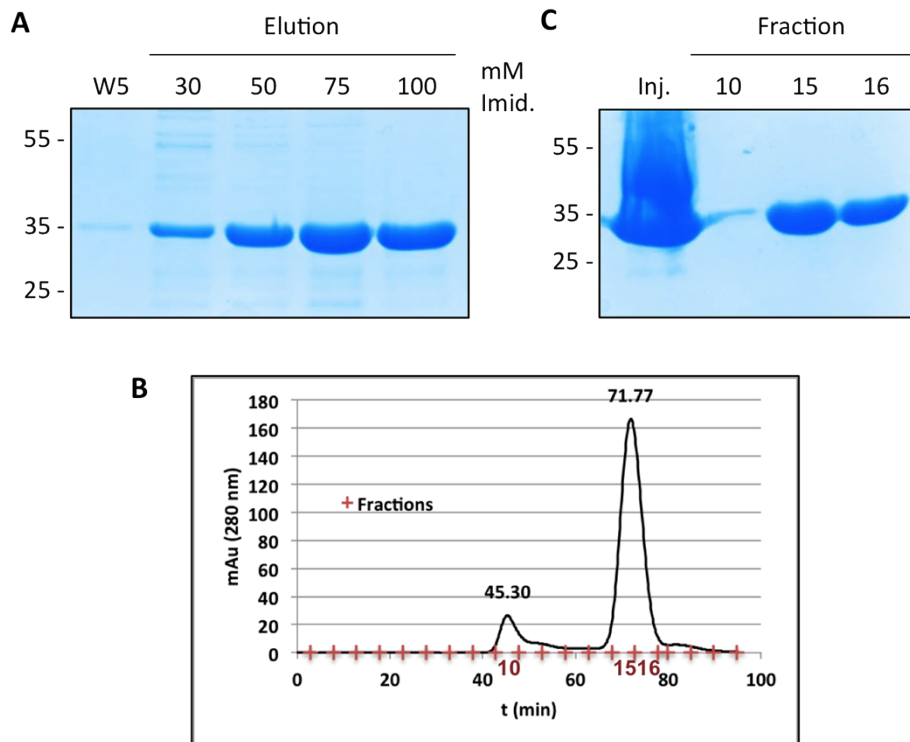
Figure 27. **Purification of His$_6$-PfkA from DH5α::pGP393 and size-exclusion chromatography.** Expression of His-tagged PfkA was induced by addition of 1 mM IPTG to a culture of *E. coli* harbouring the pGP393 plasmid. **(A)** The cells were disrupted and purification was performed as described above, and the fractions were analysed by SDS-PAGE and Coomassie staining. **(B)** Relevant elution fractions were pooled and applied to a size-exclusion chromatography column as described in Materials and methods. **(C)** The fractions were analysed by SDS-PAGE and Coomassie staining and the ones containing enzyme were concentrated and preserved in aliquots at -80 °C. Inj., injection; Imid., imidazole; W5, wash 5.

3.3.3. Degradation activity of PNPase *in vitro*

The purified PNPase was used to assay its activity *in vitro*. However, the conditions could only be improved in this time for the degradation activity. Nonetheless, degradation activity by the purified enzyme *in vitro* was also observed (not shown). To study the degradation of PNPase, the conditions were improved by following the already published assay for *in vitro* activity of PNPase from *E. coli* (Nurmohamed *et al.*, 2011). Briefly, a reaction mix was prepared that contained 15mer poly(A) RNA, inorganic phosphate, Tris-HCl pH 8.0 buffer, MgCl$_2$, and 250 nM of purified PNPase. The reaction was performed for 2 minutes at 25 °C. The RNA was analyzed by ion-exchange chromatography, as described above (Figure 10). The 15mer poly(A) RNA runs as a discrete peak (Figure 28A). However, the retention times displayed an enormous variability. This could be attributed to the room temperature, since the column was not temperature-regulated. The retention times showed a linear correlation with the room temperature (not shown). Furthermore, the temperature also affected the elution spectra. For this reason, some of the

curves in Figure 28 were automatically smoothed, for presentation purposes. The analysis of the integral was, however, performed in the original spectra. To obtain the percentage of degradation, the integral of each peak was calculated and compared to the control spectrum.

Activity at different concentrations of Mg^{2+}

The enzyme requires a divalent cation to be active. Although the enzyme is also active in the presence of Mn^{2+} (not shown), only the dependence on Mg^{2+} was studied. For this, several concentrations of $MgCl_2$ were applied to the reaction described above, and the enzyme was allowed to react for 2 minutes. The activity of the enzyme at concentrations 1, 2, 5 10, and 100 mM is displayed (Figure 28). However, reactions with lower concentrations of $MgCl_2$ (100, 200 and 500 µM) were performed, where the enzyme showed no degradation activity (not shown).
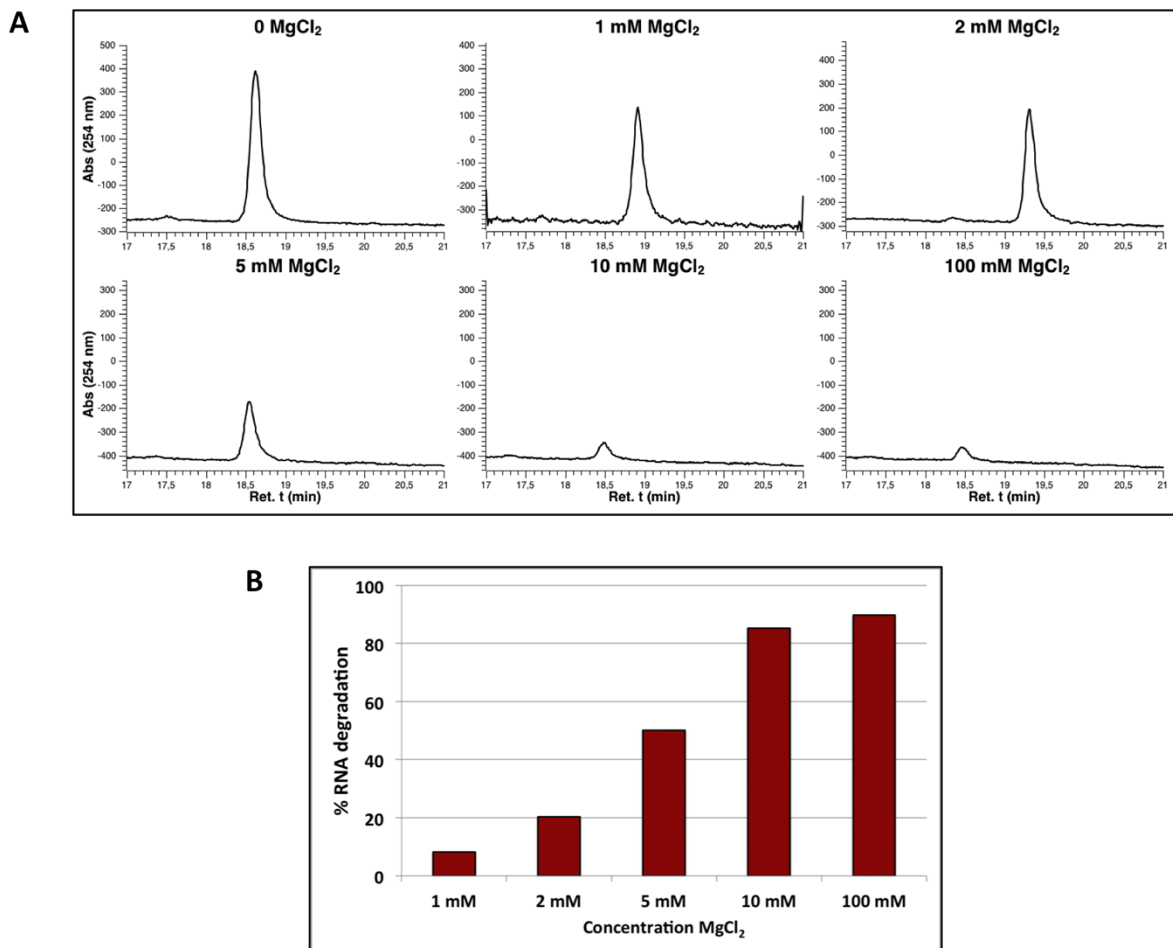
Figure 28. **Degradation of RNA by PNPase with different concentrations of $MgCl_2$.** The activity of PNPase *in vitro* on a 15mer poly(A) RNA molecule was assayed, by it incubating with the enzyme, magnesium, and Pi, for 2 minutes at 25°C. Different concentrations of magnesium were applied to the reaction **(A)**. When the reaction was stopped, it was injected to and HPLC ion-exchange chromatography column. The peaks corresponding to the RNA were integrated and compared to the reaction mix without magnesium **(B)**.

Effects of several metabolites and proteins on the *in vitro* degradation activity of PNPase

The effect of several metabolites on the degradation activity of PNPase *in vitro* was studied. The activity of PNPase form *E. coli* is enhanced by c-di-GMP in the range from 0.1 to 10 μM (Tuckerman *et al.*, 2011). To assay the effect of cyclic nucleotides, 5 μM of c-di-AMP or c-di-GMP were added to the reaction mix. The assay was performed for 2 minutes in the conditions described above. However, no difference could be seen in this conditions compared to the enzyme in the absence of cyclic nucleotides. Furthermore, the effect of citrate was assayed, since it was seen that it had an effect on the activity of the PNPase from *E. coli* (Nurmohamed *et al.*, 2011). Citrate in different concentrations was added to the reaction (1, 5, and 10 mM). The degradation activity of PNPase was reduced with increasing concentrations of citrate. However, repeating the experiment with Mg-citrate at the same concentrations revealed no difference in the degradation activity of PNPase. Thus, it can be assumed that, in the first experiment, citrate is chelating the magnesium available for the reaction, consequently reducing the degradation activity of PNPase, as was seen before (Figure 28). Furthermore, since PNPase has been proposed to be part of the RNA degradosome, the effect of the glycolytic enzymes enolase and PfkA on the activity of PNPase was assayed *in vitro.* For this purpose, the enzymes were added to the reaction mix, and a control was performed in which only PNPase was present. PNPase has been shown to be a trimer, PfkA a tetramer, and enolase an octamer. For this reason, the enzymes were added in a ration of 3:8 and 3:4 of PNPase to enolase and PfkA, respectively. However, in these conditions, no effect could be seen on the degradation activity of PNPase.

3.3.4. Conclusions

PNPase oligomerizes as a trimer, where both PH domains of each protomer organize in a ring structure, leaving a central channel for the entrance of RNA. The active site is located in the second PH domain. Furthermore, PNPase activity is sensitive to concentrations of magnesium as expected, showing higher degradation activity at 10-100 mM. The enzyme is not active at concentrations of magnesium lower than 1 mM. Moreover, the degradation activity of PNPase is not affected *in vitro* by citrate, c-di-AMP, c-di-GMP, enolase or PfkA.

4. Discussion

4.1. The RNA degradosome of *B. subtilis*, does it exist?

The regulation of the gene expression is of major importance for the organisms to adapt to the changing environmental conditions. In bacteria, this control occurs mainly by regulating the transcription initiation, stability, and degradation of the mRNAs by the joint work of RNases and associated proteins. It is common that these proteins organize in complexes, the RNA degradosomes, to improve the regulation of the pathways. The degradosomes of several organisms have been extensively studied to unravel the collaboration of the enzymes within these pathways. In *B. subtilis,* the existence of such a complex was hypothesized, following up the discovery of several *in vivo* interactions between RNases, RNA-related proteins, and glycolytic enzymes. Although these interactions were performed in artificial conditions such as bacterial two-hybrid or in the presence of a crosslinker, several could be reproduced *in vitro* and *in vivo*. However, the complex could not be purified as a whole, raising the question of whether this complex exists *in vivo* or not.

In this work the sub-cellular localization of each of the members of this putative RNA degradosome by fluorescence microscopy has been analyzed. As has been shown, the fusion of proteins to tags such as GFP can affect the activity, interactions, and localization of the proteins. For this reason, the viability of the protein fusions has been studied, by comparing them to deletion mutants to confirm that the proteins preserved the wild type characteristics. Since these fusions were introduced in the chromosome in the original locus, no additional copy of the enzymes is available. This has proven that the strains that harboured the fusions are viable, showing a wild-type phenotype (Figure 11 and Figure 13). RNase J2, however, does not cause a phenotype when absent, but it strongly interacts *in vivo* with its paralogue RNase J1 (Figure 12). The fact that both enzymes exhibit a similar localization is, then, enough to assume the RNase J2-GFP fusion is viable.

RNase Y, the central endonuclease of the RNA degradosome, is encoded by *rny* (*ymdA*), the first gene of a bicistronic operon with *ymdB.* For this reason, the fusion of RNase Y to GFP was introduced in the *amyE* gene, and was expressed under the control of a xylose-inducible promoter, keeping a second copy of RNase Y in its native locus. However, RNase Y is a membrane-bound protein, and its membrane localization has been confirmed in several independent studies. The experiments presented here are in execellent agreement with these observations, and the localization of RNase Y perfectly corresponds to that of Nile Red, a membrane-specific stain (Figure 14). Moreover, it can be observed higher fluorescence intensity at the cell septa. In a

recent study, RNase Y was found to interact with the dynamin-like protein DynA, which also localizes to the division septa (Bürmann *et al.*, 2012). In *E. coli*, the central endoribonuclease of the RNA degradosome is also a membrane-associated protein. Furthermore, it was shown that RhlB, the RNA helicase associated to the RNA degradosome, localizes to the membrane, depending on its interaction with RNase E (Strahl *et al.*, 2015). However, the results presented here show that CshA, the RNA helicase associated to the *B. subtilis* RNA degradosome, is localized to the cytoplasm (Figure 16), as had been reported before (Weber *et al.*, 2001). CshA localizes around the nucleoid, in the area where ribosomes are located. Furthermore, the paralogous RNases J1 and J2 show a similar localization to CshA. It was shown before that the localization of ribosomes is dependent on active transcription, since treating the cells with the inhibitor rifampicin, results in relaxation of the nucleoid a delocalization of the ribosomal fraction. This phenomenon can be observed for CshA, RNase J1 and RNase J2 (Figure 17), suggesting that the localization of these proteins depends on the presence of RNA. Interestingly, in *E. coli* the RNase E also delocalizes in response to rifampicin treatment (Strahl et al., 2015); such a delocalization, however, was not observed for RNase Y in *B. subtilis* (data not shown). This difference may be caused by the different attachment of the two RNases to the membrane: RNase E is membrane-attached *via* an amphipathic helix (Khemici et al., 2008), whereas RNase Y is inserted to the membrane *via* a trans-membrane helix (Lehnik-Habrink et al., 2011a). It is interesting to note that, in *E. coli*, the major fraction of the RNA helicase RhlB localizes to the membrane *via* RNase E, even though the protein is also engaged in the cytoplasmic complex with PNPase (Lin and Lin-Chao, 2005; Strahl *et al.*, 2015). In *B. subtilis*, the major fractions of the exoribonucleases and the RNA helicase CshA are clearly not associated to the membrane, i. e. these major fractions do not interact with RNase Y.

The analysis of the localization of PNPase, the 3'-5' exonuclease associated to the degradosome, showed that the protein is evenly distributed throughout the cytoplasm and not excluded from the nucleoid (Figure 15). It is tempting to speculate that the differential localization of polynucleotide phosphorylase as compared to the other exoribonucleases, J1 and J2, and the helicase CshA, is related to the fact that PNPase also exerts functions that are not related to RNA degradation: PNPase does also bind single-stranded DNA and participates in DNA repair (Cardenas *et al.*, 2009; Cardenas *et al.*, 2011).

Furthermore, the glycolytic enzymes, enolase and PfkA, are located to the cytoplasm, where they are evenly distributed (Figure 15). Interestingly, enolase shows a different localization at 28°C than at 37°C. Although it is always localized to the cytoplasm, at 37°C bright spots at the cell poles appear in some cells. Polar localization of enolase has been reported before, and was shown

to depend on phosphorylation of the enzyme on a tyrosine residue by the protein tyrosine kinase, PtkA (Jers *et al.*, 2010).

At a glance, these observations contradict previous reports on the interactions between the proteins involved in RNA degradation. However, there are several independent *in vivo* and *in vitro* reports that confirm the binary interactions of the potential RNA degradosome enzymes strongly suggesting that these interactions are real (Commichau *et al.*, 2009; Lehnik-Habrink *et al.*, 2010; Lehnik-Habrink *et al.*, 2011a; Newman *et al.*, 2012; Salvo *et al.*, 2016). All potential degradosome proteins are likely to be very abundant proteins as has been shown for PNPase, PfkA, or Eno (Eymann *et al.*, 2004). This hypothesis is supported by the fact that the genes encoding the degradosome proteins all belong to the most strongly expressed genes in *B. subtilis* (Nicolas *et al.*, 2012). Thus, these abundant proteins may be present at multiple places in the cell, and they may serve multiple functions. Indeed, it has been shown that polynucleotide phosphorylase and the RNA helicase RhlB of *E. coli* are part of two distinct complexes: the two proteins form a complex in the cytoplasm, and they are also part of the membrane-attached RNA degradosome (Lin and Lin-Chao, 2005; Strahl *et al.*, 2015). Similarly, enolase is not only part of the degradosome but also a cytoplasmic glycolytic enzyme. Thus, it is important to study the relative localization of the proteins in the different compartments. Given the clear evidence for the multiple binary protein-protein interactions on one hand, and the lack of purification of the *B. subtilis* RNA degradosome on the other, it is tempting to speculate that these interactions are rather transient, and may not always involve all components. Possibly, the RNA degrading enzymes engage in a variety of different interactions to achieve specificity in RNA degradation and processing. Indeed, it has recently been shown that the glycolytic enzyme glyceraldehyde 3-phosphate dehydrogenase (GapA) form a complex with RNase Y and RNase J1 to modulate J1 activity. This study also revealed that only a minor fraction of GapA (1 - 2%) interacts with RNase J1 and RNase Y (Gimpel and Brantl, 2016). Interestingly, this interaction of a minor part of the total GapA population in the cell correlates perfectly with the fact that GapA is a cytoplasmic protein, even though a part of the protein is found associated to the membrane (Meile *et al.*, 2006; Hahne *et al.*, 2008).

All in all, the existence of an RNA degradosome seems plausible under certain conditions and in a transient manner; however, it does not seem to be the major state of the proteins that we have investigated.

4.2. RNases J1 and J2: their complex *in vivo*

RNase J1 is a 5'-3' exoribonuclease that also possesses endoribonuclease activity, and it is encoded by the *rnjA* gene. Although it is not essential, the deletion of *rnjA* severely affects the

division, competence, and resistance to antibiotics, besides altering the cell morphology. RNase J1 has a paralogue in *B. subtilis* encoded by the *rnjB* gene. The deletion of *rnjB* does not cause as severe a phenotype as the deletion of *rnjA*. Furthermore, RNase J2 has endonuclease activity, but only very weak exonuclease activity. Both proteins interact *in vivo* and *in vitro*, in a complex that modifies the specificity of the individual proteins. Although the proteins have been extensively studied, the relevance of the existence of the two paralogues, as well as the oligomerization state *in vivo* is still unknown. Furthermore, it is known that RNase J1 and RNase J2 can self-interact *in vitro* to form homodimers that seem more stable than the heterodimers. Moreover, it is known that the C-terminal domain of RNase J1 is necessary for its self-interaction and activity. It has been speculated that this C-terminal domain is also the dimer interface of the heterodimer. However, the importance of this domain has not been studied *in vivo.* Moreover, it is not known what the real state of the proteins *in vivo* is. Furthermore, although the localization of the proteins has been studied, little is known about the subcellular localization of each of the paralogues in the absence of the other. In this work, the oligomerization state of the proteins has been studied *in vivo*, emphasizing the importance of the C-terminal domain of RNase J2 for this complex formation. Furthermore, the localization of RNase J1 and J2 was analyzed by fluorescence microscopy, in combination with the deletion of the *rnjB* and *rnjA* genes, respectively.

As has been already demonstrated, the paralogous RNases J1 and J2 interact *in vivo* (Figure 12 and Figure 18)*.* The truncation of the C-terminal domain of RNase J2, however, impedes the interaction of RNases J1 and J2 (Figure 18). Furthermore, RNase J1 and J2 oligomerize *in vivo* as dimers and tetramers. It had been proposed that the proteins would associate in homodimers that would interact to form a heterotetramer (Newman *et al.*, 2011). However, the fact that the analysis of the fraction of a pull-down assay shows that both dimers and tetramers contain both RNases J1 and J2 implies that the proteins form heterodimers *in vivo* (Figure 19 lanes 1 and 3). Nonetheless, RNase J1 can also-self-interact in the absence of RNase J2, forming both dimers and tetramers (Figure 19A lane 2). However, in the absence of RNA, RNase J1 is only able to form dimers (Figure 20A lanes 2 and 3). It is tempting to speculate that the tetramers form upon binding to RNA. Moreover, RNase J2 can also self-interact in the absence of RNase J1 to form dimers (Figure 20A lane 5). Interestingly, in the absence of RNA, the homodimers seem to be more stable than the heterodimers, which dissociate to their monomeric state (Figure 20A lanes 1 and 4). This raises the question of why and how are the heterodimers forming in the cell, and not the homodimers. Therefore, an experiment should be performed as in Figure 20, where the cells are not treated with RNase A. This experiment could not be performed due to time restrictions.

Furthermore, it would be interesting to see if RNase J2, in the absence of RNase J1, is also able to for tetramers, and if indeed the tetramers form upong binding to RNA.

The localization of RNase J1 and J2 has been analyzed *in vivo.* RNase J1 and J2 localize surrounding the nucleoid, where the ribosomal and RNA fractions are found. Furthermore, the localization is dependent on transcription, since a rifampicin treatment results in spreading of both proteins in the cytoplasm (Figure 17). Upon truncation of the C-terminal domain of RNase J2 or deletion of the *rnjB* gene, the localization of RNase J1 remains the same (Figure 22A). This is not surprising, since RNase J1 is able to form dimers and tetramers when it does not interact with RNase J2. However, the absence of RNase J1 affects the localization of RNase J2, which localizes to spots that are spread within the cell (Figure 22B). It can be speculated from this localization that its interaction of RNase J1 is necessary for its normal localization. This would imply, however, that RNase J2 cannot interact with RNA by itself. However, the localization of ribosomes and, by extension, of RNA is not known in an *rnjA* deletion mutant. It is possible that the RNA also localizes in discreet spots in the aforementioned deletion strain. Nonetheless, the localization of the nucleoid has been studied in an RNase J1 deletion mutant and, although some cells were anucleate, the nucleoid was still visibly condensed (Hunt *et al.*, 2006). Consequently, it can be assumed that the RNA would not be localized to spots in the cell, but still surrounding the nucleoid and occupying the rest of the cytoplasm. Thus, it would be interesting to observe the effect of rifampicin on the localization of RNase J2 as well as the localization of ribosomes in the absence of RNase J1. Also, it would be interesting to know the effect of the deletion of RNase J1 on the localization of the truncated RNase J2, which is not in spots, but evenly disperse in the cytoplasm. Another hypothesis is, however, that, in the absence of RNase J1, RNase J2 interacts with other proteins, which are localized in this spotty pattern. This could easily be analyzed by a pull-down of RNase J2 as decribed above, but in the absence of RNase J1.

An interesting observation is that, upon deletion of RNase J2 in the presence of RNase J1-GFP, the cell morphology resembles that of the deletion of RNase J1: elongated, curly, and thickened. However, neither the deletion of *rnjB,* nor the fusion of GFP to RNase J1 seem to provoke such a strong phenotype. Indeed, the RNase J1-GFP shows a wild type phenotype (Figure 11B), and the deletion of RNase J2 induces the formation of only some long cells (Figure 21). It can be hypothesized that the fusion of RNase J1 to GFP hinders the activity of RNase J1 or its oligomerization capabilities slightly, but it can be recovered by the presence of RNase J2. Moreover, the same can be observed in the strain where RNase J1 is fused to GFP and the C-terminal domain of RNase J2 is truncated.

Interestingly, the analysis of the cell extracts from different strains has shown that the truncation of the C-terminal domain of RNase J2 results in an increased amount of RNase J2

protein. This could have several interpretations. First, the full-length protein could have a reduced stability in comparison to the truncated RNase J2, or the shortened mRNA has increased stability. Second, RNase J2 might be regulating its own expression; the truncated RNase J2 does not oligomerize and has, most likely, no activity, since the phenotype of the deletion of *rnjB* and the deletion of the C-terminal domain of RNase J2 are similar (see Figure 21). Moreover, the deletion of RNase J1 results in an increased amount of RNase J2 (Figure 20B lanes 3 and 4). This contradicts a recent publication, which finds no evidence of increased levels of RNase J2 in the absence of RNase J1. However, these experiments were performed with a depletion mutant and not a complete deletion (Jamalli *et al.*, 2014). Nonetheless, the pull-down experiment revealed that several proteins that bind unspecifically to the column (like PycA) were also increased in the absence of RNase J1 (not shown), suggesting that it might be a more general effect from the deletion of a very important RNase.

All in all, it has been shown that RNase J1 and J2 interact *in vivo* in heterodimers and heterotetramers, but that the proteins can self-interact in the absence of the other. However, RNase J1 is not affected in its localization by the absence of RNase J2, while RNase J2 is in the absence of RNase J1. Furthermore, it can be speculated that the tetramers are formed upon interaction with RNA, and that RNase J2 cannot bind RNA on its own. Moreover, the fusion of RNase J1 to GFP seems to slightly affect the activity or interactions of the protein, although this can be rescued by the presence of full-length RNase J2.

4.3. The degradation activity of PNPase *in vitro*

Polyribonucleoride phosphorylase is a very well known enzyme that was discovered in the 1950s. It was the first enzyme discovered to be able to polymerize RNA from nucleotides. It catalyzes the reversible reaction of the phosphorolytic degradation of RNA molecules *in vivo*. Although its major activity in the cell seems to be the degradative activity, it has been shown that it can also polymerize *in vivo*. In *E. coli*, the enzyme is regulated by several metabolites and second messengers like ATP, c-di-GMP and citrate. Concentrations in the mM range of ATP inhibit both phosphorolytic and polymerizing activity (Del Favero *et al.*, 2008). The second messenger c-di-GMP activates both activities; 10 μM increases 40-fold the phosphorolytic activity, while concentrations as low as 0.1 μM can accelerate poly(A) synthesis (Tuckerman *et al.*, 2011). Moreover, citrate also affects both activities of PNPase, both *in vivo* and *in vitro* (Nurmohamed *et al.*, 2011). In addition, it has been shown that it is part of a complex that involves other RNA-related proteins and the glycolytic enzyme enolase. In *B. subtilis*, the enzyme has been also proposed to be part of complex that includes RNA-related proteins and the glycolytic enzymes

enolase and phosphofructokinase (PFK or PfkA). However, little is known of the regulation of PNPase in the latter organism. In this work, the activity of PNPase on a short poly(A) RNA fragment was analyzed *in vitro* at 25°C, and the effect of several putative effectors was assayed. It has been observed that the enzyme is able to polymerize and degrade this short fragment *in vitro* (not shown), however, the optimized reaction conditions were only obtained for the degradation activity. Furthermore, the PNPase is active in the presence of magnesium and manganese ions (not shown). The results here presented show that the enzyme is active at a wide range of magnesium concentrations, with the activity increasing with increasing amounts of the ion (Figure 28). Interestingly, the enzyme is not inhibited by concentrations of the ion as high as 100 mM. Preliminary studies also show, that the acitivity of the enzyme also increases with increasing amounts of inorganic phosphate, from 1 mM to 50 mM. It was shown that the concentration of Pi *in vivo* in *E. coli* is 30 mM (Andoh *et al.*, 1963), meaning that the enzyme most likely exerts its degradative function *in vivo*.

In addition, the study of several effectors on the phosphorolytic activity of PNPase shows that the regulation of this enzyme might differ from that of the PNPase from *E. coli.* The second messenger c-di-GMP seems to not affect the degradation activity of PNPase. A similar second messenger, c-di-AMP, is essential in *B. subtilis* and not present in *E. coli* (Gundlach *et al.*, 2015)*. However, it also does not affect the phosphorolytic activity of PNPase in the conditions tested. An experiment in which increasing concentrations of citrate were added to the reaction of PNPase (1,5, and 10 mM) showed that the degradation activity of PNPase was inhibited by 10 mM of citrate. This had already been shown for *E. coli*. However, addition of magnesium citrate at the same concentration showed no effect on the activity. This could be explained by the coordination of the magnesium ions present in the medium by citrate, which was present in the same concentration as magnesium. This would reduce the amount of magnesium ions available for the enzyme and, thus, reducing the percentage of degradation of PNPase. It would be interesting to assay the effect of citrate in the presence of manganese as a cofactor of PNPase, since it was shown that, for the *E. coli* PNPase, citrate does not inhibit the enzyme in the presence of manganese. This experiment could not be performed due to time restrictions.

PNPase has been related to enolase and phosphofructokinase, since they have been involved in the same the degradation complex. It was interesting to study whether these moonlighting enzymes could alter the activity of PNPase *in vitro.* The results are showing, however, that this is not the case in these conditions.

Polynucleotide phsphorylase is a very conserved enzyme and it is present in all three domains of life. The PNPases of *E. coli* and *B. subtilis* share a high percentage of identity and similarity. However, it seems that the regulation of these enzymes, as well as their relevance *in vivo* is not

comparable. The result here presented show that the degradation acivity of PNPase is not regulated in the same way as its homologue from *E. coli*. Nonetheless, further analyses have to be made, including the effect of these metabolites and enzymes on the polymerization activity of PNPase.

5. Bibliography

Aït-Bara, S., Carpousis, A.J., and Quentin, Y. (2014) RNase E in the γ-Proteobacteria: conservation of intrinsically disordered noncatalytic region and molecular evolution of microdomains. *Mol Genet Genomics* **290**: 847–862.

Ando, Y., and Nakamura, K. (2006) *Bacillus subtilis* DEAD protein YdbR possesses ATPase, RNA binding, and RNA unwinding activities. *Biosci Biotechnol Biochem* **70**: 1606–1615.

Andoh, T., Natori, S., and Mizuno, D. (1963) The degradation of *E. coli* Messenger RNA by polynucleotide phosphorylase. *J Biochem* **54**: 477-479.

Apirion, D. (1978) Isolation, genetic mapping and some characterization of a mutation in *Escherichia coli* that affects the processing of ribonucleic acid. *Genetics* **90**: 659–671.

Aravind, L., and Koonin, E. V. (1998) The HD domain defines a new superfamily of metal-dependent phosphohydrolases. *Trends Biochem Sci* **23**: 469–472.

Aravind, L., and Koonin, E. V. (2001) A natural classification of ribonucleases. *Methods Enzymol* **341**: 3–28.

Arens, J. (2015) Structural analysis of different *Bacillus subtilis* RNA degrading enzymes and of the diadenylatcyclase. Georg-August Univeristät Göttingen.

Arraiano, C.M., Andrade, J.M., Domingues, S., Guinote, I.B., Malecki, M., Matos, R.G., *et al.* (2010) The critical role of RNA processing and degradation in the control of gene expression. *FEMS Microbiol Rev* **34**: 883–923.

Awano, N., Inouye, M., and Phadtare, S. (2008) RNase activity of polynucleotide phosphorylase is critical at low temperature in *Escherichia coli* and is complemented by RNase II. *J Bacteriol* **190**: 5924–5933.

Babitzke, P., and Kushner, S.R. (1991) The Ams (altered mRNA stability) protein and ribonuclease E are encoded by the same structural gene of *Escherichia coli*. *Proc Natl Acad Sci U S A* **88**: 1–5.

Bandyra, K.J., Bouvier, M., Carpousis, A.J., and Luisi, B.F. (2013) The social fabric of the RNA degradosome. *Biochim Biophys Acta - Gene Regul Mech* **1829**: 514–522.

Bechhofer, D.H. (2011) *Bacillus subtilis* mRNA decay: new parts in the toolkit. *Wiley Interdiscip Rev RNA* **2**: 387–394.

Bechhofer, D.H., and Wang, W. (1998) Decay of *ermC* mRNA in a polynucleotide phosphorylase mutant of *Bacillus subtilis*. *J Bacteriol* **180**: 5968–5977.

Beckering, C.L., Steil, L., Weber, M.H.W., Völker, U., and Marahiel, M.A. (2002) Genomewide transcriptional analysis of the cold shock response in *Bacillus subtilis*. *J Bacteriol* **184**: 6395–6402.

Belasco, J.G., and Higgins, C.F. (1988) Mechanisms of mRNA decay in bacteria: a perspective. *Gene* **72**: 15–23.

Bermúdez-Cruz, R.M., Ramírez, F., Kameyama-Kawabe, L., and Montañez, C. (2005) Conserved domains in polynucleotide phosphorylase among eubacteria. *Biochimie* **87**: 737–745.

Bernstein, J. a, Lin, P.-H., Cohen, S.N., and Lin-Chao, S. (2004) Global analysis of *Escherichia coli* RNA degradosome function using DNA microarrays. *Proc Natl Acad Sci U S A* **101**: 2758–2763.

Blötz, C. (2015) Structural and functional characterization of RNase J2 from *Bacillus subtilis*. Georg-August Universität Göttingen.

Bouvet, P., and Belasco, J.G. (1992) Control of RNase E-mediated RNA degradation by 5'-terminal base pairing in *E. coli*. *Nature* **360**: 488–491.

Bouvier, M., and Carpousis, A.J. (2011) A tale of two mRNA degradation pathways mediated by RNase E. *Mol Microbiol* **82**: 1305–1310.

Bradford, M.M. (1976) A rapid and sensitive method for the quantitation of microgram quantities of protein utilizing the principle of protein-dye binding. *Anal Biochem* **72**: 248–254.

Braun, F., Hajnsdorf, E., and Regnier, P. (1996) Polynucleotide phosphorylase is required for the rapid degradation of the RNase E-processed *rpsO* mRNA of *Escherichia coli* devoid of its 3' hairpin. *Mol Microbiol* **19**: 997–1005.

Briani, F., Carzaniga, T., and Dehò, G. (2016) Regulation and functions of bacterial PNPase. *Wiley Interdiscip Rev RNA* **7**: 241–258.

Briani, F., Favero, M. Del, Capizzuto, R., Consonni, C., Zangrossi, S., Greco, C., *et al.* (2007) Genetic analysis of polynucleotide phosphorylase structure and functions. *Biochimie* **89**: 145–157.

Britton, R.A., Wen, T., Schaefer, L., Pellegrini, O., Uicker, W.C., Mathy, N., *et al.* (2007) Maturation of the 5' end of *Bacillus subtilis* 16S rRNA by the essential ribonuclease YkqC/RNase J1. *Mol Microbiol* **63**: 127–138.

Bürmann, F., Sawant, P., and Bramkamp, M. (2012) Identification of interaction partners of the dynamin-like protein DynA from *Bacillus subtilis*. *Commun Integr Biol* **5**: 362–369.

Callaghan, A.J., Aurikko, J.P., Ilag, L.L., Günter Grossmann, J., Chandran, V., Kühnel, K., *et al.* (2004) Studies of the RNA degradosome-organizing domain of the *Escherichia coli* ribonuclease RNase E. *J Mol Biol* **340**: 965–979.

Callaghan, A.J., Marcaida, M.J., Stead, J.A., McDowall, K.J., Scott, W.G., and Luisi, B.F. (2005a) Structure of *Escherichia coli* RNase E catalytic domain and implications for RNA turnover. *Nature* **437**: 1187–1191.

Callaghan, A.J., Redko, Y., Murphy, L.M., Grossmann, J.G., Yates, D., Garman, E., *et al.* (2005b) 'Zn-Link': A metal-sharing interface that organizes the quaternary structure and catalytic site of the endoribonuclease, RNase E. *Biochemistry* **44**: 4667–4675.

Callebaut, I., Moshous, D., Mornon, J.-P., and Villartay, J.-P. de (2002) Metallo-beta-lactamase fold within nucleic acids processing enzymes: the beta-CASP family. *Nucleic Acids Res* **30**: 3592–3601.

Campos-Guillén, J., Bralley, P., Jones, G.H., Bechhofer, D.H., and Olmedo-Alvarez, G. (2005) Addition of poly(A) and heteropolymeric 3' ends in *Bacillus subtilis* wild-type and polynucleotide phosphorylase-deficient strains. *J Bacteriol* **187**: 4698–4706.

Cardenas, P.P., Carrasco, B., Sanchez, H., Deikus, G., Bechhofer, D.H., and Alonso, J.C. (2009) *Bacillus subtilis* polynucleotide phosphorylase 3'-to-5' DNase activity is involved in DNA repair. *Nucleic Acids Res* **37**: 4157–4169.

Cardenas, P.P., Carzaniga, T., Zangrossi, S., Briani, F., Garcia-Tirado, E., Dehò, G., *et al.* (2011) Polynucleotide phosphorylase exonuclease and polymerase activities on single-stranded DNA ends are modulated by RecN, SsbA and RecA proteins. *Nucleic Acids Res* **39**: 9250–9261.

Carpousis, A.J. (2002) The *Escherichia coli* RNA degradosome: structure, function and relationship in other ribonucleolytic multienzyme complexes. *Biochem Soc Trans* **30**: 150–155.

Carpousis, A.J. (2007) The RNA Degradosome of *Escherichia coli* : An mRNA-degrading machine assembled on RNase E. *Annu Rev Microbiol* **61**: 71–87.

Carpousis, A.J., Houwe, G. Van, Ehretsmann, C., and Krisch, H.M. (1994) Copurification of *E. coli* RNAase E and PNPase: Evidence for a specific association between two enzymes important in RNA processing and degradation. *Cell* **76**: 889–900.

Carpousis, A.J., Khemici, V., and Poljak, L. (2008) Chapter 10 Assaying DEAD-box RNA helicases and their role in mRNA degradation in *Escherichia coli*. *Methods Enzymol* **447**: 183–197.

Cascante-Estepa, N. (2014) Carbon metabolism and RNA processing in *Bacillus subtilis*. Georg-August Universität Göttingen.

Cascante-Estepa, N., Gunka, K., and Stülke, J. (2016) Localization of components of the RNA-degrading machine in *Bacillus subtilis*. *Front Microbiol* **7**: 1492.

Chalfie, M., Tu, Y., Euskirchen, G., W. W. Ward, and Prasher, D.C. (1994) Green fluorescent protein as a marker for gene expression. *Science (80-)* **263**: 802–805.

Chandran, V., and Luisi, B.F. (2006) Recognition of enolase in the *Escherichia coli* RNA degradosome. *J Mol Biol* **358**: 8–15.

Chandran, V., Poljak, L., Vanzo, N.F., Leroy, A., Miguel, R.N., Fernandez-Recio, J., *et al.* (2007) Recognition and cooperation between the ATP-dependent RNA helicase RhlB and ribonuclease RNase E. *J Mol Biol* **367**: 113–132.

Cheng, Z.F., and Deutscher, M.P. (2003) Quality control of ribosomal RNA mediated by polynucleotide phosphorylase and RNase R. *Proc Natl Acad Sci U S A* **100**: 6388–6393.

Clouet-d'Orval, B.B., Phung, D.K., Langendijk-Genevaux, P.S., and Quentin, Y. (2015) Universal RNA-degrading enzymes in Archaea: Prevalence, activities and functions of beta-CASP ribonucleases. *Biochimie* **118**: 279–285.

Coburn, G.A., Miao, X., Briant, D.J., and Mackie, G.A. (1999) Reconstitution of a minimal RNA degradosome demonstrates functional coordination between a 3' exonuclease and a DEAD-box RNA helicase. *Genes Dev* **13**: 2594–2603.

Collins, J.A., Irnov, I., Baker, S., and Winkler, W.C. (2007) Mechanism of mRNA destabilization by the *glmS* ribozyme. *Genes Dev* **21**: 3356–3368.

Commichau, F.M., Pietack, N., and Stülke, J. (2013) Essential genes in *Bacillus subtilis*: a re-evaluation after ten years. *Mol Biosyst* **9**: 1068–1075.

Commichau, F.M., Rothe, F.M., Herzberg, C., Wagner, E., Hellwig, D., Lehnik-Habrink, M., *et al.* (2009) Novel activities of glycolytic enzymes in *Bacillus subtilis*: interactions with essential proteins involved in mRNA processing. *Mol Cell Proteomics* **8**: 1350–1360.

Condon, C. (2007) Maturation and degradation of RNA in bacteria. *Curr Opin Microbiol* **10**: 271–278.

Condon, C. (2010) What is the role of RNase J in mRNA turnover? *RNA Biol* **7**: 316–321.

Condon, C., and Bechhofer, D.H. (2011) Regulated RNA stability in the Gram positives. *Curr Opin Microbiol* **14**: 148–154.

Daou-Chabo, R., Mathy, N., Bénard, L., and Condon, C. (2009) Ribosomes initiating translation of the *hbs* mRNA protect it from 5'-to-3' exoribonucleolytic degradation by RNase J1. *Mol Microbiol* **71**: 1538–1550.

Deikus, G., and Bechhofer, D.H. (2007) Initiation of decay of *Bacillus subtilis trp* leader RNA. *J Biol Chem* **282**: 20238–20244.

Deikus, G., and Bechhofer, D.H. (2011) 5' End-independent RNase J1 endonuclease cleavage of *Bacillus subtilis* model RNA. *J Biol Chem* **286**: 34932–34940.

Deikus, G., Condon, C., and Bechhofer, D.H. (2008) Role of *Bacillus subtilis* RNase J1 endonuclease and 5'-exonuclease activities in *trp* leader RNA turnover. *J Biol Chem* **283**: 17158–17167.

Deutscher, M.P. (2009) Maturation and degradation of ribosomal RNA in bacteria. *Prog Mol Biol Transl Sci* **85**: 369–391.

Deutscher, M.P. (2015) Twenty years of bacterial RNases and RNA processing : how we've matured. *RNA* **21**: 597–600.

Deutscher, M.P., and Reuven, N.B. (1991) Enzymatic basis for hydrolytic versus phosphorolytic mRNA degradation in *Escherichia coli* and *Bacillus subtilis*. *Proc Natl Acad Sci U S A* **88**: 3277–3280.

DiChiara, J.M., Liu, B., Figaro, S., Condon, C., and Bechhofer, D.H. (2016) Mapping of internal monophosphate 5' ends of *Bacillus subtilis* messenger RNAs and ribosomal RNAs in wild-type and ribonuclease-mutant strains. *Nucleic Acids Res* **44**: 3373–3389.

Diethmaier, C., Pietack, N., Gunka, K., Wrede, C., Lehnik-Habrink, M., Herzberg, C., *et al.* (2011) A novel factor controlling bistability in *Bacillus subtilis*: The YmdB protein affects flagellin expression and biofilm formation. *J Bacteriol* **193**: 5997–6007.

Domínguez-Malfavón, L., Islas, L.D., Luisi, B.F., García-Villegas, R., and García-Mena, J. (2013) The assembly and distribution *in vivo* of the *Escherichia coli* RNA degradosome. *Biochimie* **95**: 2034–2041.

Dominski, Z., Carpousis, A.J., and Clouet-d'Orval, B. (2013) Emergence of the β-CASP ribonucleases: Highly conserved and ubiquitous metallo-enzymes involved in messenger RNA maturation and degradation. *Biochim Biophys Acta - Gene Regul Mech* **1829**: 532–551.

Dorléans, A., Li De La Sierra-Gallay, I., Piton, J., Zig, L., Gilet, L., Putzer, H., and Condon, C. (2011) Molecular basis for the recognition and cleavage of RNA by the bifunctional 5'-3' exo/endoribonuclease RNase J. *Structure* **19**: 1252–1261.

Durand, S., Gilet, L., Bessiè Res, P., Nicolas, P., and Condon, C.N. (2012) Three Essential Ribonucleases—RNase Y, J1, and III—Control the Abundance of a Majority of *Bacillus subtilis* mRNAs. *PLoS Genet* **8**: e1002520.

Errington, J. (2003) Dynamic proteins and a cytoskeleton in bacteria. *Nat Cell Biol* **5**: 175–178.

Even, S., Pellegrini, O., Zig, L., Labas, V., Vinh, J., Bréchemmier-Baey, D., *et al.* (2005) Ribonucleases J1 and J2: Two novel endoribonucleases in *B. subtilis* with functional homology to *E. coli* RNase E. *Nucleic Acids Res* **33**: 2141–2152.

Eymann, C., Dreisbach, A., Albrecht, D., Bernhardt, J., Becher, D., Gentner, S., *et al.* (2004) A comprehensive proteome map of growing *Bacillus subtilis* cells. *Proteomics* **4**: 2849–2876.

Farr, G.A., Oussenko, I.A., and Bechhofer, D.H. (1999) Protection against 3'-to-5' RNA decay in *Bacillus subtilis*. *J Bacteriol* **181**: 7323–7330.

Favero, M. Del, Mazzantini, E., Briani, F., Zangrossi, S., Tortora, P., and Dehò, G. (2008) Regulation of *Escherichia coli* polynucleotide phosphorylase by ATP. *J Biol Chem* **283**: 27355–27359.

Figaro, S., Durand, S., Gilet, L., Cayet, N., Sachse, M., and Condon, C. (2013) *Bacillus subtilis* mutants with knockouts of the genes encoding ribonucleases RNase Y and RNase J1 are viable, with major defects in cell morphology, sporulation, and competence. *J Bacteriol* **195**: 2340–2348.

Gamba, P., Jonker, M.J., and Hamoen, L.W. (2015) A novel feedback loop that controls bimodal expression of genetic competence. *PLoS Genet* **11**: e1005047.

Gimpel, M., and Brantl, S. (2016) Dual-function sRNA encoded peptide SR1P modulates moonlighting activity of *B. subtilis* GapA. *RNA Biol* **6286**: 1–11.

Górna, M.W., Carpousis, A.J., and Luisi, B.F. (2012) From conformational chaos to robust regulation: the structure and function of the multi-enzyme RNA degradosome. *Q Rev Biophys* **45**: 105–145.

Górna, M.W., Pietras, Z., Tsai, Y.-C., Callaghan, A.J., Hernández, H., Robinson, C. V, and Luisi, B.F. (2010) The regulatory protein RraA modulates RNA-binding and helicase activities of the *E. coli* RNA degradosome. *RNA* **16**: 553–562.

Guérout-Fleury, A.M., Shazand, K., Frandsen, N., and Stragier, P. (1995) Antibiotic-resistance cassettes for *Bacillus subtilis*. *Gene* **167**: 335–336.

Gundlach, J., Mehne, F.M.P., Herzberg, C., Kampf, J., Valerius, O., Kaever, V., and Stülke, J. (2015) An essential poison: Synthesis and degradation of cyclic di-AMP in *Bacillus subtilis*. *J Bacteriol* **197**: 3265–3274.

Gunka, K., Stannek, L., Care, R.A., and Commichau, F.M. (2013) Selection-driven accumulation of suppressor mutants in *Bacillus subtilis*: The apparent high mutation frequency of the cryptic *gudB* gene and the rapid clonal expansion of *gudB+* suppressors are due to growth under selection. *PLoS One* **8**: e66120.

Hahne, H., Wolff, S., Hecker, M., and Becher, D. (2008) From complementarity to comprehensiveness - Targeting the membrane proteome of growing *Bacillus subtilis* by divergent approaches. *Proteomics* **8**: 4123–4136.

Hardwick, S.W., Gubbey, T., Hug, I., Jenal, U., and Luisi, B.F. (2012) Crystal structure of *Caulobacter crescentus* polynucleotide phosphorylase reveals a mechanism of RNA substrate channelling and RNA degradosome assembly. *Open Biol* **2**: 120028.

Hardwick, S.W., and Luisi, B.F. (2013) Rarely at rest: RNA helicases and their busy contributions to RNA degradation, regulation and quality control. *RNA Biol* **10**: 56–70.

Hartmann, R.K., Gößringer, M., Späth, B., Fischer, S., and Marchfelder, A. (2009) The making of tRNAs and more - RNase P and tRNase Z. *Prog Mol Biol Transl Sci* **85**: 319–368.

Herzberg, C., Weidinger, L.A.F., Dörrbecker, B., Hübner, S., Stülke, J., and Commichau, F.M. (2007) SPINE: A method for the rapid detection and analysis of protein-protein interactions *in vivo*. *Proteomics* **7**: 4032–4035.

Hui, M.P., Foley, P.L., and Belasco, J.G. (2014) Messenger RNA degradation in bacterial Cells. *Annu Rev Genet* **48**: 537–559.

Hunger, K., Beckering, C.L., Wiegeshoff, F., Graumann, P.L., and Marahiel, M.A. (2006) Cold-induced putative DEAD box RNA helicases CshA and CshB are essential for cold adaptation and interact with cold shock protein B in *Bacillus subtilis*. *J Bacteriol* **188**: 240–248.

Hunt, A., Rawlins, J.P., Thomaides, H.B., and Errington, J. (2006) Functional analysis of 11 putative essential genes in *Bacillus subtilis*. *Microbiology* **152**: 2895–2907.

Jahn, N., and Brantl, S. (2016) Heat-shock-induced refolding entails rapid degradation of *bsrG* toxin mRNA by RNases Y and J1. *Microbiology* **162**: 590–599.

Jamalli, A., Hébert, A., Zig, L., and Putzer, H. (2014) Control of expression of the RNases J1 and J2 in *Bacillus subtilis*. *J Bacteriol* **196**: 318–324.

Jarrige, A.-C., Bré Chemier-Baey, D., Mathy, N., Lie Duché, O., and Portier, C. (2002) Mutational analysis of polynucleotide phosphorylase from *Escherichia coli*. *J Mol Biol* **321**: 397–409.

Jarvis, E.D., Widom, R.L., LaFauci, G., Setoguchi, Y., Richter, I.R., and Rudner, R. (1988) Chromosomal organization of rRNA operons in *Bacillus subtilis*. *Genetics* **120**: 625–635.

Jers, C., Pedersen, M.M., Paspaliari, D.K., Schütz, W., Johnsson, C., Soufi, B., *et al.* (2010) *Bacillus subtilis* BY-kinase PtkA controls enzyme activity and localization of its protein substrates. *Mol Microbiol* **77**: 287–299.

Kaberdin, V.R., and Lin-Chao, S. (2009) Unraveling new roles for minor components of the *E. coli* RNA degradosome. *RNA Biol* **6**: 402–405.

Kalman, M., Murphy, H., and Cashel, M. (1991) *rhlB*, a new *Escherichia coli* K-12 gene with an RNA helicase-like protein sequence motif, one of at least five such possible genes in a prokaryote. *New Biol* **3**: 886–895.

Kawai, Y., Asai, K., and Errington, J. (2009) Partial functional redundancy of MreB isoforms, MreB, Mbl and MreBHp in cell morphogenesis of *Bacillus subtilis*. *Mol Microbiol* **73**: 719–731.

Khemici, V., Poljak, L., Luisi, B.F., and Carpousis, A.J. (2008) The RNase E of *Escherichia coli* is a membrane-binding protein. *Mol Microbiol* **70**: 799–813.

Khemici, V., Poljak, L., Toesca, I., and Carpousis, A.J. (2005) Evidence *in vivo* that the DEAD-box RNA helicase RhlB facilitates the degradation of ribosome-free mRNA by RNase E. *Proc Natl Acad Sci U S A* **102**: 6913–6018.

Khemici, V., Prados, J., Linder, P., and Redder, P. (2015) Decay-initiating endoribonucleolytic cleavage by RNase Y is kept under tight control *via* sequence preference and sub-cellular localisation. *PLoS Genet* **11**: e1005577.

Kobayashi, K., Ehrlich, S.D., Albertini, A., Amati, G., Andersen, K.K., Arnaud, M., *et al.* (2003) Essential *Bacillus subtilis* genes. *Proc Natl Acad Sci U S A* **100**: 4678–4683.

Koslover, D.J., Callaghan, A.J., Marcaida, M.J., Garman, E.F., Martick, M., Scott, W.G., and Luisi, B.F. (2008) The crystal structure of the *Escherichia coli* RNase E apoprotein and a mechanism for RNA degradation. *Structure* **16**: 1238–1244.

Kühnel, K., and Luisi, B.F. (2001) Crystal structure of the *Escherichia coli* RNA degradosome component enolase. *J Mol Biol* **313**: 583–592.

Kunst, F., Ogasawara, N., Moszer, I., Albertini, A.M., Alloni, G., Azevedo, V., *et al.* (1997) The complete genome sequence of the Gram-positive bacterium *Bacillus subtilis*. *Nature* **390**: 249–256.

Laalami, S., Bessières, P., Rocca, A., Zig, L., Nicolas, P., and Putzer, H. (2013) *Bacillus subtilis* RNase Y activity *in vivo* analysed by tiling microarrays. *PLoS One* **8**: e54062.

Laalami, S., Zig, L., and Putzer, H. (2014) Initiation of mRNA decay in bacteria. *Cell Mol Life Sci* **71**: 1799–1828.

Laemmli, U.K. (1970) Cleavage of structural proteins during the assembly of the head of bacteriophage T4. *Nature* **227**: 680–685.

Lehnik-Habrink, M. (2011) An mRNA degradation complex in *Bacillus subtilis*. Georg-August Universität Göttingen.

Lehnik-Habrink, M., Lewis, R.J., Mäder, U., and Stülke, J. (2012) RNA degradation in *Bacillus subtilis*: An interplay of essential endo- and exoribonucleases. *Mol Microbiol* **84**: 1005–1017.

Lehnik-Habrink, M., Newman, J., Rothe, F.M., Solovyova, A.S., Rodrigues, C., Herzberg, C., *et al.* (2011a) RNase Y in *Bacillus subtilis*: A natively disordered protein that is the functional equivalent of RNase E from *Escherichia coli*. *J Bacteriol* **193**: 5431–5441.

Lehnik-Habrink, M., Pförtner, H., Rempeters, L., Pietack, N., Herzberg, C., and Stülke, J. (2010) The RNA degradosome in *Bacillus subtilis*: Identification of CshA as the major RNA helicase in the multiprotein complex. *Mol Microbiol* **77**: 958–971.

Lehnik-Habrink, M., Rempeters, L., Kovács, Á.T., Wrede, C., Baierlein, C., Krebber, H., *et al.* (2013) DEAD-box RNA helicases in *Bacillus subtilis* have multiple functions and act independently from each other. *J Bacteriol* **195**: 534–544.

Lehnik-Habrink, M., Schaffer, M., Mäder, U., Diethmaier, C., Herzberg, C., and Stülke, J. (2011b) RNA processing in *Bacillus subtilis*: Identification of targets of the essential RNase Y. *Mol Microbiol* **81**: 1459–1473.

Leroy, A., Vanzo, N.F., Sousa, S., Dreyfus, M., and Carpousis, A.J. (2002) Function in *Escherichia coli* of the non-catalytic part of RNase E: Role in the degradation of ribosome-free mRNA. *Mol Microbiol* **45**: 1231–1243.

Lewis, P.J., Thaker, S.D., and Errington, J. (2000) Compartmentalization of transcription and translation in *Bacillus subtilis*. *EMBO J* **19**: 710–718.

Leyva-Vazquez, M.A., and Setlow, P. (1994) Cloning and nucleotide sequences of the genes encoding triose phosphate isomerase, phosphoglycerate mutase, and enolase from *Bacillus subtilis*. *J Bacteriol* **176**: 3903–3910.

Li de la Sierra-Gallay, I., Zig, L., Jamalli, A., and Putzer, H. (2008) Structural insights into the dual activity of RNase J. *Nat Struct Mol Biol* **15**: 206–212.

Lin, P.-H., and Lin-Chao, S. (2005) RhlB helicase rather than enolase is the beta-subunit of the *Escherichia coli* polynucleotide phosphorylase (PNPase)-exoribonucleolytic complex. *Proc Natl Acad Sci U S A* **102**: 16590–16595.

Liou, G.G., Chang, H.Y., Lin, C.S., and Lin-Chao, S. (2002) DEAD-box RhlB RNA helicase physically associates with exoribonuclease PNPase to degrade double-stranded RNA independent of the degradosome-assembling region of RNase E. *J Biol Chem* **277**: 41157–41162.

Liou, G.G., Jane, W.N., Cohen, S.N., Lin, N.S., and Lin-Chao, S. (2001) RNA degradosomes exist *in vivo* in *Escherichia coli* as multicomponent complexes associated with the cytoplasmic membrane via the N-terminal region of ribonuclease E. *Proc Natl Acad Sci U S A* **98**: 63–68.

Littauer, U.Z., and Grunberg-Manago, M. (1999) Polynucleotide Phosphorylase. John Wiley & Sons, Inc., Hoboken, NJ, USA.

Liu, B., Deikus, G., Bree, A., Durand, S., Kearns, D.B., and Bechhofer, D.H. (2014) Global analysis of mRNA decay intermediates in *Bacillus subtilis* wild-type and polynucleotide phosphorylase-deletion strains. *Mol Microbiol* **94**: 41–55.

Loughney, K., Lund, E., and Dahlberg, J.E. (1982) tRNA genes are found between the 16S and 23S rRNA genes in *Bacillus subtilis*. *Nucleic Acids Res* **10**: 1607–1624.

Lu, F., and Taghbalout, A. (2014) The *Escherichia coli* major exoribonuclease RNase II is a component of the RNA degradosome. *Biosci Rep* **34**: e00166.

Luttinger, A., Hahn, J., and Dubnau, D. (1996) Polynucleotide phosphorylase is necessary for competence development in *Bacillus subtilis*. *Mol Microbiol* **19**: 343–356.

Mackie, G.A. (1998) Ribonuclease E is a 5'-end-dependent endonuclease. *Nature* **395**: 720–723.

Mäder, U., Zig, L., Kretschmer, J., Homuth, G., and Putzer, H. (2008) mRNA processing by RNases J1 and J2 affects *Bacillus subtilis* gene expression on a global scale. *Mol Microbiol* **70**: 183–196.

Marcaida, M.J., DePristo, M.A., Chandran, V., Carpousis, A.J., and Luisi, B.F. (2006) The RNA degradosome: Life in the fast lane of adaptive molecular evolution. *Trends Biochem Sci* **31**: 359–365.

Margolin, W. (2012) The price of tags in protein localization studies. *J Bacteriol* **194**: 6369–6371.

Mascarenhas, J., Weber, M.H.W., and Graumann, P.L. (2001) Specific polar localization of ribosomes in *Bacillus subtilis* depends on active transcription. *EMBO Rep* **2**: 685–689.

Mathy, N., Bénard, L., Pellegrini, O., Daou, R., Wen, T., and Condon, C. (2007) 5'-to-3' exoribonuclease activity in bacteria: Role of RNase J1 in rRNA maturation and 5' stability of mRNA. *Cell* **129**: 681–692.

Mathy, N., Hébert, A., Mervelet, P., Bénard, L., Dorléans, A., Li de la Sierra-Gallay, I., *et al.* (2010) *Bacillus subtilis* ribonucleases J1 and J2 form a complex with altered enzyme behaviour. *Mol Microbiol* **75**: 489–498.

Matus-Ortega, M.E., Regonesi, M.E., Piña-Escobedo, A., Tortora, P., Dehò, G., and García-Mena, J. (2007) The KH and S1 domains of *Escherichia coli* polynucleotide phosphorylase are necessary for autoregulation and growth at low temperature. *Biochim Biophys Acta - Gene Struct Expr* **1769**: 194–203.

Mauri, P., and Dehò, G. (2008) Chapter 6: A proteomic approach to the analysis of RNA degradosome composition in *Escherichia coli. Methods Enzymol* **447**: 99-117.

Meile, J.-C.C., Wu, L.J., Ehrlich, S.D., Errington, J., and Noirot, P. (2006) Systematic localisation of proteins fused to the green fluorescent protein in *Bacillus subtilis*: Identification of new proteins at the DNA replication factory. *Proteomics* **6**: 2135–2146.

Meinken, C., Blencke, H.M., Ludwig, H., and Stülke, J. (2003) Expression of the glycolytic *gapA* operon in *Bacillus subtilis*: Differential syntheses of proteins encoded by the operon. *Microbiology* **149**: 751–761.

Meyer, F.M., Gerwig, J., Hammer, E., Herzberg, C., Commichau, F.M., Völker, U., and Stülke, J. (2011) Physical interactions between tricarboxylic acid cycle enzymes in *Bacillus subtilis*: Evidence for a metabolon. *Metab Eng* **13**: 18–27.

Miczak, A., Kaberdin, V.R., Wei, C., and Lin-Chao, S. (1996) Proteins associated with RNase E in a multicomponent ribonucleolytic complex. *Proc Natl Acad Sci U S A* **93**: 3865–3869.

Mitra, S., Hue, K., and Bechhofer, D.H. (1996) *In vitro* processing activity of *Bacillus subtilis* polynucleotide phosphorylase. *Mol Microbiol* **19**: 329–342.

Miyawaki, A. (2011) Proteins on the move: Insights gained from fluorescent protein technologies. *Nat Rev Mol Cell Biol* **12**: 656–668.

Mohanty, B.K., and Kushner, S.R. (2000) Polynucleotide phosphorylase functions both as a 3' right-arrow 5' exonuclease and a poly(A) polymerase in *Escherichia coli*. *Proc Natl Acad Sci U S A* **97**: 11966–11971.

Mohanty, B.K., and Kushner, S.R. (2010) Bacterial/archaeal/organellar polyadenylation. *Wiley Interdiscip Rev RNA* **2**: 256–276.

Mohanty, B.K., and Kushner, S.R. (2016) Regulation of mRNA decay in bacteria. *Annu Rev Microbiol* **70**: 25–44.

Morita, T., Kawamoto, H., Mizota, T., Inada, T., and Aiba, H. (2004) Enolase in the RNA degradosome plays a crucial role in the rapid decay of glucose transporter mRNA in the response to phosphosugar stress in *Escherichia coli*. *Mol Microbiol* **54**: 1063–1075.

Mudd, E.A., Krisch, H.M., and Higgins, C.F. (1990) RNase E, an endoribonuclease, has a general role in the chemical decay of *Escherichia coli* mRNA: Evidence that *rne* and *ams* are the same genetic locus. *Mol Microbiol* **4**: 2127–2135.

Müller, P., Jahn, N., Ring, C., Maiwald, C., Neubert, R., Meißner, C., and Brantl, S. (2016) A multistress responsive type I toxin-antitoxin system: *bsrE*/SR5 from the *B. subtilis* chromosome. *RNA Biol* **6286**: 1–13.

Muñoz-Márquez, M.E., and Ponce-Rivas, E. (2010) Effect of *pfkA* chromosomal interruption on growth, sporulation, and production of organic acids in *Bacillus subtilis*. *J Basic Microbiol* **50**: 232–240.

Newman, J.A., Hewitt, L., Rodrigues, C., Solovyova, A., Harwood, C.R., and Lewis, R.J. (2011) Unusual, dual endo- and exonuclease activity in the degradosome explained by crystal structure analysis of RNase J1. *Structure* **19**: 1241–1251.

Newman, J.A., Hewitt, L., Rodrigues, C., Solovyova, A.S., Harwood, C.R., and Lewis, R.J. (2012) Dissection of the network of interactions that links RNA processing with glycolysis in the *Bacillus subtilis* degradosome. *J Mol Biol* **416**: 121–136.

Nicolas, P., Mäder, U., Dervyn, E., Rochat, T., Leduc, A., Pigeonneau, N., *et al.* (2012) Condition-dependent transcriptome reveals high-level regulatory architecture in *Bacillus subtilis*. *Science (80-)* **335**: 1103–1106.

Niepmann, M. and Zheng, J, (2006) Discontinuous native protein gel electrophoresis: pros and cons. *Expert Rev Proteomics* **4**: 355–361.

Noone, D., Salzberg, L.I., Botella, E., Bäsell, K., Becher, D., Antelmann, H., and Devine, K.M. (2014) A highly unstable transcript makes CwlO D,L-endopeptidase expression responsive to growth conditions in *Bacillus subtilis*. *J Bacteriol* **196**: 237–247.

Nurmohamed, S., Vaidialingam, B., Callaghan, A.J., and Luisi, B.F. (2009) Crystal structure of *Escherichia coli* polynucleotide phosphorylase core bound to RNase E, RNA and manganese: Implications for catalytic mechanism and RNA degradosome assembly. *J Mol Biol* **389**: 17–33.

Nurmohamed, S., Vincent, H.A., Titman, C.M., Chandran, V., Pears, M.R., Du, D., *et al.* (2011) Polynucleotide phosphorylase activity may be modulated by metabolites in *Escherichia coli*. *J Biol Chem* **286**: 14315–14323.

Oliva, M.A., Halbedel, S., Freund, S.M., Dutow, P., Leonard, T.A., Veprintsev, D.B., *et al.* (2010) Features critical for membrane binding revealed by DivIVA crystal structure. *EMBO J* **29**: 1988–2001.

Ow, M.C., and Kushner, S.R. (2002) Initiation of tRNA maturation by RNase E is essential for cell viability in *E. coli*. *Genes Dev* **16**: 1102–1115.

Pei, X.Y., Bralley, P., Jones, G.H., and Luisi, B.F. (2015) Linkage of catalysis and 5' end recognition in ribonuclease RNase J. *Nucleic Acids Res* **43**: 8066–8076.

Pietack, N. (2010) Investigation of glycolysis in *Bacillus subtilis*. Georg-August Universität Göttingen.

Pietack, N., Becher, D., Schmidl, S.R., Saier, M.H., Hecker, M., Commichau, F.M., and Stülke, J. (2010) *In vitro* phosphorylation of key metabolic enzymes from *Bacillus subtilis*: PrkC phosphorylates enzymes from different branches of basic metabolism. *J Mol Microbiol Biotechnol* **18**: 129–140.

Pietras, Z., Hardwick, S.W., Swiezewski, S., and Luisi, B.F. (2013) Potential regulatory interactions of *Escherichia coli* RraA protein with DEAD-box helicases. *J Biol Chem* **288**: 31919–31929.

Portier, C. (1975a) Quaternary structure of *Escherichia coli* polynucleotide phosphorylase: New evidence for a trimeric structure. *FEBS Lett* **50**: 79–81.

Portier, C. (1975b) Quaternary structure of polynucleotide phosphorylase from *Escherichia coli*: Evidence of a complex between two types of polypeptide chains. *Eur J Biochem* **582**: 573–582.

Py, B., Higgins, C.F., Krisch, H.M., and Carpousis, a J. (1996) A DEAD-box RNA helicase in the *Escherichia coli* RNA degradosome. *Nature* **381**: 169–172.

Rath, D., Mangoli, S.H., Pagedar, A.R., and Jawali, N. (2012) Involvement of *pnp* in survival of UV radiation in *Escherichia coli* K-12. *Microbiology* **158**: 1196–1205.

Redder, P., and Linder, P. (2012) Chapter 17: DEAD-box RNA helicases in Gram-positive RNA decay. *Methods Enzymol* **511**: 369-383.

Redko, Y., Aubert, S., Stachowicz, A., Lenormand, P., Namane, A., Darfeuille, F., *et al.* (2013) A minimal bacterial RNase J-based degradosome is associated with translating ribosomes. *Nucleic Acids Res* **41**: 288–301.

Regonesi, M.E., Favero, M. Del, Basilico, F., Briani, F., Benazzi, L., Tortora, P., *et al.* (2006) Analysis of the *Escherichia coli* RNA degradosome composition by a proteomic approach. *Biochimie* **88**: 151–161.

Roy, M.K., and Apirion, D. (1983) Purification and properties of ribonuclease E, an RNA-processing enzyme from *Escherichia coli*. *Biochim Biophys Acta* **747**: 200–208.

Salvo, E., Alabi, S., Liu, B., Schlessinger, A., and Bechhofer, D.H. (2016) Interaction of *Bacillus subtilis* polynucleotide phosphorylase and RNase Y: Structural mapping and effect on mRNA turnover. *J Biol Chem* **291**: 6655-6663.

Sambrook, J.; Fritsch, E. F. and Maniatis, T. (1989) Molecular cloning: A laboratory manual. 2nd Edition. *Cold Spring Harb Lab Press*.

Sanger, F., Nicklen, S., and Coulson, A.R. (1977) DNA sequencing with chain-terminating inhibitors. *Proc Natl Acad Sci U S A* **74**: 5463–5467.

Sarkar, B., Cao, G.-J., and Sarkar, N. (1997) Identification of two poly(A) polymerases in *Bacillus subtilis*. *Biochem Mol Biol Int Pages* **41**: 1045–1050.

Sarkar, N. (1997) Polyadenylation of mRNA in prokaryotes. *Annu Rev Biochem* **66**: 173–197.

Sekiguchi, M., and Cohen, S.S. (1963) The selective degradation of phage-induced ribonucleic acid by polynucleotide phosphorylase. *J Biol Chem* **238**: 349–356.

Shahbabian, K., Jamalli, A., Zig, L., and Putzer, H. (2009) RNase Y, a novel endoribonuclease, initiates riboswitch turnover in *Bacillus subtilis*. *EMBO J* **28**: 3523–3533.

Shapiro, L., and Losick, R. (2000) Dynamic spatial regulation in the bacterial cell. *Cell* **100**: 89–98.

Shi, Z., Yang, W.-Z., Lin-Chao, S., Chak, K.-F., and Yuan, H.S. (2008) Crystal structure of *Escherichia coli* PNPase: central channel residues are involved in processive RNA degradation. *RNA* **14**: 2361–2371.

Spring, T.G., and Wold, F. (1971) The purification and characterization of *Escherichia coli* enolase. **246(22)**: 6797–6802.

Stewart, C., Wilson, F.E., and Bott, K.F. (1982) Detailed physical mapping of the ribosomal RNA genes of *Bacillus subtilis*. *Elsevier Biomed Press* **19**: 153–162.

Stickney, L.M., Hankins, J.S., Miao, X., and Mackie, G.A. (2005) Function of the conserved S1 and KH domains in polynucleotide phosphorylase. *J Bacteriol* **187**: 7214–7221.

Strahl, H., Bürmann, F., and Hamoen, L.W. (2014) The actin homologue MreB organizes the bacterial cell membrane. *Nat Commun* **5**: 1–11.

Strahl, H., Turlan, C., Khalid, S., Bond, P.P.J., Kebalo, J.-M.M., Peyron, P., *et al.* (2015) Membrane recognition and dynamics of the RNA degradosome. *PLoS Genet* **11**: 1–23.

Symmons, M.F., Jones, G.H., and Luisi, B.F. (2000) A duplicated fold is the structural basis for polynucleotide phosphorylase catalytic activity, processivity, and regulation. *Structure* **8**: 1215–1226.

Symmons, M.F., Williams, M.G., Luisi, B.F., Jones, G.H., and Carpousis, A.J. (2002) Running rings around RNA: A superfamily of phosphate-dependent RNases. *Trends Biochem Sci* **27**: 11–18.

Taraseviciene, L., Bjork, G.R., and Uhlin, B.E. (1995) Evidence for an RNA binding region in the *Escherichia coli* processing endoribonuclease RNase E. *J Biol Chem* **270**: 26391–26398.

Taraseviciene, L., Miczak, A., and Apirion, D. (1991) The gene specifying RNase E (*rne*) and a gene affecting mRNA stability (ams) are the same gene. *Mol Microbiol* **5**: 851–855.

Tseng, Y.-T., Chiou, N.-T., Gogiraju, R., and Lin-Chao, S. (2015) The protein interaction of RNA helicase B (RhlB) and polynucleotide Phosphorylase (PNPase) contributes to the homeostatic control of cysteine in *Escherichia coli*. *J Biol Chem* **290**: 29953–29963.

Tuckerman, J.R., Gonzalez, G., and Gilles-Gonzalez, M.A. (2011) Cyclic di-GMP activation of polynucleotide phosphorylase signal-dependent RNA processing. *J Mol Biol* **407**: 633–639.

Vanzo, N.F., Li, Y.S., Py, B., Blum, E., Higgins, C.F., Raynal, L.C., *et al.* (1998) Ribonuclease E organizes the protein interactions in the *Escherichia coli* RNA degradosome. *Genes Dev* **12**: 2770–2781.

Wach, A. (1996) PCR-synthesis of marker cassettes with long flanking homology regions for gene disruptions in *S. cerevisiae*. *Yeast* **12**: 259–265.

Wade, H.E., and Lovett, S. (1961) Polynucleotide phosphorylase in ribosomes from *Escherichia coli*. *Biochem J* **81**: 319-328.

Wang, W., and Bechhofer, D.H. (1996) Properties of a *Bacillus subtilis* polynucleotide phosphorylase deletion strain. *J Bacteriol* **178**: 2375–2382.

Waters, S.M., Zeigler, D.R., and Nicholson, W.L. (2015) Experimental evolution of enhanced growth by *Bacillus subtilis* at low atmospheric pressure: Genomic changes revealed by whole-genome sequencing. *Appl Environ Microbiol* **81**: 7525–7532.

Weber, M.H.W., Volkov, A. V., Fricke, I., Marahiel, M.A., and Graumann, P.L. (2001) Localization of cold shock proteins to cytosolic spaces surrounding nucleoids in *Bacillus subtilis* depends on active transcription. *J Bacteriol* **183**: 6435–6443.

Weiss, W., Weiland, F., and Görg, A. (2009) Protein detection and quantitation technologies for gel-based proteome analysis. *Methods Mol Biol* **564**: 59–82.

Wilusz, C.J., and Wilusz, J. (2004) Bringing the role of mRNA decay in the control of gene expression into focus. *Trends Genet* **20**: 491–497.

Worrall, J.A.R., Górna, M., Crump, N.T., Phillips, L.G., Tuck, A.C., Price, A.J., *et al.* (2008) Reconstitution and analysis of the multienzyme *Escherichia coli* RNA degradosome. *J Mol Biol* **382**: 870–883.

Worrall, J.A.R., Howe, F.S., McKay, A.R., Robinson, C. V, and Luisi, B.F. (2007) Allosteric activation of the ATPase activity of the *Escherichia coli* RhlB RNA helicase. *J Biol Chem* **283**: 5567–5576.

Wu, J., Jiang, Z., Liu, M., Gong, X., Wu, S., Burns, C.M., and Li, Z. (2009) Polynucleotide phosphorylase protects *Escherichia coli* against oxidative stress. *Biochemistry* **48**: 2012–2020.

Xu, F., and Cohen, S.N. (1995) RNA degradation in *Escherichia coli* regulated by 3' adenylation and 5' phosphorylation. *Nature* **374**: 180–183.

Yao, S., Blaustein, J.B., and Bechhofer, D.H. (2008) Erythromycin-induced ribosome stalling and RNase J1-mediated mRNA processing in *Bacillus subtilis*. *Mol Microbiol* **69**: 1439–1449.

Yao, S., Sharp, J.S., and Bechhofer, D.H. (2009) *Bacillus subtilis* RNase J1 endonuclease and 5' exonuclease activities in the turnover of *DeltaermC* mRNA. *RNA* **15**: 2331–2339.

Yehudai-Resheff, S., Hirsh, M., and Schuster, G. (2001) Polynucleotide phosphorylase functions as both an exonuclease and a poly(A) polymerase in spinach chloroplasts. *Mol Cell Biol* **21**: 5408–5416.

Zhao, Y., Lu, M., Zhang, H., Hu, J., Zhou, C., Xu, Q., *et al.* (2015) Structural insights into catalysis and dimerization enhanced exonuclease activity of RNase J. *Nucleic Acids Res* **43**: 5550–5559.

Zweers, J.C., Wiegert, T., and Dijl, J.M. Van (2009) Stress-responsive systems set specific limits to the overproduction of membrane proteins in *Bacillus subtilis*. *Appl Environ Microbiol* **75**: 7356–7364.

6. Appendix

6.1. Bacterial strains

Table 20. Bacterial strains used in this work

Strain	Genotype	Reference
E. coli		
DH5α	*F⁻ endA1 glnV44 thi-1 recA1 relA1 gyrA96 deoR nupG Φ80dlacZΔM15 Δ(lacZYA-argF)U169, hsdR17(r$_K^-$ m$_K^+$), λ–*	Sambrook *et al.*, 1989
B. subtilis		
168	*trpC2*	Laboratory collection
BSB1	168 *trp⁺*	Nicolas *et al.*, 2012
CCB434	W168 *ΔrnjA::spec*	Figaro *et al.*, 2013
GP594	*trpC2 Δeno::cat*	Commichau *et al.*, 2013
GP1034	*trpC2 rnjA*-Strep-*spec*	Lehnik-Habrink, 2011
GP1035	*trpC2 ΔcshA::aphA3*	Lehnik-Habrink *et al.*, 2013
GP1042	*trpC2 rnjA*-Strep-*cat*	Lehnik-Habrink, 2011
GP1048	*trpC2 rnjA*-Strep-*cat rnjB*-3xFLAG-*spec*	Lehnik-Habrink, 2011
GP1075	*trpC2 rnjA*-3xFLAG-*aphA3*	Lehnik-Habrink, 2011
GP1291	*trpC ΔrnjB::cat*	Blötz, 2015
GP1684	*trpC2 amyE::(Pxyl-rny-mSFgfpV206K-spec)*	pGP1449 → 168 Cascante-Estepa *et al.*, 2016
GP1687	*trpC2 rnjB*-Strep-*aphA3*	LFH → 168
GP1694	*trpC2 amyE::(Pxyl-mSFgfpV206K-rnjA-spec)*	pGP2802 → 168 Cascante-Estepa *et al.*, 2016

GP1695	*trpC2 amyE::(Pxyl-mSFgfpV206K-rnjB-spec)*	pGP2803→ 168
		Cascante-Estepa *et al.*, 2016
GP1698	*trpC2 pnpA-gfpA206K-spec*	pGP2806→ 168
		Cascante-Estepa *et al.*, 2016
GP1699	*trpC2 rnjB-gfpA206K-spec*	pGP2807 → 168
		Cascante-Estepa *et al.*, 2016
GP1700	*trpC2 eno-gfpA206K-spec*	pGP2808→ 168
		Cascante-Estepa *et al.*, 2016
GP1720	*trpC2 pfkA-gfpA206K-spec*	pGP2810 → 168
		Cascante-Estepa *et al.*, 2016
GP1721	*trpC2 cshA-gfpA206K-spec*	pGP2811 → 168
		Cascante-Estepa *et al.*, 2016
GP1722	*trpC2 rnjA-gfpA206K-spec*	pGP2812 → 168
		Cascante-Estepa *et al.*, 2016
GP1723	*trpC2 rnjA-Strep-spec ΔrnjB::cat*	GP1291 → GP1034
GP1724	*trpC2 rnjB-Strep-spec*	pGP2816 → 168
GP1731	*trpC2 rnjB-Strep-spec rnjA*-3xFLAG-*aphA3*	GP1724 → GP1075
GP1732	*trpC2 rnjB-ΔCter::cat*	LFH → 168
GP1733	*trpC2 rnjB-ΔCter-gfpA206K-spec*	pGP2818 → 168
GP1734	*trpC2 rnjA-gfpA206K-spec rnjB-ΔCter::cat*	GP1732 → GP1722
GP1736	*trpC2 rnjA-Strep-spec rnjB-ΔCter::cat*	GP1732 → GP1034
GP1737	*trpC2 rnjB-ΔCter-*Strep-*spec*	pGP1827 → 168
GP1740	*trpC2 rnjA-Strep-cat rnjB-ΔCter-*3xFLAG-*spec*	pGP2821 → GP1042
GP1741	*trpC2 rnjB-ΔCter-*Strep-*spec rnjA*-3xFLAG-*aphA3*	GP1737 → GP1075
GP1744	BSB1 Δ*pfkA::aphA3*	LFH → BSB1
GP1747	*trpC2 ΔpfkA::aphA3*	LFH → 168
		Cascante-Estepa *et al.*, 2016
GP1748	*trpC2 ΔpnpA::aphA3*	LFH → 168
		Cascante-Estepa *et al.*, 2016

GP1749	*trpC2 rnjB-gfpA206K-aphA3*		LFH → 168
GP1750	*trpC2 rnjB-gfpA206K-aphA3 ΔrnjA::spec*		GP2502 → GP1749
GP2317	*trpC2 rnjA-gfpA206K-spec ΔrnjB::cat*		GP1291 → GP1722
GP2318	*trpC2 rnjB-Strep-aphA3 ΔrnjA::spec*		GP2502 → GP1687
GP2502	*trpC ΔrnjA::spec*		CCB434 → 168 Cascante-Estepa *et al.*, 2016

ᵃ Arrows indicate construction by transformation.

6.2. Plasmids

Table 21.   Plasmids used in this work

Plasmid	Relevant Characteristics	Primers	Reference
pBP43	pUS19-*gfpA206K*	ML220/ML221	Cascante-Estepa *et al.*, 2016
pDG780	Amplification of *aphA3* cassette	-	Guérout-Fleury *et al.*, 1995
pGEM-cat	Amplification of cm^R cassette	-	Guérout-Fleury *et al.*, 1995
pGP393	His₆-*pfkA*	-	Pietack, 2010
pGP563	His₆-*eno*	-	Pietack *et al.*, 2010
pGP838	His₆-*pnpA*	-	Pietack, 2010
pGP1331	C-terminal 3xFLAG tag	-	Lehnik-Habrink *et al.*, 2010
pGP1389	C-terminal Strep tag	-	Lehnik-Habrink *et al.*, 2011a
pGP1449	pHJS105-*rny*	NC51/NC52 NC53/NC54	Cascante-Estepa *et al.*, 2016
pGP2802	pHJS105-*rnjA*	NC63/NC64	Cascante-Estepa *et al.*, 2016
pGP2803	pHJS105-*rnjB*	NC65/NC2	Cascante-Estepa *et al.*, 2016
pGP2806	pBP43-*pnpA*	ML91/ML92	Cascante-Estepa *et al.*, 2016

pGP2807	pBP43-*rnjB*	ML173/ML174	Cascante-Estepa *et al.*, 2016
pGP2808	pBP43-*eno*	FR86/FR90	Cascante-Estepa *et al.*, 2016
pGP2810	pBP43-*pfkA*	ML56/ML57	Cascante-Estepa *et al.*, 2016
pGP2811	pBP43-*cshA*	ML11/ML12	Cascante-Estepa *et al.*, 2016
pGP2812	pBP43-*rnjA*	ML58/ML59	Cascante-Estepa *et al.*, 2016
pGP2816	pGP1389-*rnjB*	ML173/ML174	This work
pGP2817	pGP1389-*rnjB-ΔCter*	NC78/NC79	This work
pGP2818	pBP43-*rnjB-ΔCter*	NC78/NC79	This work
pGP2821	pGP1331-*rnjB-ΔCter*	NC78/NC79	This work
pHJS105	*amyE::(Pxyl-mSFgfpV206K spec)*	-	Gamba *et al.*, 2015

6.3. Oligonucleotides

All the oligonucleotides were purchased from Sigma-Aldrich. Overlapping sequences are in italics; restriction sites for endonucleases are underlined

Table 22. **Oligonucleotides used in this work**

Primer	Sequence [a]	Purpose
cat fwd (kan)	*CAGCGAACCATTTGAGGTGATAGG*CGGCAATAGTTACCCTTATTATCAAG	Fwd; amplification of *cat* cassette from pGEMcat
cat rev (kan)	*CGATACAAATTCCTCGTAGGCGCTCGG*CCAGCGTGGACCGGCGAGGCTAGTTACCC	Rev; amplification of *cat* cassette from pGEMcat
CB21	*CGCCTACGAGGAATTTGTATCGAT*TGACTGACTAAAGACCGGAGCT	Fwd; down fragment LFH GP1687, GP1732, GP1749
CB25	TTCAGCAAGTCATTCATGCAGC	Fwd; up fragment LFH GP1687

FR21	CACTTAATCAGACGTGCGACATTGGCG	Fwd; check primer LFHs *rnjB*
FR86	TTT<u>GTCGAC</u>CTTGTTTAAGTTGTAGAAAGAGTTGATACCGTGG	Rev; amplification of *eno* (no STOP codon) for cloning into pBP43
FR90	AAA<u>GGATCC</u>CGCTTCAAACAATCGTTGAAGC	Fwd; amplification of *eno* for cloning into pBP43
kan fwd	CAGCGAACCATTTGAGGTGATAGG	Fwd; amplification of *aphA3* cassette from pDG780
kan rev	CGATACAAATTCCTCGTAGGCGCTCGG	Rev; amplification of *aphA3* cassette from pDG780
ML11	ACA<u>GTCGAC</u>GTAAGATTTTTTCTGGCGTCTGTCACCTG	Rev; amplification of *cshA* (no STOP codon) for cloning into pBP43
ML12	ACA<u>GGATCC</u>CTGGCTGAAGCTCTGAACCTTCG	Fwd; amplification of *cshA* for cloning into pBP43
ML56	ACA<u>GTCGAC</u>GATAGACAGTTCTTTTGAAAGCTGATACA	Rev; amplification of p*fkA* (no STOP codon) for cloning into pBP43
ML57	ACA<u>GGATCC</u>GTGGAGACGGTTCCTATATGG	Fwd; amplification of *pfkA* for cloning into pBP43
ML58	ACA<u>GTCGAC</u>AACCTCCATAATGATCGGCAGG	Rev; amplification of *rnjA* (no STOP codon) for cloning into pBP43
ML59	ACA<u>GGATCC</u>CGAACAATCAACCAGCTGTATCG	Fwd; amplification of *rnjA* for cloning into pBP43
ML91	5'-CCTATCACCTCAAATGGTTCGCTGTTATCACTTGTCGTCATCGTCTTTGTAG	Rev; amplification of *pnpA* (no STOP codon) for cloning into pBP43
ML92	ACA<u>GGATCC</u>GCTCGGAGATATGGACTTTAAAG	Fwd; amplification of *pnpA* for cloning into pBP43
ML94	CCTATCACCTCAAATGGTTCGCTGAGCTATTATCATTTTTCGAACTGCGG	Rev; down fragment LFH GP1687 (from GP1724)
ML149	AAAAGCTCATTCAAAAATCGCTGAAG	Fwd; up fragment LFH GP1749
ML173	ACA<u>GTCGAC</u>TACTTCCATAATAATTGGGATGATCATCG	Rev; amplification of *rnjB* (no STOP codon) for cloning into pBP43

ML174	ACA<u>GGATCC</u>CTCATTTACTCTAAAACAGTAGATCTTC	Fwd; amplification of *rnjB* for cloning into pBP43
ML220	ATA<u>AAGCTT</u>ATGAGTAAAGGAGAAGAACTTTTCACTG	Fwd; amplification of *gfp* from pSH3
ML221	ATA<u>AAGCTT</u>TTATTTGTATAGTTCATCCATGCCATGTG	Rev; amplification of *gfp* from pSH3
NC1	AAA<u>GGATCC</u>TTGAAAAAGAAAAATACAGAAAACGTTAGAATTATCGCCC	Fwd; up fragment LFH GP1732
NC2	TTT<u>AAGCTT</u>TTATACTTCCATAATAATTGGGATGATCATCGGTTTAC	Rev; amplification of *rnjB* for cloning into pHJS105
NC51	AAA<u>CCTAGG</u>ATGACCCCAATTATGATGGTTCTCA	Fwd; amplification of *rny* for cloning into pHJS105
NC52	TTT<u>GGATCC</u>TTTTGCATACTCTACGGCTCGA	Rev; amplification of *rny* (no STOP codon) for cloning into pHJS105
NC53	AAA<u>GGATCC</u>GGCTCAGGAAGCGGTATGGGTACCCTGCAGATGAG	Fwd; amplification of *gfp* from pHJS105
NC54	TTT<u>GCGGCCGC</u>TTATTTGTAGAGCTCATCCATGCCA	Rev; amplification of *gfp* from pHJS105 (with STOP codon)
NC63	AAA<u>GGATCC</u>AAATGAAATTTGTAAAAAATGATCAGACTG	Fwd; amplification of *rnjA* for cloning into pHJS105
NC64	TTT<u>AAGCTT</u>TTAAACCTCCATAATGATCGGCAG	Rev; amplification of *rnjA* for cloning into pHJS105
NC65	AAA<u>GGATCC</u>AAATGAAAAAGAAAAATACAGAAAACGTTAG	Fwd; amplification of *rnjB* for cloning into pHJS105
NC78	ACA*<u>GTCGAC</u>*ATCACCGACACCTAAACCATCA	Rev; amplification of *rnjB* (w/o C-ter domain) for cloning into pGP1389 (w/o STOP)
NC79	ACA*<u>GGATCC</u>*TCAATCTGTCCTGCAGCTGG	Fwd; amplification of *rnjB* (w/o C-ter) cloning into pGP1389
NC80	*CCTATCACCTCAAATGGTTCGCTG*TTAATCACCGACACCTAAACCATCA	Rev; up fragment LFH GP1732
NC107	AATTTGAAGCCGTGGGACCG	Fwd; up fragment LFH GP1747

NC108	*CCGGTGATATTCTCATTTTAGCC*ATTCTCCATT CACCTCAGCAACATA	Rev; up fragment LFH GP1747
NC109	*TATTATATTTTACTGGATGAATTGTTTTAG*TGT ACAGCTGAAGGCTGAAGAT	Fwd; down fragment LFH GP1747
NC110	GCATGATCGCATCTGTTCCG	Rev; down fragment LFH GP1747
NC111	ATGGCTAAAATGAGAATATCACCGGA	Fwd; amplification of *aphA3* (from pDG780)
NC112	CTAAAACAATTCATCCAGTAAAATATAATA	Rev; amplification of *aphA3* (from pDG780)
NC113	ATCTGGCCGATGTGGATTGC	Fwd; sequencing in *aphA3*
NC114	AGATGTTGCTGTCTCCCAGG	Rev; sequencing in *aphA3*
NC115	TCCGATATGGATCTAAGTGCGG	Fwd; sequencing GP1747
NC116	TGCATTGTTTGAACTGCTTCAACC	Rev; sequencing GP1747
NC126	*CCGGTGATATTCTCATTTTAGCCAT*ACAATTAC GAACTCCTCTCTTCG	Rev; up fragment LFH GP1748
NC127	ATCGGGTTTCCGACAGCGA	Fwd; up fragment LFH GP1748
NC128	*TATTATATTTTACTGGATGAATTGTTTTAG*ATG AAAACATAAAAGGAGCCTGGG	Fwd; down fragment LFH GP1748
NC129	CCATTATGTATCTTGCTTAACACTC	Rev; down fragment LFH GP1748
NC130	ATTAAAGGAATTGTCATTCATGGTG	Fwd; sequencing GP1748
NC131	GTTCAGTGACTGTTCCAAGCG	Rev; sequencing GP1748
NC132	*TCAAATGGTTCGCTGGGTTTATC*TTATTTGTA GAGCTCATCCATGCCAT	Rev; up fragment LFH GP1749

NC133	CGGTGAAATGTCCGGATGC	Rev; sequencing GP1749
NC135	*TGGAGCCACCCGCAGTTCGAAAAATGATAAA*GAAAAGAGGAAGGAAATAATAAATGG	Fwd; amplification of *aphA3* cassette from pDG780
NC136	*AGCTCCGGTCTTTAGTCAGTCA*CTAGGTACTAAAACAATTCATCCAG	Rev; amplification of *aphA3* cassette from pDG780
SHU12	GCTCATGTGCGCTTGTCTCTTG	Rev; down fragment LFH GP1749, GP1732, GP1687

ª Underlined bases indicate restriction sites. *Italic* indicates homology regions.

6.4. Materials

6.4.1. Chemicals

Acetic acid	ChemSolute
Acryl-:Bisacrylamide	Roth
c-di-AMP	Biolog
Agar	Roth
Agarose	PEQLAB
AgNO$_3$	Roth
Ammonium peroxydisulfate	Roth
Ampicillin	Roth
Bromophenol blue	Riedel-de Haën
BSA	AppliChem
Casamino acids (CAA)	Oxoid
CaCl$_2$ · 2H$_2$O	Roth
Casamino acids	Roth
CDP-Star	Roche
Chloramphenicol	Serva
Coomassie Brilliant Blue, G-250	Roth
DAPI	AppliChem
D-desthiobiotin	IBA

DMSO	Roth
dNTPs	Thermo Scientific
Ethanol	VWR Prolabo chemicals
Ethidium bromide	Roth
Ferric ammonium citrate (CAF)	Fluka
Formaldehyde	Roth
D-(+)-Glucose	AppliChem
L-glutamic acid	Roth
Glycerol	Roth
Glycine	AppliChem
c-di-GMP	Biolog
HDGreen Plus DNA stain	Intas
HEPES	Roth
Imidazole	Sigma-Aldrich
IPTG	PEQLAB
Isopropyl β-*D*-1-thiogalactopyranoside	Sigma-Aldrich
Kanamycin	AppliChem
KCl	Roth
KH_2PO_4	Roth
$K_2HPO_4 \cdot 3H_2O$	Roth
KOH	Roth
λ-DNA	Thermo Scientific
β-mercaptoethanol	Roth
Methanol	VWR Chemicals
$MgCl_2 \cdot 3H_2O$	Roth
$MgSO_4 \cdot 7H_2O$	Roth
$MnCl_2 \cdot 4H_2O$	Roth
Na_3-citrate	AppliChem
NaCl	Roth
Na_2CO_3	Roth

Na$_2$-EDTA · 2H$_2$O	Roth
(NH$_4$)$_2$SO$_4$	Fluka
NaOH	Roth
Na$_2$S$_2$O$_3$ · 5H$_2$O	Merck
Nile Red	SIgma-Aldrich
Ni^{2+}-NTA Sepharose	IBA
Nutrient broth	Roth
PIPES disodium salt	Serva
Poly(A) 15mer RNA	SIgma-Aldrich
Rifampicin	Sigma
Sodium dodecyl sulfate (SDS)	Roth
Spectinomycin	Sigma Life Sciences
Strep-Tactin Sepharose	IBA
D-(+)-Sucrose	AppliChem
Tetramethylethylenediamine	Roth
Tris	Roth
Tryptone	Roth
L-Tryptophan	AppliChem
Tween-20	Sigma-Aldrich
Yeast extract	Oxoid
Xylene cyanol	Merck

6.4.2. Auxiliary material

Centrifuge cups	Beckmann
Cuvettes (microlitre, plastic)	Greiner
Eppendorf tubes	Greiner
Falcon tubes	Sarstedt
Glas beads 0.1 mm	Roth
Glas pipettes	Brad

Micropipettes (2.5; 20; 200; 1000 μl and 5 ml)	Eppendorf
PageRulerTM Plus Protein Ladder	Thermo Scientific
Petri dishes	Greiner
Pipette tips	Greiner
Poly-prep chromatography columns	BioRad
PVDF membrane	BioRad
Vivaspin® turbo 15	Sartorius

6.4.3. Instrumentation

ÄKTAprime plus	GE Healthcare
Autoclave LTA 2x3x4	Zirbus Technology
AxioCam MRm	Zeiss
AxioImager M2 Microscope	Zeiss
Axioskop 40 Microscope	Zeiss
BioLC DNA Pac PA200 4x50 mm Guard	Dionex
BioLC DNA Pac PA200 4x250 mm	Dionex
Centrifuge Heraeus FRESCO 21	Thermo Scientific
Centrifuge Heraeus Megafuge 16R	Thermo Scientific
Centrifuge Sorvall RC 6+	Thermo Scientific
Centrifuge Sorvall WX Ultraseries	Thermo Scientific
Chrom. Data System LC-NetII/ADC	Jasco
Degasser DG-2080-53	Jasco
ECPlan-NEOFLUAR 100X/1.3	Zeiss
Filterset 2	AHF Analysentechnik
Filterset 38 BP470/40, FT495, BP525/50	Zeiss
Filterset 43 BP545/25, FT570, BP605/70	Zeiss
Filterset 49 G365, FT395, BP445/50	Zeiss
French pressure cell press	Thermo Scientific
Horizontal shaker 3006	GFL

HPLC Pump PU-2080Plus	Jasco
Ice machine MF 36	Scotsman
Incubator Heraeus	Thermo Scientific
Incubator shaker Innova®44 series	Eppendorf
Labcycler	SensoQuest
Magnetic stirrer KMO 2 basic	IKA-Werke
Mini PROTEAN® System	BioRad
Molecular Imager® Gel Doc™XR+	BioRad
NanoDrop ND-1000	PeqLab Biotechnologie
pH-meter Calimatic 766	Knick
Plan Neofluar 100x/1.30	Zeiss
Plan Neofluar 40x/0.75	Zeiss
Power Pac Basic™	BioRad
Press machine	G. Heinemann
Scale CP22025	Sartorius
Ultrospec 2100 pro spectroph.	Amersham Biosciences
UV Detector UV-2075Plus	Jasco
Sterile bench HERA safe KS12	Thermo Scientific
HiLoad 16/600 Superdex 200 pg	GE Healthcare
ThermoStat Plus	Eppendorf
Tyssue Lyser II	QIAGEN
Vortex	Schütt Labortechnik
Water desalination plant	Millipore

6.4.4. Commercial systems

DNeasy® Blood & Tissue Kit	QIAGEN
NucleoSpin® Plasmid	Macherey-Nagel
peqGOLD Bacterial DNA kit	PEQLAB
QIAquick® PCR purification Kit	QIAGEN
Roti®-Quant	Roth

6.4.5. Enzymes and antibodies

Alkaline phosphatase (AP)	Thermo Scientific
DNase I	Roche
Phusion DNA polymerase	Thermo Scientific
RNase A	Roche
Restriction enzymes	Thermo Scientific
T4-DNA ligase	Thermo Scientific
Anti-Strep antibody	PromoKine
Anti-FLAG antibody	Sigma-Aldrich
Anti-GapA antibody	Meinken *et al.*, 2003
Anti-Rabbit IgG	Promega

6.5. Websites and software

6.5.1. Websites

URL	Provider	Usage
http://biotools.nubic.northwestern.edu/OligoCalc.html	Northwestern University, USA	Calculation of oligonucleotide properties
http://www.ncbi.nlm.nih.gov/pubmed	National Institutes of Health, Bethesda, USA	Literature
http://subtiwiki.uni-goettingen.de	General Microbiology, University of Göttingen	*B. subtilis* knowledge
http://www.wikipedia.org	Wikimedia Foundation, Inc.	General knowledge
http://www.rcsb.org/pdb/home/home.do	Reasearch Collaboratory for Structural Bioinformatics (RCSB)	Protein structures
http://www.expasy.org	Swiss Institute of Bioinformatics (SIB)	Protein properties predictor

6.5.2. Software

Program	Provider	Usage
AxioVision Rel. 4.7	Zeiss	Image uptake
AxioVision Rel. 4.8	Zeiss	Image uptake
Borwin 1.50	Jasco	Spectra analysis
ChemDraw 14	PerkinElmer Informatics	Chemical scheme
ChemoStar Imager	Intas	Image processing
Geneious 7.0.2	Biomatters Ltd	Bioinformatics
Image J 1.49p	NIH	Image processing
ImageLab™ Software	BioRad	Image processing
Mendeley Desktop 1.17.6	PDFTron™ Systems Inc.	References
Microsoft Office 2010	Microsoft Inc.	Data processing
PrimeView Evaluation	GE Healthcare	Spectra analysis
PyMOL™ 1.7	Schrödinger	Protein structures
SciDAVis 1.D009	scidavis.sourceforge.net	Plotting

6.6. List of abbreviations

% (v/v)	% (volume/volume)
% (w/v)	% (weight/volume)
ADP	adenosine diphosphate
amp	ampicillin
AP	alkaline phosphatase
APS	ammonium peroxodisulfate
ATP	adenosine triphosphate
B2H	bacterial two-hybrid assay
bp	base pair
BSA	Bovine serum albumin
CAA	casamino acids
CAF	ferric ammonium citrate
cat/cm^R	chloramphenicol

DAPI	4',6-diamino-2-fenilindol
dH$_2$O	deionized water
DMSO	dimethylsulfoxide
DNA	deoxyribonucleic acid
DNase	DNA nuclease
dNTP	deoxyribonucleoside triphosphate
EDTA	ethylendiaminetetraacetic acid
et al.	*et alia*
FA	formaldehyde
FD	fast digest
fwd	forward
GFP	green fluorescent protein
HPLC	High-Performance Liquid Chromatography
IPTG	isopropyl-*β-D*-thiogalactopyranoside
kan/aphA3	kanamycin
LB	Luria-Bertani
LFH	long-flanking homology
mRNA	messenger RNA
NIH	National Institutes of Health
Ni^{2+}-NTA	nickel-nitrilotriacetic acid
NTP	nucleoside triphosphate
OD	optical density
PAGE	polyacrylamide gel electrophoresis
PCR	polymerase chain reaction
PFK/PfkA	phosphofructokinase
Pi	inorganic phosphate
PIPES	piperazine-*N,N'*-bis(2-ethanesulfonic acid)
PVDF	polyvinylidene fluoride
rev	reverse
RNA	ribonucleic acid

100

RNase	ribonuclease
rRNA	ribosomal RNA
tRNA	tranfer RNA
RT	room temperature
SEC	size-exclusion chromatography
SDS	sodium dodecylsulfate
SP	sporulation
spec/*spc*	spectinomycin
SPINE	Strep Protein INteraction Experiment
TAE	Tris acetic EDTA
TBS	Tris buffer saline
TEMED	tetramethylethylenediamine
Tris	tris-(hydroxymethyl)-aminomethane
U	units
WT	wild-type

Curriculum vitae

PERSONAL INFORMATION

Name: Nora Cascante Estepa

Date of birth: August 17th 1989

Place of birth: Soria (Spain)

Nationality: Spanish

EDUCATION AND TRAINING

09/13-02/17   Ph.D. in Molecular Biology

Georg-August University Göttingen, Göttingen (Germany).
Title of thesis: Localization and Function of RNases in *Bacillus subtilis*. Department of General Microbiology, Institute for Genetics and Microbiology. Supervisor: Prof. Dr. Jörg Stülke.

09/12-03/13   M.Sc. in Molecular Biology

Georg-August University Göttingen, Göttingen (Germany).
Title of thesis: Carbon metabolism and RNA processing in *Bacillus subtilis*. Department of General Microbiology, Institute for Genetics and Microbiology. Supervisor: Prof. Dr. Jörg Stülke.

10/11-06/12   M.Sc. in Genetics and Cell Biology

Autonomous University of Madrid (UAM), University of Alcalá (UAH) and Complutense University of Madrid (UCM), Madrid (Spain).
Title of thesis: "Reprogramación de la actividad mitocondrial en condiciones de hipoxia: regulación de la proteína NDUFA4." (Reprogramming of mitochondrial activity in hypoxia: regulation of protein NDUFA4). Department of Immunology. Supervisor: Manuel Ortiz de Landázuri

10/07-09/11   Licenciatura en Bioquímica (B.Sc. in Biochemistry)

Autonomous University of Madrid (UAM), Madrid (Spain)
Final degree project (B.Sc. Thesis): "Reprogramación de la actividad mitocondrial vía hipoxia: regulación de las proteínas NDUFA4L2 y NDUFA4." (Reprogramming of mitochondrial activity *via* hypoxia: regulation of the proteins NDUFA4L2 and NDUFA4). Department of Immunology, La Princesa University Hospital, Madrid. Supervisor: Dr. Manuel Ortiz de Landázuri

PUBLICATIONS

Cascante-Estepa N., Gunka K. and Stülke J. (2016) Localization of Components of the RNA-Degrading Machine in *Bacillus subtilis*. *Front. Microbiol.* 7: 1492.